



Technische Universität Wien

Fakultät für Technische Chemie  
Institut für chemische Technologien und Analytik



# Diplomarbeit

## Source apportionment of particulate matter in Styria, Austria

Ausgeführt am Institut für  
Chemische Technologien und Analytik  
der Technischen Universität Wien

Unter der Leitung von:      Ao. Univ. Prof. Dipl.-Ing. Dr.techn. Anne Kasper-Giebl  
Univ. Ass. Mag. Dr. techn. Magdalena Kistler

Durchgeführt von:      Bernadette Kirchsteiger, BSc  
Schachen bei Vorau 81  
8250 Vorau

Matrikelnummer: 1305620  
Studienkennzahl: 066 490

---

Betreuerin

---

Bernadette Kirchsteiger

Wien, am 27. März 2018

*„Remember to look up at the stars and not down at your feet. Try to make sense of what you see and wonder about what makes the universe exist. Be curious. And however difficult life may seem, there is always something you can do and succeed at.*

*It matters that you don't just give up.”*

*Stephen Hawking*

## **Acknowledgments**

---

First of all, I would like to thank gratefully and sincerely Prof. Anne Kasper- Giebl for giving me the opportunity to work in her research group and for supporting me with her knowledge and patience.

Also, a big thank you goes to Dr. Magdalena Kistler for supporting me not only during this time. Thank both of you for your help, understanding and always answering my questions.

Furthermore, I would like to thank all members of our research group for making this time so enjoyable, for listening to all of my problems and for all the funny moments together.

My sincerest gratitude goes to my family and friends. I thank my parents and grandparents for making my education possible and supporting me my whole life. They always believed in me and shared encouraging words when desperation was big and the end out of sight. Special thanks go to my brothers and friends for pushing me to the limit, for the amazing arrangement of my leisure time and for telling me repeatedly to get my stuff together.

## Abstract

---

In 2017 high pollution of particulate matter occurred in mid- Europe and thus also in Austria. To identify particle sources the chemical analysis of quartz fiber filters of four sampling sites in Styria was performed. To allocate the major sources of these high PM concentrations three of these sampling sites were situated in Graz. The fourth sampling site describes a rural area with clearly lower PM concentrations and is located in Vorau, a little town in the east part of Styria. The source apportionment was realized on basis of the macro-tracer approach, which enables the apportionment of source contribution to the bulk PM in the atmosphere.

Sampling was carried out with quartz fiber filters with a High-Volume Sampler at all four sampling sites. For quantification, PM<sub>2.5</sub> samples of the sampling sites Graz Don Bosco and Graz Süd and PM<sub>10</sub> samples of Graz Ost and Vorau were available.

Over the whole sampling period major particle sources were identified:

- Secondary inorganic aerosol (NH<sub>4</sub><sup>+</sup>, NO<sub>3</sub><sup>-</sup> and SO<sub>4</sub><sup>2-</sup>)
- Wood burning aerosol
- Traffic related aerosols (exhaust and abrasion)

An alternating predominance of major sources (SIA and wood burning aerosol) can be observed at both sites.

Vorau

Within the project „CleanAir by Biomass“ measurements of PM<sub>10</sub> samples took place from August 2016 to September 2017 in Vorau. Aim of this project is the evaluation of a real-life study of air quality in a mountain valley and its changes after implementation of improvements into the residential biomass heating systems. The determination of the impact of mitigation strategies requires a detailed knowledge of PM. Measurements describe the situation of ambient air quality of a rural area. The classification of sample pools was carried out to generate representative annual profiles, i.e. to account for elevated and lower concentrations. Furthermore, the occurrence of precipitation was considered.

The source apportionment enables the identification of major sources. Secondary inorganic aerosols (SIA) are identified as major source of pollution. The predominance of SIA can be seen during the whole year and is followed by the contribution of wood burning aerosol and not defined organic material (including humic like substances). Although the PM<sub>10</sub> samples were quantified, comparable low contributions of traffic related aerosols (exhaust and abrasion) and of mineral dust can be observed.

Graz

Because of the numerous exceedances of the limit value for daily mean of 50 µg\*m<sup>-3</sup> of PM<sub>10</sub> concentrations in Graz the analysis of filters of three different sampling sites was done. Measurements were carried out at sampling sites Graz Don Bosco (PM<sub>2.5</sub>), Graz Süd (PM<sub>2.5</sub>) and Graz Ost (PM<sub>10</sub>). Within this project sampling site Graz Don Bosco was focused. Because of this, sampling site Graz Don Bosco had the greatest amount of sample pools. Pools of Graz Süd and Graz Ost cover some time periods of pools from Graz Don Bosco only. So, the comparison of different sampling sites was available. The classification of pools was carried on the basis of the PM<sub>10</sub> concentrations of the sampling site Graz Don Bosco and was compared with the continuous measured PM<sub>10</sub> concentrations at sampling site Bockberg. The sampling site Bockberg (449m) was already used as background site in past studies. [1]

High polluted pools show a predominance of secondary inorganic aerosol followed by the contribution of wood burning aerosol. Major source of pools with lower concentrations of PM mass are wood burning aerosol. Within the timeline of these pools a clear decreasing trend of wood burning aerosol can be observed. The contribution of secondary inorganic aerosol also decreases while an increasing trend of mineral dust can be seen. This clearly occurred at sampling site Graz Ost, where PM<sub>10</sub> samples were available for analysis.

## Kurzfassung

---

Um die Quellen der Feinstaubbelastung zu identifizieren, wurde eine umfassende chemische Analyse von vier Messstationen in der Steiermark durchgeführt. Drei der Messstationen lagen im Raum Graz und eine im oststeirischen Ort Vorau. Die Quellenzuordnung erfolgte mit Hilfe des Makrotracermodells, wodurch die Quellenzuordnung durch spezifische Analyten hochgerechnet wird.

An allen genannten Standorten erfolgte die Probennahmen auf Quarzfaserfiltern mit einem „High- Volume“- Sammler. Zur Analyse standen die  $PM_{2,5}$  Fraktionen der Messstationen Graz Don Bosco sowie Graz Süd und die  $PM_{10}$  Fraktionen der Messstationen Graz Ost und Vorau zur Verfügung.

An allen genannten Standorten erfolgte die Probennahmen auf Quarzfaserfiltern durch einen High Volume Sammler. Zur Analyse standen die  $PM_{2,5}$  Fraktionen der Messstationen Graz Don Bosco sowie Graz Süd und die  $PM_{10}$  Fraktionen der Messstationen Graz Ost und Vorau zur Verfügung.

Die massenmäßig wichtigsten Feinstaubquellen über den Beobachtungszeitraum waren:

- das anorganische Sekundäraerosol ( $NH_4^+$ ,  $NO_3^-$  und  $SO_4^{2-}$ )
- der Holzrauch und
- der Kfz- Verkehr

Die Dominanz der massenmäßig stärksten Quellen (anorganisches Sekundäraerosol und Holzrauch) alternierte beim Vergleich der beiden Messstationen.

Vorau

Aufgrund eines laufenden Projektes fanden im Zeitraum von August 2016 bis September 2017 erste Sammlungen der PM<sub>10</sub> Fraktion in Vorau statt. Ziel dieses Projektes ist die Erstellung einer Real – Life Studie welche die Reduktion des Holzrauchanteiles durch Umsetzung von Maßnahmen in der Raumwärmebereitstellung aufzeigt. Die gewählten Pools der PM<sub>10</sub> Fraktionen beschreiben die Immissionssituation einer ländlichen Region. Die Einteilung der Filter in Probenpools basierte auf der Erstellung repräsentativer Jahresprofile, wobei das Auftreten von Niederschlag berücksichtigt wurde.

Durch die Quellenzuordnung wurde das anorganische Sekundäraerosol als wirksamste Quelle identifiziert. Die Dominanz des SIA wird bleibt über das gesamte Jahr hinweg bestehen. Der Holzrauch, gefolgt vom nicht definierten organischen Material (inklusive HULIS) nimmt ebenso einen Großteil der Staubmasse ein. Der Beitrag des Verkehrs (Emissionen und Abrieb) sowie des Mineralstaubes, sind, obwohl die PM<sub>10</sub> Fraktion zur Analyse zur Verfügung stand, verhältnismäßig gering.

Graz

Aufgrund der zahlreichen Überschreitungen des Grenzwertes für den Tagesmittelwert von 50 µg\*m<sup>-3</sup> der PM<sub>10</sub> Fraktion in Graz, wurden drei Messstationen ausgewählt. Die Messungen erfolgten an den Messstationen Graz Don Bosco (PM<sub>2,5</sub>), Graz Süd (PM<sub>2,5</sub>) und Graz Ost (PM<sub>10</sub>), wobei der Fokus auf der Messstation Graz Don Bosco lag. Dadurch war der Umfang der analysierten Pools dieser Messstation am größten. Die Probenpools der Messstationen Graz Süd und Graz Ost beschreiben ausgewählte Zeitintervalle, welche sich mit Pools der Messstation Graz Don Bosco überschneiden und so einen Vergleich der Stationen ermöglicht. Die Einteilung der Pools erfolgte aufgrund der PM<sub>10</sub> Belastungen der Messstation Graz Don Bosco und wurde mit den kontinuierlich ermittelten PM<sub>10</sub> Daten der Messstation Bockberg abgeglichen. Die Messstation Bockberg (449m) wurde auch schon in vorherigen Messungen als Hintergrundstation gewählt. [1]

Die Quellenzuordnung mittels Makrotracermmodell zeigt unterschiedliche Hauptverursacher der einzelnen Belastungsperioden. Hoch belastete Probenpools sind geprägt von hohen Anteilen an anorganischem Sekundäraerosol gefolgt vom Holzrauch. Bei Probenpools, welche geringere Belastungssituationen darstellten, dominiert der Anteil an Holzrauch, welcher bei geringen Belastungen im März deutlich abfällt. Der Anteil an anorganischem Sekundäraerosol nimmt ebenfalls an, während ein Anstieg des Anteil, welcher dem Mineralstaub zugeordnet wird, zu beobachten ist. Dieser wird speziell bei der Messstation Graz Ost deutlich sichtbar, da hier, anders als bei Graz Don Bosco und Graz Süd, die PM<sub>10</sub> Fraktion zur Analyse zur Verfügung stand.

## List of abbreviations

Abbreviation	Denotation
Milli- Q water	Ultrapure water (Milli-Q, Millipore)
MSA	Methanesulfonic acid
HULIS	Humic like substances
PAHs	Polycyclic hydrocarbons
TC	Total Carbon
EC	Elemental Carbon
OC	Organic Carbon
PM	Particulate Matter
PE	Polyethylene
NYE	New Year's Eve
FID	Flame Ionisation Detector
BaP	Benzo(a)pyren
BeP	Benzo(e)pyren
BghiP	Benzo(ghi)perylene
B(a)A	Benz(a)anthracene
B(b, k)F	Benzo(b, k)fluoranthene
I(1,2,3-cd)P	Indeno(1,2,3-cd)pyrene
DiB(a)A	Dibenz(a, h)anthracene
d <sub>12</sub> -Chr	d <sub>12</sub> - Chrysene
d <sub>12</sub> -BaP	d <sub>12</sub> - Benzo(a)pyren
k	Slope of regression
d	Intercept of regression
sd	Standard deviation
$\bar{x}$	Mean value
LOD	Limit of detection
SIA	Secondary inorganic aerosol
CEF	Crustal enrichment factor
CMB	Chemical Mass Balance
PMF	Positive Matrix Factorization

## Table of contents

---

1	Introduction and aims	- 1 -
1.1	Particulate matter	- 1 -
1.2	Ambient air quality and legislative regulations in Austria	- 1 -
1.3	Motivation of this work	- 2 -
2	The macro-tracer approach	- 3 -
3	Experimental part	- 6 -
3.1	Soluble ions	- 6 -
3.2	Anhydrosugars	- 7 -
3.3	Humic like substances	- 7 -
3.4	Polycyclic aromatic hydrocarbons	- 8 -
3.5	Carbonaceous fractions	- 9 -
3.6	Crustal and trace metals	- 9 -
4	Quality assurance and limits of detection	- 10 -
5	Sampling site – Vorau	- 12 -
5.1	PM <sub>10</sub> sampling sites in Vorau	- 12 -
5.2	Classification of sample pools	- 12 -
5.3	PM <sub>10</sub> concentration trends	- 14 -
5.4	Source apportionment with macrotracer approach	- 17 -
5.5	Annual trend of aerosols	- 21 -
5.5.1	Secondary inorganic aerosol	- 21 -
5.5.2	Wood burning aerosol	- 24 -
5.5.3	Mineral dust	- 28 -
5.5.4	Crustal and trace elements	- 29 -
5.6	Conclusion - Vorau	- 32 -
6	Sampling site - Graz	- 34 -
6.1	PM <sub>10</sub> and PM <sub>2.5</sub> sampling sites in Graz	- 34 -
6.2	Classification of sample pools	- 35 -
6.3	PM <sub>2.5</sub> and PM <sub>10</sub> concentration trends	- 36 -

6.4 Source apportionment with macro-tracer approach - Graz	- 41 -
6.4.1 Days with maximum PM concentrations (January and February)	- 41 -
6.4.2 Days with medium PM concentrations (January and February)	- 45 -
6.4.3 Days with proportionally low PM concentrations (January and February)	- 47 -
6.4.4 Representation of ambient aerosol concentrations and sources in March	- 50 -
6.4.5 Comparison of pools with different ratios PM concentrations between urban and background site	- 53 -
6.4.6 Comparison of New Year's Eve 2016 and 2017	- 54 -
6.5 Polycyclic aromatic hydrocarbons	- 55 -
6.6 Conclusion – Graz	- 59 -
7 Comparison Graz Don Bosco – Vorau	- 62 -
7.1 PM <sub>10</sub> concentrations	- 62 -
7.2 Source apportionment with macro-tracer approach	- 62 -
7.2.1 Secondary inorganic aerosol	- 63 -
7.2.2 Wood burning aerosol	- 64 -
7.2.3 Traffic related aerosols	- 66 -
7.2.4 Mineral dust	- 67 -
8 Limitations of the macro-tracer approach and other methods used for source apportionment	- 68 -
9 Summary and Conclusions	- 72 -
10 List of figures	- 73 -
11 List of tables	- 75 -
12 Bibliography	- 76 -
13 Annex	i

# 1 Introduction and aims

## 1.1 Particulate matter

---

Particulate matter generally describes a dispersions of solid and liquid particles of different size in air. The term particulate matter (PM) refers to all particles suspended in the atmosphere. PM<sub>10</sub> comprises all particles with an aerodynamic diameter  $\leq 10 \mu\text{m}$  (PM<sub>10</sub>). This fraction and also the PM<sub>2.5</sub> fraction, which describes particles with an aerodynamic diameter of  $2,5 \mu\text{m}$  (PM<sub>2.5</sub>), have an important impact on human health and climate. The impact of these particles on human health depends on their shape, size and chemical properties. Even though the human respiratory tract filters inhaled air, PM<sub>2.5</sub> particles reach the pulmonary alveoli. Respiratory and cardiovascular diseases and the reduction of life expectancy is related to particulate matter. [2] Despite this, particles also interact with solar radiation and so influence the climate. Changes in concentrations of greenhouse gases, aerosols and particles in the atmosphere violent the earth's radiative equilibrium and temperature fluctuates. The impact of particulate matter to climate can be classified in direct (absorption and scattering of solar radiation) and indirect effects (change in cloud formation). [3]

PM<sub>2.5</sub> particles are usually formed from anthropogenic sources like combustion processes or from precursors like NO<sub>x</sub>, SO<sub>2</sub> and NH<sub>3</sub>, which furthermore react to ammonium nitrate and -sulphate in the atmosphere. [4]

## 1.2 Ambient air quality and legislative regulations in Austria

---

In Austria, ambient air quality control is carried out regularly and systematically and is published on the respective homepage of each federal state. Legal basis of the air quality control is the national law called "Immissionsschutzgesetz- Luft (IG-L)". Goals of this law are the regulation of measurements, the permanent protection of fauna, flora and the human health, as well as the precautionary reduction of the ambient air pollutants. Furthermore, this law arranges some limit and target values for air pollutants like Benzo(a)pyren, PM<sub>10</sub> and NO<sub>x</sub>. For example the daily limit value for the PM<sub>10</sub> concentration is  $50 \mu\text{g}\cdot\text{m}^{-3}$  and the annual limit value for Benzo(a)pyren, a polycyclic aromatic hydrocarbon, is  $1 \text{ng}\cdot\text{m}^{-3}$  for PM<sub>10</sub> samples. [5]

In Austria, the monitoring of PM<sub>10</sub> concentration started in 1999; in recent years the IG-L sampling network was permanently supported. In general, a decrease of the PM<sub>10</sub> pollution can be observed during last years. In 2017, some exceedances of the limit value for the PM<sub>10</sub> concentration were observed at IG- L sampling sites in some parts of Austria; also three sampling sites in Graz were affected of exceedances. [6]

If there are exceedances of this limit values the reason has to be analyzed. Therefore, the characterization of active sources for particulate matter is of great importance. Chemical different substances which represent particulate matter can be formed by different sources. Because of their variety and the complex chemical composition of the particles different methods for source apportionment have been established.

### **1.3 Motivation of this work**

---

Because of repeated exceedances of the daily limit value for PM<sub>10</sub> concentrations some areas in Austria are characterized as regions of special interest for the monitoring of ambient air quality. At the beginning of 2017 high pollutions of particulate matter were measured in some regions of Styria. The limit value for the PM<sub>10</sub> concentration (50 µg\*m<sup>-3</sup> as daily mean) was exceeded several times at most sampling sites; where maximum values above 100 µg\*m<sup>-3</sup> were measured. Because of that, PM samples are analyzed and the major sources are identified.

This work focuses on the source apportionment of particulate matter performed with the macro-tracer approach at four sampling sites. Three of the sites are located in the capital of Styria: Graz Don Bosco, Graz Süd and Graz Ost. The fourth monitoring site is located in the east of Styria, in Vorau. These sampling site represents areas with different geographical and community issues.

Following questions are answered:

- Which different effects have to be considered, during classification of sample pools?
- Are there spatial or temporal trends or is there a uniformly pollution of PM over time?
- What are the major sources of PM mass at the different sampling sites?
- Which sources show spatial or temporal (seasonal) trends?

The macro-tracer approach focusses on the source apportionment based on the concentrations of tracer substances. During source apportionment with this simple and robust approach several questions occurred, which are briefly discussed as a starting point for future work.

- What are the limitations of the macro-tracer approach?
- Are there other possibilities for source apportionment within the scope of quantified sample pools and what are the requirements?

## 2 The macro-tracer approach

The macro-tracer approach is one method which allows the apportionment of chemical species of PM to specific sources. This concept was established at TU Wien within the AQUELLA and AQUELLIS group studies. It permits the identification of sources and the quantitative classification of PM. [1]

The basic principle of this approach is the idea of the classification of portions and contributions of pollutants of ambient data to different sources. This receptor model enables the identification of following sources and contributions:

- Wood burning aerosol
- Secondary inorganic aerosols (ammonium nitrate and –sulphate)
- Mineral dust (silicates and carbonates)
- Traffic related aerosols (exhaust and abrasion)
- Water-soluble secondary organic aerosols (incl. HULIS)
- De-icing salt (NaCl)

The calculation of the contributions of macro-tracers to different sources, is carried out on the basis of the concentrations of tracer substances with appropriate conversion factors. These factors are optimized for regions which are already investigated in detail, e.g. for Austria. The relationships and factors, which are based on the AQUELLA and PMInter projects, are listed in the table below and are optimized for the situation in Austria. [1], [7]

*Table 1: List of conversion factors to calculate the source contribution I*

Tracer	Calculation	Source	Referenz
Levoglucosan	$M_{WS} = c_{Lev} * 10,7$	Wood burning aerosol, small-scale residential heating	[8]-[10]
Elemental Carbon (EC)	$E_{WS} = M_{WS} * 0,1$ $EC_D = EC$ $D_{EX} = EC_D + (EC_D * 0,33)$ $D_{AB} = D_{EX} * 0,3$	Traffic (exhaust & abrasion) $E_{WS}$ = EC from Wood burning $E_{CD}$ = EC emission from diesel $D_{EX}$ = diesel emissions	Tunnel measurements [11]
Organic Carbon (OC)	$OC_D = EC * 0,33$ $OC_{ND} = OC - OC_D - OC_{WS}$ $OM_{ND} = OC_{ND} * 1,5$	$OC_{ND}$ = not defined OC $OC_{WS}$ = OC from Wood burning $OC_D$ = OC from Diesel $OM_{ND}$ = not defined OM	Tunnel measurements [8]-[10], [12]
HULIS	$HULIS - OC * 1$	Humic like substances, part of secondary organic aerosol	[13]

Table 1 continued: List of conversion factors to calculate the source contribution

Tracer	Calculation	Source	Referenz
NaCl	-	De-icing salt	De-icing agent, Na/Cl relation
Ca, Si, Al	Ca* 2,5 Si = Al *3 Si * 2,7	Mineral dust (silicates, carbonates)	Geogenic relations, street dust profiles
NH <sub>4</sub> <sup>+</sup> , SO <sub>4</sub> <sup>2-</sup> , NO <sub>3</sub> <sup>-</sup>	SIA = $\Sigma$ (NH <sub>4</sub> <sup>+</sup> , SO <sub>4</sub> <sup>2-</sup> , NO <sub>3</sub> <sup>-</sup> ) *1,1	Secondary inorganic aerosol (Humidity respected)	-
HULIS	HULIS - OC * 1	Humic like substances, part of secondary organic aerosol	[13]

The contribution of wood burning aerosol is calculated based on the concentrations of the anhydrosugar levoglucosan. Levoglucosan is an important macro-tracer, which is mostly generated during combustion processes of organic material like wood, is stable at low temperatures and not emitted through other sources than burning. [14] The conversion factor used to calculate the contribution of wood burning aerosol is adjusted to the situation in Austria. [15] The stereoisomers of levoglucosan (mannosan and galactosan) can also be found in PM; but in much lower concentrations than levoglucosan. Mannosan and galactosan are also formed during the pyrolytic conversion of cellulose and hemicelluloses. The distribution of these anhydrosugars depends on the type of biomass burnt and the burning temperature. The sort of burning material (soft- or hardwood) can be calculated out of the ratio between mannosan and galactosan in PM samples. [14], [15]

Elemental carbon (EC) is formed during the combustion of fossil fuels and biomass. The contribution of elemental carbon which is formed by biomass burning depends on the used technology and the used burning material. Although it is an essential simplification of source apportionment, the correction of elemental carbon with the amount of EC caused by biomass burning was not considered within this work. The concentration of EC was directly used to calculate the contribution of traffic related aerosols. Besides EC also the contribution of organic carbon (OC) in the exhaust and the abrasion has to be considered. The conversion factors were derived from tunnel measurements; the conversion factor is based on measured ratios of OM/EC of PM<sub>2.5</sub> concentration. [11]

Secondary inorganic aerosols (SIA) also comprise a big part of PM. They are generated from precursor gases like NO<sub>x</sub>, SO<sub>2</sub> and NH<sub>3</sub> in the atmosphere. The main sources of these gaseous compounds are agriculture, industry processes and traffic. The concentration of secondary inorganic aerosol depends on the transport of air masses, the temperature and the relative humidity of the ambient air; they are used as indicators to calculate the contribution for regional transport. [7]

Particulate matter (PM) also contains organic material (OM); the calculation is based on the concentration of organic carbon (OC). To calculate the amount of OM conversion factors which consider the hetero atoms of airborne substances are used. The contribution of organic material is attributed to water-soluble secondary organic aerosols (e.g. HULIS), the emissions caused by biomass burning and not defined organic material. Humic like substances (HULIS) count to the secondary organic aerosol and capture an essential contribution of water-soluble organic compounds of PM. [16] Due to their structure and chemical properties they are important in reactions of atmospheric chemistry. The amount which is contributed to HULIS is calculated on basis of the concentration of the total carbon amount of the samples. The contribution of not defined organic material (not defined OM) is calculated out of the amount of total carbon of the samples after deduction of the amount of the contribution of wood burning aerosol and HULIS.

Especially in summer season, also bio aerosols contribute to the mass of organic material. In the scope of this work no quantification of markers for this source were analyzed, so the contribution of bio aerosols cannot be given.

Mineral dust is emitted by both, anthropogenic and natural sources and the amount which is caused by erosion processes can be preferably found in  $PM_{10}$  samples. [17] The contribution of mineral dust is based on the geogenic ratio between aluminum and silicium as well as on the concentration of calcium. Mineral dust consists mostly of silicates and carbonates which are considered within the calculation with conversion factors. High amounts of mineral dust are related to resuspension of soil, erosion, construction works or already beginning agricultural activities.

Like mineral dust also the amounts of de-icing salt can also be related to resuspensions of soil. In the scope of this work the input of sea-salt contributions was neglected. [7]

## 3 Experimental part

### 3.1 Soluble ions

---

To determine the soluble inorganic anions ( $\text{Cl}^-$ ,  $\text{NO}_2^-$ ,  $\text{NO}_3^-$ ,  $\text{SO}_4^{2-}$ ) a filter aliquot ( $\varnothing=10\text{mm}$ ) out of each filter contributing to a pool was taken. All aliquots per pool were usually extracted with 5 mL Milli-Q water. After sonification for 30 minutes and centrifugation the extract was analyzed by ion chromatography.

The quantification was carried out with isocratic ion chromatography with conductivity detection. The system parameters are listed in the table below.

*Table 2: Parameters of the anion chromatography system*

System	Thermo Scientific Dionex ICS 1100
Autosampler	Spark Holland Basic Marathon
Precolumn	Dionex Ion Pac AG22A
Column	Dionex Ion Pac AS22A
Suppressor	Dionex ASRS 300-4mm
Detector	Conductivity detector
Eluent	4,5 mM $\text{Na}_2\text{CO}_3$ / 1,4 mM $\text{NaHCO}_3$
Flow	1 mL/min

Similarly, a filter aliquot of the same size ( $\varnothing=10\text{mm}$ ) was used to extract soluble cations ( $\text{Na}^+$ ,  $\text{K}^+$ ,  $\text{Ca}^{2+}$ ,  $\text{NH}_4^+$ ,  $\text{Mg}^{2+}$ ) with 5 mL Methanesulfonic acid. After sonification for 30 minutes and centrifugation the extract was also analyzed by ion chromatography.

The quantification of cations was carried out with isocratic ion chromatography and conductivity detection. The used system and parameters are listed in the table below.

*Table 3: Parameters of the cation chromatography system*

System	Thermo Scientific Dionex ICS 3000
Autosampler	Knauer Autosampler 3800
Precolumn	Dionex Ion Pac CG16A
Column	Dionex Ion Pac CS16A
Suppressor	Dionex CSRS 500-4mm
Detector	Conductivity detector
Eluent	38 mM MSA
Flow	1 mL/min

### 3.2 Anhydrosugars

For the quantification of Saccharides (levoglucosan, mannosan, galactosan, xylitol, glucose, galactosan, fructose and sucrose) the same extract, which was prepared for anion analysis was used. After sonification for 30 minutes and centrifugation the extract was analyzed by ion chromatography with electrochemical detection (pulsed amperometry). [18]

*Table 4: Parameters of the Saccharides chromatography system*

System	Thermo Scientific Dionex ICS 3000
Autosampler	Knauer Autosampler 3800
Column	CarboPack MA1
Reference electrode	Ag/AgCl pH electrode
Detector	Dionex electrochemical detector (Au electrode)
Eluent	1 mM NaOH / Milli- Q water (52% / 48%)
Flow	0,4 mL/min

### 3.3 Humic like substances

For the quantification of humic like substances (HULIS) filter aliquots were taken, so the total area for measurement of each pool summed up about 10 cm<sup>2</sup>; the exact area was determined for each pool. Aliquots were extracted threefold with 3 mL Milli- Q water, sonicated for 20 minutes and acidulated with 0,9 mL pH2 solution to a resulting pH of 3. Subsequently the same filter aliquots were extracted threefold with 3 mL NaOH (pH13) in the ultrasonic bath for 20 minutes and afterwards acidulated with 0,7 mL pH 0 solution to a resulting pH of 2.. The isolation of the HULIS fraction was carried out in two steps. In the first step, protonated HULIS and other apolar substances were retained via solid phase extraction (SPE) with a C<sub>18</sub> phase. The second step separated retained HULIS from other remaining organic substances with a SAX- column. The quantification of the carbon portion of the HULIS fraction the sample is burnt and the generated CO<sub>2</sub> is quantified with an NDIR Detector. [13]

In the following table the sample preparation sequence for HULIS extraction is listed. [19]

Table 5: Parameters of HULIS quantification [19]

Isolation step 1	Solid Phase Extraction with C18- phase (ISOLUTE C18-EC, Biotage) Retention of protonated HULIS and other apolar substances in aqueous or alkaline solution
Elution of the C18-phase	With 400 $\mu\text{L}$ Methanol
Isolation step 2	Separation of remaining organic substances and methanol with SAX (ISOLATE SAX, self-built column installed in flow injection system)
Separation	Of Mono- and Dicarboxylic acids with diluted nitric acid
Elution of HULIS	With Ammonia
Analysis of HULIS-C	Pyrolysis with a catalytic oven at 800 $^{\circ}\text{C}$ to form $\text{CO}_2$ and subsequent detection of $\text{CO}_2$ with NDIR

### 3.4 Polycyclic aromatic hydrocarbons

Aliquots prepared according to the pool size (exact extraction area was determined for each pool and accounted at least 10  $\text{cm}^2$ ) were spiked with 50  $\mu\text{L}$  of the recovery standard ( $d_{12}$ - BaP) and extracted two times with 3 mL Cyclohexane and 3 mL Dichloromethane. After sonification for 30 minutes the extracts were centrifuged and each supernatant was transferred into an "Turbovap- Vial". This vial was stored close-lipped until the second extract of the appropriate sample was transferred into it. After coalition of the two extracts in the "Turbovap- Vial" 50  $\mu\text{L}$  of the internal standard ( $d_{12}$ - Chrysene) was added and the extract was contracted from a 12 to 0,5 mL. [20]

The contracted extract was then transferred into the GC- Vial with an inlet and analyzed.

Table 6: Parameters of PAH quantification

System	Hewlett- Packard HP 6890 Series (GC) Hewlett- Packard HP 5973 (MS)
Injection mode	Pulsed splitless
Sample volume	1,0 $\mu\text{L}$
Purge flow	30,0 $\text{mL} \cdot \text{min}^{-1}$
Saver flow	15 $\text{mL} \cdot \text{min}^{-1}$
Start temperature	55,0 $^{\circ}\text{C}$
Temperature gradient	25 $^{\circ}\text{C} \cdot \text{min}^{-1}$ ramp: 55,0 – 320,0 $^{\circ}\text{C}$ with 25 $^{\circ}\text{C} \cdot \text{min}^{-1}$ 320 $^{\circ}\text{C}$ hold for 8 minutes 550 $^{\circ}\text{C}$ hold for 1 minute total analysis time: 19,6 minutes
Maximum temperature	320,0 $^{\circ}\text{C}$
Gastype	Helium 5.0
Pre column	Ulitimate Plus FS ID = 0,25 mm; l = 30 m
Capillary column	HP- 5MS 5% Phenylmethylsiloxane DB – 5 MS (30 x 25 x 0,25 mm)
Inlet Liner	Single-Taper, 900 $\mu\text{L}$ , deactivated
Quadrupol temperature	180 $^{\circ}\text{C}$
Ion source temperature	300 $^{\circ}\text{C}$

### 3.5 Carbonaceous fractions

For the quantification of carbonaceous fractions (OC and EC) a filter aliquot ( $\varnothing=10\text{mm}$ ) out of each filter was taken and day by day determined with an OCEC analyzer from Sunset Laboratory Inc.. The measurement is a thermal- optical method based on the combustion of EC, OC in inert- or an oxidizing atmosphere. [21] [22]

Within the temperature program EC and OC are converted into carbon dioxide ( $\text{CO}_2$ ) in different steps of the temperature program under different conditions. [23] The resulting carbon dioxide is subsequently converted into methane ( $\text{CH}_4$ ) which was quantified with an FID. First parts of the temperature program include the heating of the filter punch in (inert) helium atmosphere. While heating of the punch there is a continuous determination of the laser transmission. This laser signal decreased during the determination because of desorption and partly pyrolyzation of the organic compounds. After that the filter punch is heated in an oxidizing helium/oxygen atmosphere to convert the EC into carbon dioxide so the transmission signal rises again. The split point between OC and EC is set automatically within the evaluation when the laser signal reached its initial value again or at the end of the temperature program. As method EUSAAR 2 was used and the gained information was evaluated with the OCEC (Calc 415) software. [23]

### 3.6 Crustal and trace metals

For the quantification of trace metals the filter aliquots were chemically digested with aqua regia and then analyzed with ICP-OES. An aliquot of each filter with a diameter of 27 mm was taken and summarized to the appropriate pool. The pools were transferred in Teflon-high pressure vessels and digested with 8 mL aqua regia in the microwave. During the 45 minutes of digestion the sample vessels heated up to 170 – 190 °C (depending on the number of filter aliquots in the vessel). Afterwards the cooled vessels were vent and the extract was diluted with Milli- Q water to a total volume of 40 mL. [17]

Before quantification with ICP- OES takes places, the samples were diluted 1:5 and spiked with 2 ppm (40  $\mu\text{L}$ ) Europium as an internal standard. [24]

Analyses were carried out in the research group inorganic trace analysis under supervision of Prof. Dipl.-Ing. Dr. techn. Andreas Limbeck.

*Table 7: Parameters of crustal and trace element quantification*

System	Thermo Scientific iCap 6000 Series
Measure mode	Radial
Auxiliary gas flow	0,8 L*min <sup>-1</sup>
Nebulizer gas flow	0,85 L*min <sup>-1</sup>
Viewing height	12 mm
Quantified wavelengths	Al 309,271 nm; Ba 445,403 nm; Fe 259,940 nm; B 249,773 nm; Zn 213,856 nm; Mn 257,610 nm; Cr 267,716 nm

## 4 Quality assurance and limits of detection

Depending on the parameter analyzed the quality assurance was checked via laboratory inter-comparisons or the use of standards or certified reference materials (CRM).

To ensure the quality of quantification of polycyclic aromatic hydrocarbons a certified reference material (ERM – CZ 100) was quantified regularly as advised by the European norm EN 15549. Within the research group an intercomparison with other laboratories analyzing BaP for Austrian Air Quality Network was conducted.

To ensure the quality of the analysis of carbonaceous fractions, reference filters with different PM mass and sucrose standards were quantified in specified time intervals. Based on their PM mass the reference filters were separated in HighLoad, MidLoad and LowLoad fractions. Additionally, a liquid sucrose standard with 50 µg C was measured at the beginning of each day.

To ensure the quality of the quantification of anhydrosugars the laboratory of TU Wien took part at the interlaboratory comparison test “Levoglucosan and its isomers”. The results from previous intercomparison tests showed a good agreement of results achieved with the applied method with the expected values (in 2007 and 2013). [25]

Furthermore, the plausibility of the results of the ion analyses are checked in terms of ion balances whereby the equivalent concentrations of anions and cations are calculated and checked. Regularly the laboratory of TU Wien takes place on the WMO Inter-laboratory Comparison Study (LIS 57) of the World Meteorological Organization.

The calculation of the limit of detections was carried out via measurements of field blanks. These field blanks were handled as samples and analyzed with each method. Because it was not possible to calculate the LODs of each analyte on the basis of the measurement of blank filters (either because no analyte was detected or because of variations of the blanks, as for AI results), LODs were determined differently. In this case, the LOD was calculated out of the calibration in use of the calibration standard with the lowest amount of analyte.

The calculation of LOD was performed according to following formulas.

*Formula 1: Calculation of LOD  
via field blanks*

$$LOD = 6 * s_{BW}$$

LOD ..... Limit of detection (µg\*m<sup>-3</sup>)  
s<sub>BW</sub> ..... Standard deviation of multiple  
measurements

\* If analytes could not be quantified via multiple measurements of field blanks, the LOD was calculated via the calibration standard with the lowest amount of analyte. LODs calculated with this method are signed with \*

Formula 2: Calculation of LOD  
via lowest calibration standard

$$* LOD = 3 * s_{Std}$$

$s_{Std}$  ..... Standard deviation of multiple measurements

To calculate the atmospheric concentrations following assumptions have been made:

- Average air volume 700 m<sup>3</sup>
- Punch size, as used for the appropriate analysis
- Volume of elution, as used for the appropriate analysis

Table 8: List of limits of detection

	LOD	Unit		LOD	Unit	
Chloride	0,01	µg*m <sup>-3</sup>	Total-C, TC	0,63	µg*m <sup>-3</sup>	
Nitrite ▲	0,02	µg*m <sup>-3</sup>	Elemental- C, EC	0,09	µg*m <sup>-3</sup>	
Nitrate ▲	0,03	µg*m <sup>-3</sup>	Organic- C, OC	0,55	µg*m <sup>-3</sup>	
Inorganic analytes	Sulfate ▲	0,09	µg*m <sup>-3</sup>	Levogluconan *	0,03	µg*m <sup>-3</sup>
	Natrium ▲	0,01	µg*m <sup>-3</sup>	Mannosan *	0,03	µg*m <sup>-3</sup>
	Calcium	0,41	µg*m <sup>-3</sup>	Galactosan *	0,07	µg*m <sup>-3</sup>
	Ammonium	0,02	µg*m <sup>-3</sup>	HULIS	0,36	µg*m <sup>-3</sup>
	Kalium	0,06	µg*m <sup>-3</sup>	BaP	0,05	ng*m <sup>-3</sup>
	Magnesium	0,03	µg*m <sup>-3</sup>	BeP	0,19	ng*m <sup>-3</sup>
	▲ because of plausibility examinations only field blanks 1-4 were used for calculation			B(b,k)F	0,07	ng*m <sup>-3</sup>
	Aluminum	26	ng*m <sup>-3</sup>	B(a)A *	0,36	ng*m <sup>-3</sup>
The calculation of the limit of detection of aluminum was carried out on the basis of the calibration curve by the software.			I(1,2,3-c,d)P *	0,17	ng*m <sup>-3</sup>	
			DiB(a)A *	0,13	ng/m <sup>3</sup>	

# 5 Sampling site – Voral

## 5.1 PM<sub>10</sub> sampling sites in Voral

Sampling took place in Voral, a small town in the east of Styria. It has about 5000 inhabitants and represents a small community with great influence from nearby agricultural activity. The percentage of agriculture (farms and agricultural used landscapes) conducts 15 % of all households in Voral; whereat cattle breeding dominates with 90 % of all farm in this area. The sampling site was located in the center of Voral, behind the city hall, near to the park and is shown in Figure 1.

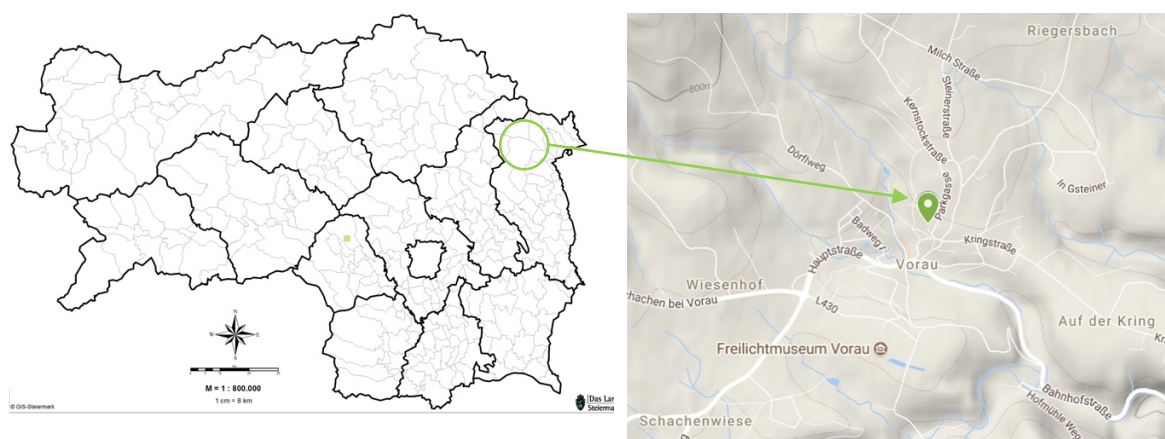


Figure 1: Sampling site in Voral, Austria [26][27]

## 5.2 Classification of sample pools

Gravimetric analysis of the quartz fiber filters (PM<sub>10</sub> samples) was performed in the laboratories of the local Government of Styria. Subsequently the filters were folded and stored in PE- bags at -20 °C until they were transferred to TU Wien for further investigations. Because a detailed chemical analysis of filters of the whole year was not possible, representative time periods were chosen. Voral represents a sampling site with generally lower concentrations of PM than Graz. Regarding the sampling period of 03.08.2016 to 12.09.2017 exceedances of the limit value of 50 µg·m<sup>-3</sup> were observed in January 2017 only.

These exceedances occurred during the time period of 23.01. – 01.02.2017 at the end of January, i.e. similar to the pollution episode determined in Graz as well. Furthermore, the aspect of occurrence of precipitation was important. Precipitation cleans the atmosphere and thus a lower concentration of PM and other air pollutants can be measured. To account for precipitation data from the background site Masenberg (1260 m) was considered. Because of the different sea levels of both sampling sites and so different meteorological conditions, only prominent amounts of precipitation  $> 10 \text{ L}\cdot\text{m}^{-2}$  were respected and precipitation in Masenberg can only be taken as an indication for similar conditions in Vorau. For the time period of 03.08.2016 to 12.09.2017 following pools were chosen:

- One pool which characterizes a maximum  $\text{PM}_{10}$  concentrations  $> 100 \mu\text{g}\cdot\text{m}^{-3}$  (31.01.2017)
- Two pools which characterize days with comparable high  $\text{PM}_{10}$  concentrations ( $> 40 \mu\text{g}\cdot\text{m}^{-3}$ ) being close to the daily limit value of  $\text{PM}_{10}$
- Six pools which characterize moderate polluted periods with  $\text{PM}_{10}$  concentrations within  $20 \mu\text{g}\cdot\text{m}^{-3}$  to  $40 \mu\text{g}\cdot\text{m}^{-3}$
- Four pools which characterize low polluted periods with  $\text{PM}_{10}$  concentrations  $< 20 \mu\text{g}\cdot\text{m}^{-3}$ . At two of them a prominent amount of precipitation occurred, so the comparison of pools with and without precipitation is possible.

Table 9 lists the pools, which were chosen for the sampling site in Vorau. Several pools consist of only one day, which mark traditional events or extraordinary high PM concentrations.

Table 9: List of sample pools Vorau

$\text{PM}_{10}$ mass [ $\mu\text{g}\cdot\text{m}^{-3}$ ]	Pool	Periode	$\text{PM}_{10}$ mass [ $\mu\text{g}\cdot\text{m}^{-3}$ ]	Pool	Periode
20-30	VO1	27.08-28.08.2016	>100	VO8	31.01.2017
20-30	VO2	07.09-16.09.2016	30-40	VO9	08.02. - 13.02.2017
>30	VO3	16.11.2016	10-20	VO10	26.03. - 02.04.2017
>30	VO4	05.12.2016	<10	VO11	12.05. - 15.05.2017
20-30	VO5	19.12. - 24.12.2016	10-20	VO12	04.06. - 10.06.2017
40-80	VO6	22.01. - 25.01.2017	<10	VO13	24.07. - 28.07.2017
40-80	VO7	28.01. - 30.01. + 01.02.2017 (except 31.01.2017)	also, blank filters have been analyzed for each period of time		

### 5.3 PM<sub>10</sub> concentration trends

Figure 2 shows temporal trends of concentrations of PM<sub>10</sub> in Vorau, Hartberg and Masenberg and the temperature over time. Hartberg is the next city and about 26 km away from the center of Vorau. Masenberg (1260 m) was chosen as background site because it is one of the mountains surrounding the Vorauer Becken. Because of different sea levels of the sampling sites in Vorau and Masenberg different meteorological issues have to be kept in mind. Elevated concentrations can be clearly detected at all sites at low temperatures in December and January.

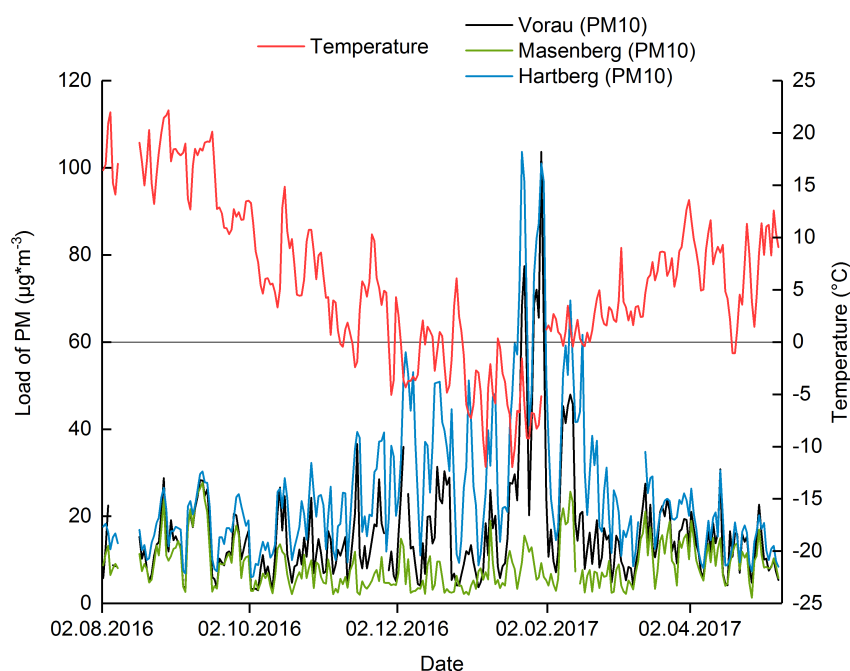


Figure 2: Comparison of PM<sub>10</sub> concentrations ( $\mu\text{g}\cdot\text{m}^{-3}$ ) of sampling sites in Vorau, Masenberg and Hartberg and trend of temperature ( $^{\circ}\text{C}$ ) during sampling period.

The PM<sub>10</sub> mass of the background site Masenberg was very low; it reached its maximum value on 14.09.2017 with  $28 \mu\text{g}\cdot\text{m}^{-3}$  during the sampling period. The maximum value at the sampling site in Vorau was detected on the 31.01.2017 with  $104 \mu\text{g}\cdot\text{m}^{-3}$ . The daily limit value of  $50 \mu\text{g}\cdot\text{m}^{-3}$  for the PM<sub>10</sub> concentration was exceeded on eight days, all within the time period of 23.01.2016 – 01.02.2017. This period is included in pools V4, V5 and V6.

Figure 3 shows the total  $PM_{10}$  concentrations of Vorau and the ratios between two urban/residential sampling sites (Vorau/Hartberg). Vorau describes a more rural area and the total area of community accounts for about 81 km<sup>2</sup> and is located 660 m above sea level. Whereas Hartberg presents a more urban area with about 6500 inhabitants on more confined space (22 km<sup>2</sup>) and is located 360 m above sea level.  $PM_{10}$  mass of Vorau is presented as grey bars and the ratio between the urban sampling sites in Vorau and Hartberg is shown as black line. Figure 3 shows the different ratios of these urban sampling sites; where the red highlighted area describes ratios between 1 and 1,5. During winter the ratio between these two sites lies under the red area, which means that  $PM_{10}$  concentrations in Hartberg were higher than in Vorau. But during summer the ratios were often located within the red highlighted area, which indicates quite similar  $PM_{10}$  concentrations of this two sampling sites. In August, some high ratios can be observed on 08.09.2017 (2,7) and on 12.08.2017 (2,9). Vorau is a more rural sampling site with more of agriculture around it than Hartberg. So, a possible source of such high ratios may be related to agricultural activities during late summer months. Furthermore, the before mentioned exceedances (23.01.2016 – 01.02.2017) can also be observed in this figure. During these days, the ratios between the  $PM_{10}$  fractions of Vorau and Hartberg were within 0,3 - 0,9; and reached its maximum on 24.01.2017 with 0,9 which means that  $PM_{10}$  concentrations were quite similar at both sites.

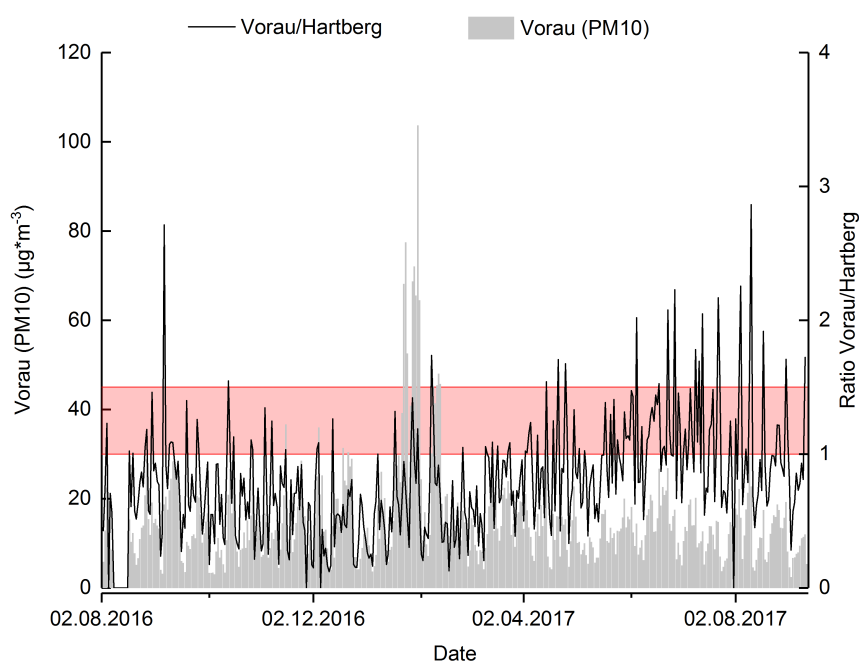


Figure 3: Ratio  $PM_{10}$  concentrations of Vorau/Hartberg and the total  $PM_{10}$  concentration ( $\mu\text{g}\cdot\text{m}^{-3}$ ) of Vorau. The red highlighted area marks the ratio between 1,0 and 1,5 which means similar pollutions at the different sampling sites.

In Figure 4 the daily means of  $PM_{10}$  concentration of Vorau and the amount of precipitation at the sampling site on Masenberg is shown. The blue pictured area marks the occurrence of precipitation while the black line describes the trend of  $PM_{10}$  mass in Vorau. The red highlighted area marks an abrupt decrease of  $PM_{10}$  concentration during 03.02. and 07.02.2017; this is caused by the occurrence of precipitation.

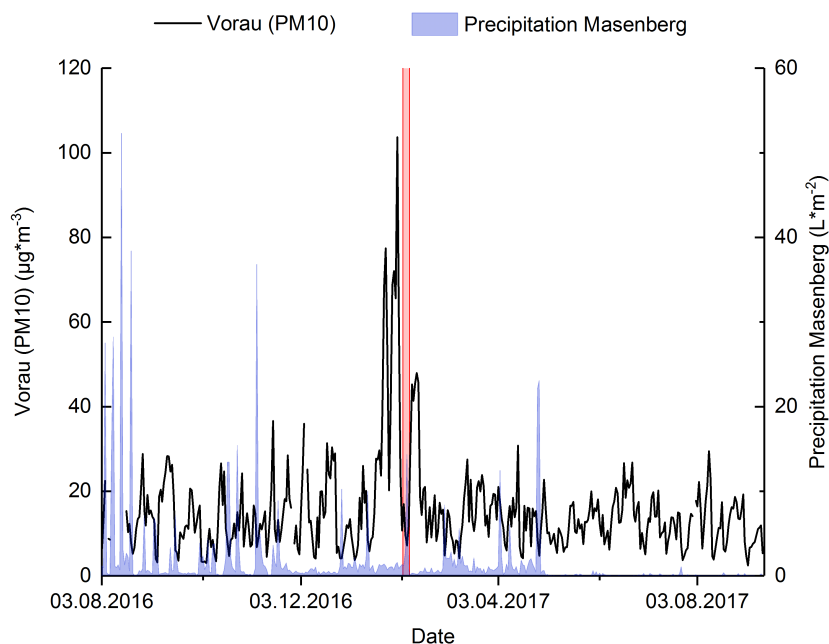


Figure 4: Trend of  $PM_{10}$  concentration ( $\mu\text{g}\cdot\text{m}^{-3}$ ) in Vorau and precipitation ( $\text{L}\cdot\text{m}^{-2}$ ) on Masenberg. The red highlighted area marks an abrupt decrease of  $PM_{10}$  concentration caused by a precipitation event.

Because of the low PM concentrations in Vorau the pool classification was realized depending on different  $PM_{10}$  masses and the occurrence of precipitation. The highest values were handled as single pool, while days with lower PM mass were summarized to bigger pools. Figure 5 shows the  $PM_{10}$  concentrations of Vorau. The light grey and dark grey highlighted areas mark the time periods of selected sampling pools; differences in colors do not display maximum PM concentrations. Blue highlighted areas mark the two pools where a prominent amount of precipitation  $> 10 \text{ L}\cdot\text{m}^{-2}$  occurred at least on one day.

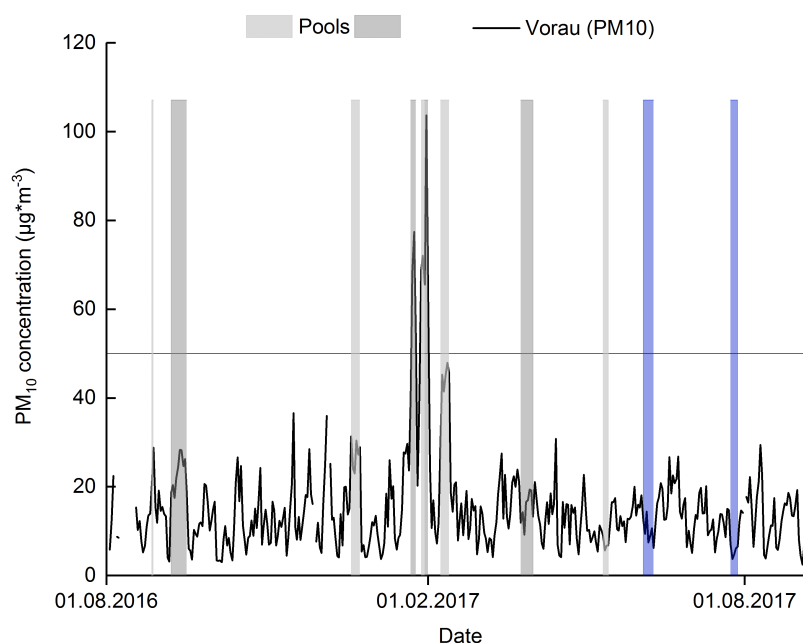


Figure 5: Sampling pools – Vorau. The red drawn line marks the daily limit value of  $PM_{10}$  concentration. Pools during or after the occurrence of precipitation  $> 10 L \cdot m^{-2}$  are highlighted blue.

Elevated  $PM_{10}$  concentrations which occurred on 16.11.2016 ( $37 \mu g \cdot m^{-3}$ ), 05.12.2016 ( $36 \mu g \cdot m^{-3}$ ) and 31.01.2017 ( $104 \mu g \cdot m^{-3}$ ) were handled as single-day- pool. Pools covering these days within their time period do not include them (VO 7 does not include 31.01.2017). The only exceedances of the limit value for the daily mean of  $50 \mu g \cdot m^{-3}$  occurred in the before mentioned time period during 23.01.2016 – 01.02.2017.

## 5.4 Source apportionment with macrotracer approach

This chapter comprises the results of source apportionment with the macro-tracer approach. All concentrations and the calculated source contributions are listed in the Annex.

To present the annual trends of the apportionment of  $PM_{10}$  13 sample pools for sampling site Vorau was chosen. So, it was possible to divide pools into summer (VO 1-2 and VO 10 – 13) and winter pools (VO 3 – 9). During winter pools the average  $PM_{10}$  concentration was about 3,5 times higher than during summer pools. Because of this classification different contributions of source apportionment were observed. The macro-tracer approach allowed the characterization of average 83 % of total  $PM_{10}$  mass during all pools. In contrast to the situation at one site in Graz the source apportionment did not overestimate the actually measured mass concentrations at the sampling site Vorau.

Figure 6 presents the source apportionment of the pollution situation during winter time, which corresponds to the time period of November to end of February. The absolute  $PM_{10}$  concentrations ranged from  $27 \mu g \cdot m^{-3}$  to  $103 \mu g \cdot m^{-3}$ . During the first pools of winter period (VO 3 – 5; November - December) no dominant source can be observed; the impact of wood burning aerosol and secondary inorganic aerosol is nearly equal. During VO 3 – 5 the concentration of wood burning aerosol accounted for in average  $10 \mu g \cdot m^{-3}$  which corresponds to average 30 % of total  $PM_{10}$  mass. The average concentration of SIA during these pools accounted  $11 \mu g \cdot m^{-3}$  which corresponds to 33 % of total  $PM_{10}$  mass. Furthermore, the impact of traffic related aerosols was about 15 % of total  $PM_{10}$  mass. This trend of source impacts shifts and a predominance of secondary inorganic aerosol can be observed during later winter pools. VO 6 – 9 describe the situation of ambient air quality during January and February, with lower average temperatures than measured during VO 3 – 5. The average concentrations of SIA accounted  $32 \mu g \cdot m^{-3}$  which corresponds 46 % of total  $PM_{10}$  mass. Furthermore, the contribution of not defined organic material increases during winter period; a part of this can be most likely attributed to humic like substances (HULIS) which had not analyzed yet.

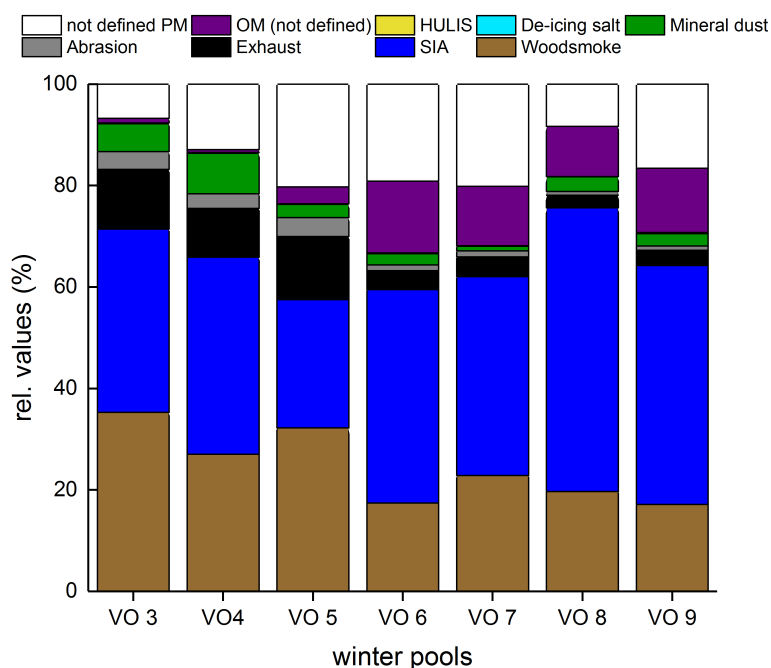


Figure 6: Presentation of source apportionment of winter pools (VO 3 – 9) of sampling site Vorau ( $PM_{10}$ )

Figure 7 shows the relative source contribution of summer pools (VO 1- 2 and VO 10 – 13) of sampling site Vorau. In contrast to winter pools, lower average  $PM_{10}$  concentrations were observed during these pools. They represent the ambient air quality at higher average temperatures during April to September. VO 10 was the only pool of this time period, where the quantification of levoglucosan was possible; in all other pools the concentration of levoglucosan dropped below the LOD. If results drop below the LOD no contribution of wood burning aerosol is calculated for this period, this does not represent the actual situation; so, the source apportionment of this pool is flawed with higher uncertainty than other ones. VO 1 is the only pool where a predominance of secondary inorganic aerosol can be observed. The concentration of SIA accounted  $14 \mu g \cdot m^{-3}$  which corresponds to 58 % of total  $PM_{10}$  mass. At the present, no defined reason for this high value can be given. One possible explanation would be high sulphate concentrations ( $8 \mu g \cdot m^{-3}$ ) which can be caused by agricultural activities like fertilization. Furthermore, an increasing concentration of not defined organic material could be observed, which ranged between  $3 \mu g \cdot m^{-3}$  and  $10 \mu g \cdot m^{-3}$  (1 – 14%). This points to sources not considered in the present approach, e.g. bioaerosols. In contrast to late winter pools a higher contribution of mineral dust can be observed during summer pools.

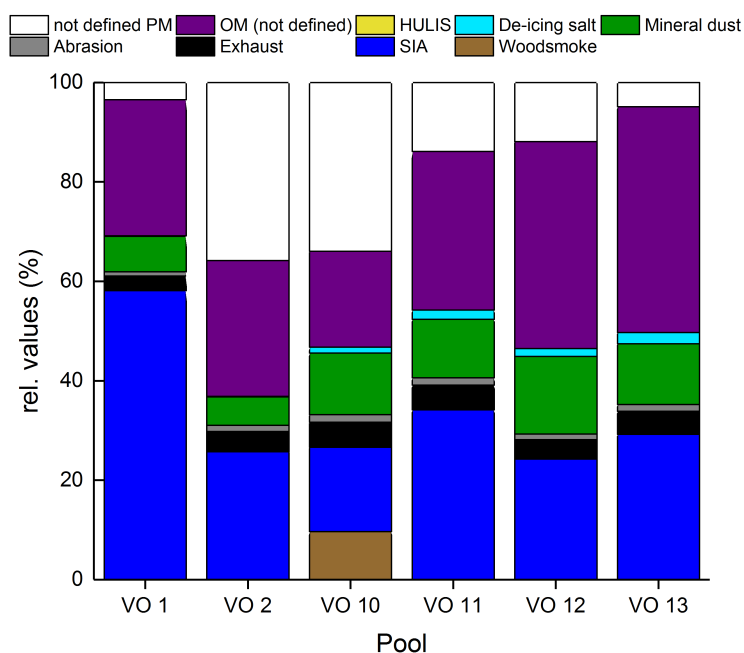


Figure 7: Presentation of source apportionment of summer pools (VO 1 – 2 and VO 10 - 13) of sampling site Vorau ( $PM_{10}$ )

Figure 8 compares the source apportionment and absolute concentrations the cold and the warm season. The difference in atmospheric PM<sub>10</sub> concentrations and the resulting source contribution can be seen. The impact of wood burning aerosol can clearly be observed during winter period, while a low concentration is contributed during summer pools. Although, the PM<sub>10</sub> concentration is clearly different, the contribution of SIA ranged between 30 % and 40 % within these two periods. An increased impact of mineraldust and not defined organic material can be observed during summer pools.

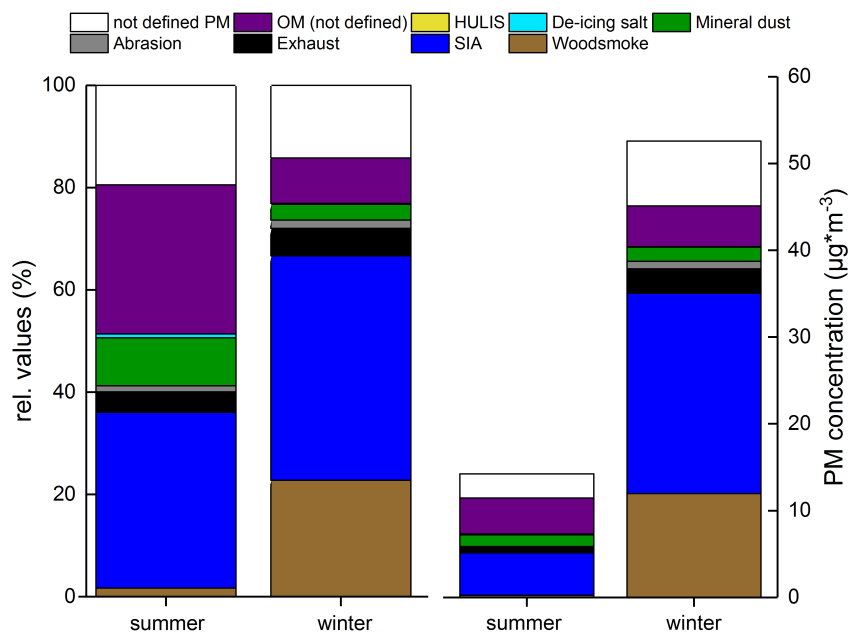


Figure 8: Comparison of the source apportionment of different sampling periods of sampling site Vorau (PM<sub>2.5</sub>)

To sum up, a clear difference in PM<sub>10</sub> concentrations and the resulting source apportionment can be observed. During winter time, a clear impact of wood burning aerosol and secondary inorganic aerosol can be observed. This can be attributed to lower average temperatures and a higher amount of small scale heating. Furthermore, low temperatures support the formation of semi volatile aerosol components.

## 5.5 Annual trend of aerosols

---

Because of their prominence at low temperatures a distinct temporal trend can be observed for wood burning aerosol and secondary inorganic aerosols. The demand of small scale heating arises with low temperatures and so a higher amount of related aerosols are emitted. Furthermore, the formation of ammonium nitrate, which counts to the secondary inorganic aerosols, depends on temperature. It is formed preferentially at low temperatures and so the amount of SIA arises at low temperatures.

The contribution of mineral dust and traffic related aerosols (exhaust and abrasion) shows an indirect proportional trend. Later on, the impact of these two sources is noticeable.

### 5.5.1 Secondary inorganic aerosol

---

Secondary inorganic aerosols summarize the concentrations of ammonium nitrate and – sulphate, which are formed in the atmosphere of the precursors  $\text{NO}_x$ ,  $\text{SO}_2$  and  $\text{NH}_3$ . These gaseous precursor substances are emitted by traffic emissions, industry or combustion processes and agriculture. The formation of ammonium nitrate depends on the temperature and is preferred at low temperatures. At high temperatures, the compound is instable and the equilibrium shifts to the side of gaseous precursors substances, so lower concentrations can be measured in the particulate phase. This temperature dependences cannot be found for the formation of ammonium sulphate. [28], [29]

The atmospheric concentrations, the average temperature and the contribution of SIA are listed in Table 10. Figure 9 shows the concentration of secondary inorganic aerosols and the trend of concentrations of ammonium, nitrate and sulphate over time period. Each time period marks one pool and the width of shown bars does not display the number of days which are summarized to a pool. Noticeable are the great different concentrations between the summer time 2016 and 2017, which need further investigations.

Table 10: Concentration of ammonium, nitrate and sulphate ( $\mu\text{g}\cdot\text{m}^{-3}$ ), contribution of secondary inorganic aerosol (%) to PM mass and average temperature ( $^{\circ}\text{C}$ ) of all pools of sampling site Vorau

	Pool	Time period	Average temperature ( $^{\circ}\text{C}$ )	$\text{NH}_4^+$ ( $\mu\text{g}\cdot\text{m}^{-3}$ )	$\text{NO}_3^-$ ( $\mu\text{g}\cdot\text{m}^{-3}$ )	$\text{SO}_4^{2-}$ ( $\mu\text{g}\cdot\text{m}^{-3}$ )	SIA (%)
summer period	VO 1	27.08. - 28.08.2016	21,6	3,4	2,1	7,5	58
	VO 2	07.09. - 16.09.2016	18,0	1,1	0,6	3,7	26
winter period	VO 3	16.11.17	-1,9	3,6	5,7	2,8	36
	VO 4	05.12.17	-3,6	4,4	6,3	2,0	39
	VO 5	19.12. - 24.12.2016	-1,8	1,3	3,2	1,9	25
	VO 6	22.01. - 25.01.2017	-5,9	4,9	9,7	8,0	42
	VO 7	28.01. - 30.01 + 01.02.2017 (except 31.01.2017)	-5,7	1,2	13,9	7,1	39
	VO 8	31.01.17	-5,2	8,9	28,6	15,3	56
	VO 9	08.02. - 13.02.2017	1,0	3,6	7,0	7,7	47
summer period	VO 10	26.03. - 02.04.2017	9,3	0,8	0,1	1,4	17
	VO 11	12.05. - 15.05.2017	13,8	0,3	1,2	0,8	34
	VO 12	04.06. - 10.06.2017	15,9	0,4	0,8	1,0	24
	VO 13	24.07. - 28.07.2017	18,1	0,1	0,9	0,5	29

An annual trend of all analytes can be observed. Especially high concentrations of nitrate correlate with high concentrations of ammonium. During summer time (VO 1 - 2 corresponds time period 27.08 – 28.08.2016 and 07.09. – 16.09.2016) higher concentrations of sulphate were measured. The ratio of nitrate and sulphate ranged between 0,2 and 0,3 during these pools. Whereas the ratio during winter pools (VO 3 – 9 corresponds time period 16.11.2016 to 08.02. – 13.02.2017) varied between 0,9 and 3,2. The highest concentrations of all analytes and the corresponding maximum value of secondary inorganic aerosol were measured at VO 8 (31.01.2017) which was also the pool with the  $\text{PM}_{10}$  mass. The maximum values on 31.01.2017 counted  $29 \mu\text{g}\cdot\text{m}^{-3}$  for nitrate, sulphate  $15 \mu\text{g}\cdot\text{m}^{-3}$  and ammonium  $9 \mu\text{g}\cdot\text{m}^{-3}$ . Pool VO 7 spans the neighboring/adjacent days, i.e. the time period of 28.01. – 01.02.2017, but not including the maximum value at 31.01.2017. For pool VO 8 already different concentrations of nitrate and sulphate can be observed. This phenomenon can also be found at the concentrations of sampling site Graz Don Bosco and so it strengthens the assumption of a regional pollution period caused by the transport of air masses during this time period.

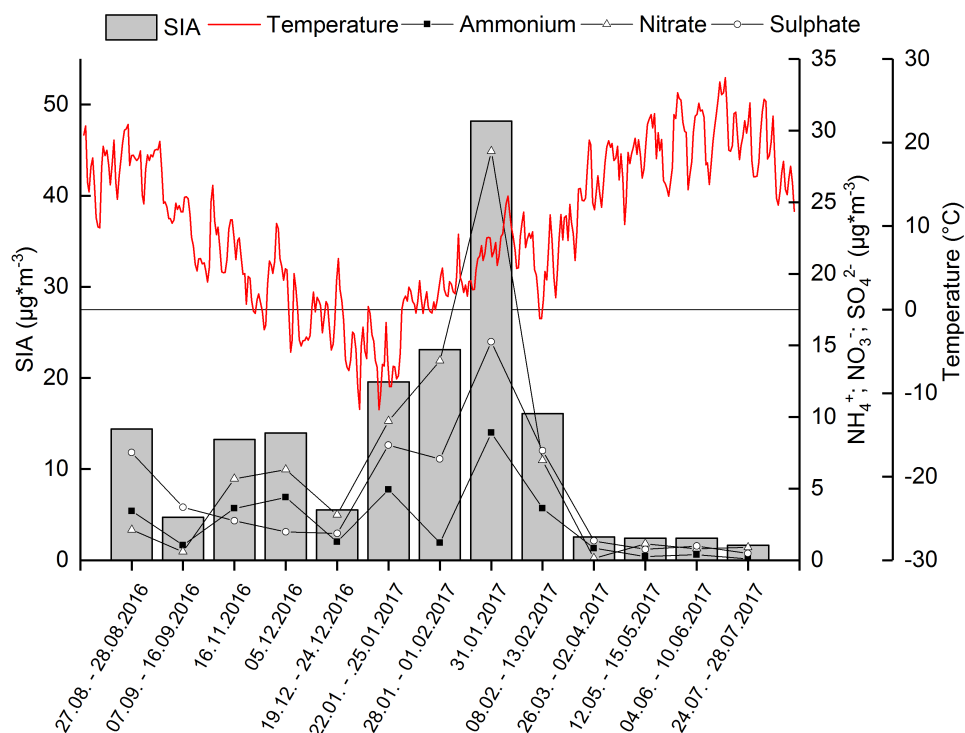


Figure 9: Atmospheric concentrations of ammonium, nitrate or sulphate ( $\mu\text{g}\cdot\text{m}^{-3}$ ) (right inner axis) and secondary inorganic aerosol ( $\mu\text{g}\cdot\text{m}^{-3}$ ) (left axis) over time period. The daily mean of temperature ( $^{\circ}\text{C}$ ) is shown as a red line.

Figure 10 shows the annual trend of secondary inorganic aerosol and the remaining  $\text{PM}_{10}$  concentration as well as the trend of temperature during sampling time. The width of bars displays the number of days which were summarized to one pool. The before mentioned trend can also be observed in Figure 10. Higher concentrations of SIA were measured at pools with higher  $\text{PM}_{10}$  concentrations. The decreasing trend of PM mass during the warmer season correlates with decreasing concentrations of SIA. This is on the one hand caused by the temperature dependence of the formation of ammonium nitrate as well as decreasing emissions of particulate matter.

During the cold season (VO 3 – 9) the contribution of SIA ranged between 25 and 56 % of total PM. The concentrations of SIA during cold time (VO 3 – 9) were in average about 4,7 times higher than during warmer time (VO 1-2 and VO 10 – 13). So, the contribution of SIA during warmer time ranged between 17 and 34 %. Because of its high contribution of SIA (58%) VO 1 is excluded in this discussion. During VO 1 a maximum concentration of sulphate of  $8 \mu\text{g}\cdot\text{m}^{-3}$  was measured; the concentrations of ammonium ( $3 \mu\text{g}\cdot\text{m}^{-3}$ ) and nitrate ( $2 \mu\text{g}\cdot\text{m}^{-3}$ ) were much lower. This work focuses on the annual trend of aerosols, for further investigations require a more detailed analysis of this elevated ion concentrations.

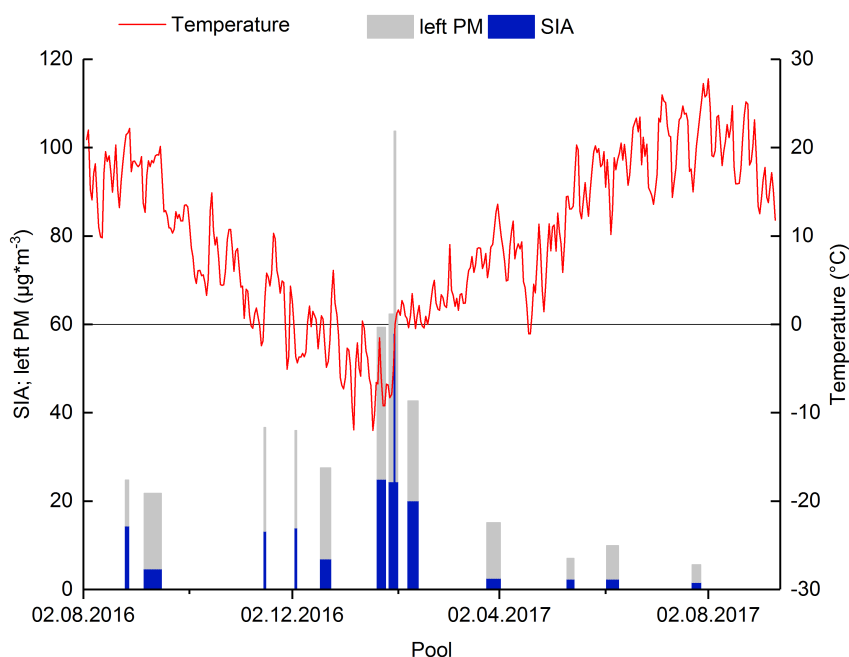


Figure 10: Annual trend of SIA concentrations and remaining PM ( $\mu\text{g}\cdot\text{m}^{-3}$ ) and temperature ( $^{\circ}\text{C}$ )

### 5.5.2 Wood burning aerosol

Anhydrosugars are formed during to combustion processes of biomass like wood but also of leafs, branches and straw. They are formed during the pyrolysis of cellulose and hemicellulose; as further anhydrosugars like mannosan and galactosan, the isomers of levoglucosan. [14] Besides this, forest fires represent a source of anhydrosugars in  $\text{PM}_{10}$  and  $\text{PM}_{2.5}$ , but during winter time the concentrations are mostly caused by wood burning and small-scale heating. To summarize the contribution of wood burning aerosol the amount of levoglucosan in PM was quantified.

In the scope of AQUELLA projects, but also in other literature, also potassium is listed as a wood burning tracer. [1], [12]

Figure 11 shows the atmospheric concentrations of wood burning tracers levoglucosan and Potassium and the temperature trend over the whole sampling period. The width of drawn bars does not display the number of days which are summarized to a pool.

Increasing concentrations of both levoglucosan and potassium can be observed when temperature decreases; this correlates to the higher demand of heating and biomass combustion. If temperature increased the concentration of both markers decreased and the concentrations of levoglucosan dropped under the limit of detection. A correlation between both markers and the trend of temperature can be seen.

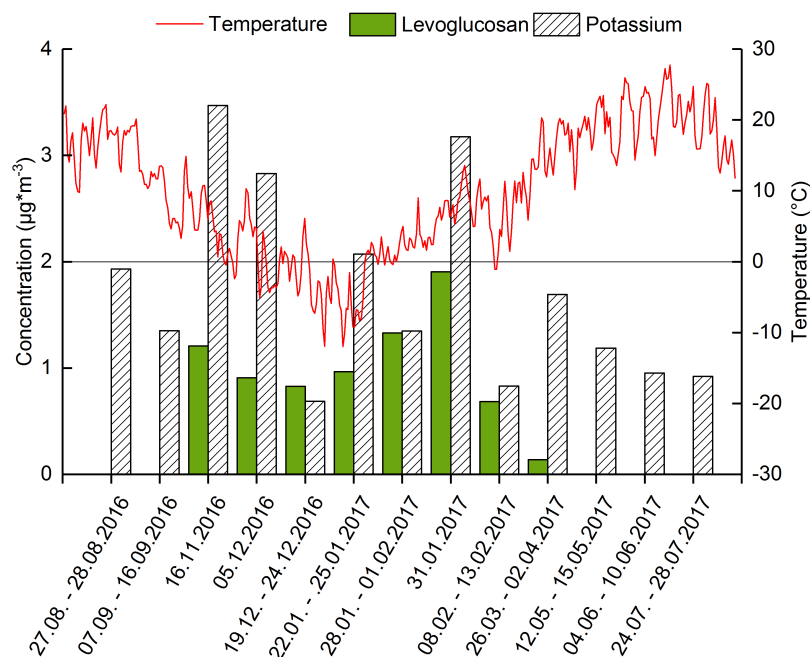


Figure 11: Trend of the atmospheric concentrations of wood burning tracers levoglucosan and potassium ( $\mu\text{g}\cdot\text{m}^{-3}$ ) and temperature ( $^{\circ}\text{C}$ ) over sampling period, Vörau. The concentration of levoglucosan dropped below the LOD ( $< 0,03 \mu\text{g}\cdot\text{m}^{-3}$ ), so quantification was not possible during summer time.

The ratio between levoglucosan and potassium ranged between 0,3 and 1,2 during November to March; while it reached a ratio of 0,1 during April to September. During April to September noticeable concentrations of potassium were measured. It has to be mentioned, that wood burning is not the only source for potassium emissions. There are several other emission sources like meat grilling or other primary biogenic emissions; like already observed in previous publications. Caseiro et al. found ratios, which pictured the same trend; where also higher concentrations of potassium were observed. [12]

The annual average concentration for levoglucosan ranged between  $0,2 \mu\text{g}\cdot\text{m}^{-3}$  (Pool VO 10, time period 26.03. – 02.04.2017) and  $1,9 \mu\text{g}\cdot\text{m}^{-3}$  (Pool VO 8, time period 31.01.2017). The average temperature during pool VO 7 was  $-5,7 \text{ }^{\circ}\text{C}$  while it was  $+9,3 \text{ }^{\circ}\text{C}$  during pool VO 10. VO 10 was the pool with the highest temperature where the concentration of levoglucosan was over the limit of detection. Pools VO 1-2 and VO 11-13 are summarized to so called “summer pools”, the concentration of levoglucosan during these pools was lower the limit of detection. If the results for levoglucosan drop under the LOD no contribution of wood burning aerosol is calculated, so the source apportionment of these pools is flawed with higher uncertainty than others. Furthermore, this does not display the real situation of wood burning aerosol because biomass is also burnt for heating purposes during summer.

The atmospheric concentrations of levoglucosan and the average temperature during winter pools are listed in Table 11. Pools VO 6 - 8 are the ones with the lowest average temperatures during sampling time. In general, an increasing trend of levoglucosan can be observed during these three pools. VO 8 is the pool with the highest PM<sub>10</sub> concentration of 104 µg\*m<sup>-3</sup>. The maximum contribution of 35 % can be observed at pool VO 3 (16.11.2016), which marks PM<sub>10</sub> mass of 37 µg\*m<sup>-3</sup>.

*Table 11: Concentration of levoglucosan (µg\*m<sup>-3</sup>), contribution of wood burning aerosol (%) and average temperature (°C) of winter pools - Vorau*

Pool	Time period	Average temperature (°C)	Levoglucosan (µg*m <sup>-3</sup> )	Wood burning aerosol (%)
VO 3	16.11.2017	-1,9	1,2	35
VO 4	05.12.2017	-3,6	0,9	27
VO 5	19.12. - 24.12.2016	-1,8	0,8	32
VO 6	22.01. - 25.01.2017	-5,9	1,0	17
VO 7	28.01. - 30.01 + 01.02.2017 (except 31.01.2017)	-5,7	1,3	23
VO 8	31.01.2017	-5,2	1,9	20
VO 9	08.02. - 13.02.2017	1,0	0,7	17

Figure 12 shows the annual trend of wood burning aerosol and the remaining PM<sub>10</sub> mass. The width of shown bars displays the number of days which are summarized to a pool. The already mentioned trend can also be observed in this figure. Pools during November to March, which mark situations with lower temperatures, showed a higher contribution of wood burning aerosol than “summer pools”. During April to September (VO 1,2 and VO 10, 12, 13) the average contribution of wood burning aerosol reached 10 %. Because of the low concentrations of levoglucosan in summer pools, only pool VO 10 could be quantified. All other pools were under the limit of detection, so no contribution of wood burning aerosol could be calculated.

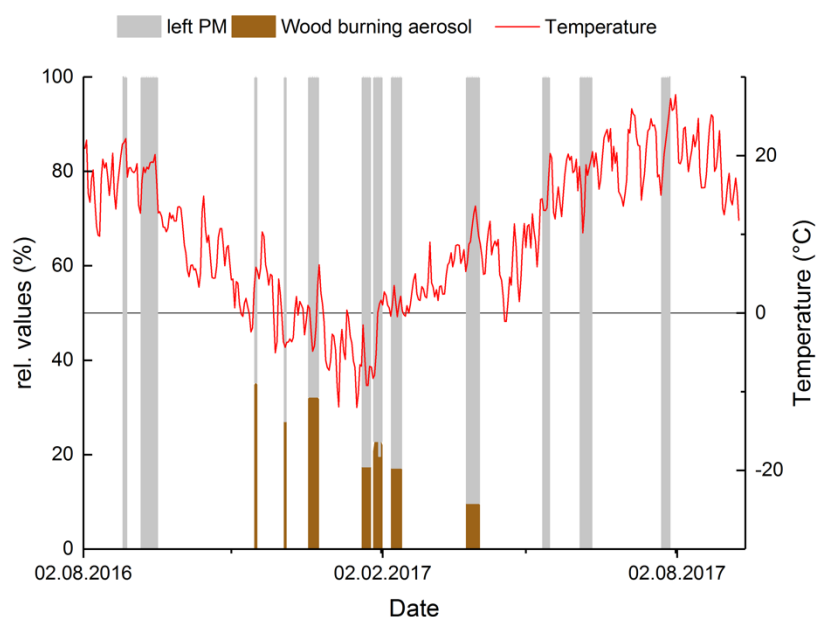


Figure 12: Relative contribution of wood burning aerosol (%) and remaining PM ( $\mu\text{g}\cdot\text{m}^{-3}$ ) and trend of temperature ( $^{\circ}\text{C}$ ). The width of showed bars displays the number of days which are summarized to a pool.

The average contribution of wood burning aerosol during November to March (VO 3 – 9) ranged between 17 to 35 % of total PM. This is 5,7 times higher than it was measured during summer pools. The highest concentration of wood burning aerosol was measured on 31.01.2017 (VO 8) with  $20,4 \mu\text{g}\cdot\text{m}^{-3}$ , this is also the pool with the highest  $\text{PM}_{10}$  concentration.

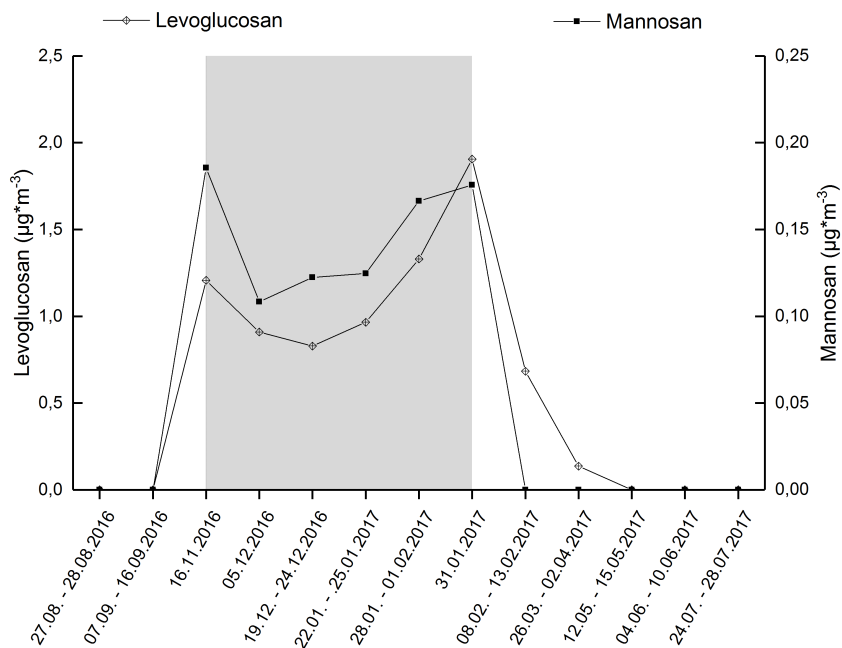


Figure 13: Annual trend of levoglucosan and Mannosan ( $\mu\text{g}\cdot\text{m}^{-3}$ ). The grey highlighted area marks pools during autumn/winter period

Mannosan and galactosan, the isomers of levoglucosan, are also formed during combustion processes. The concentrations of levoglucosan and mannosan are shown in Figure 13. Mannosan followed the same trend shown by levoglucosan while the concentrations of galactosan dropped under the limit of detection and could not be quantified. The grey highlighted area marks the pools during autumn/winter period (VO 3 – 9). Although the concentration of mannosan is about ten times lower than the concentration of levoglucosan a high correlation between this two anhydrosugars can be observed. The ratio between levoglucosan and mannosan during winter pools (VO 3 – VO 8) ranged between 7 and 10.

### 5.5.3 Mineral dust

---

As sampling was carried out with quartz fiber filters, the direct quantification of silicium was not possible. The concentrations of silicium were calculated via the geogenic ratio of aluminum and silicium; this was tested analytically for Leibnitz and Arnfels within the PMInter projects. [7] The amount of mineral dust summarizes silicates and carbonates. Besides natural sources, resuspension or erosions also gritting material, construction activities and agriculture affects the amount of mineral dust. [1], [7] Mineral dust can be preferably found in PM<sub>10</sub> samples or coarse fraction (PM<sub>10-2.5</sub>). [30]

Thus, the atmospheric concentrations of mineral dust underlie fluctuations, the relative contributions show seasonal trends which is shown in Figure 14. The maximum value of mineral dust can be observed within pool VO 8 (31.01.2017), which is caused by high concentrations of calcium (2,0 µg\*m<sup>-3</sup>). The amount of silicates within VO 8 was 1,1 µg\*m<sup>-3</sup> and correlates with concentrations of other pools.

During summer/autumn the relative amounts of mineral dust were higher than during the winter period. The average amount of mineral dust during the winter period was 4 % of PM<sub>10</sub> mass while the average amount during summer/autumn was three times higher. During summer pools (VO 1-2 and VO 10-11) the average of mineral dust was 11 % of PM<sub>10</sub> mass. This is probably a consequence of agricultural works during summer/autumn.

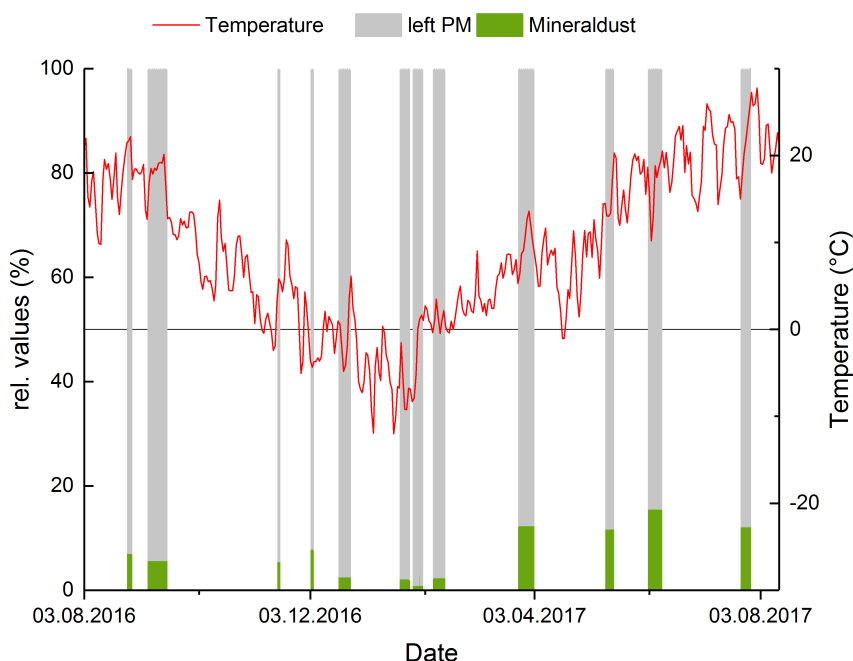


Figure 14: Annual trend of relative values of mineral dust (%) and trend of temperature (°C) – Vorau

#### 5.5.4 Crustal and trace elements

All metals with a density  $> 5 \text{ kg} \cdot \text{dm}^3$  are classified to heavy metals and have negative impacts on human health. Mineral components in particulate matter have both anthropogenic and natural sources; they are emitted through geogenic processes like volcanic eruption, erosion and dust storms. Anthropogenic emissions are for example, the combustion of fossil fuels or metallurgic industry processes. [17] Compared to the  $\text{PM}_{2.5}$  concentration, it is expected that  $\text{PM}_{10}$  samples contain greater amounts of crustal and trace elements. The  $\text{PM}_{10}$  fraction is preferably emitted through erosion, resuspension and abrasive processes and contains a greater amount of aluminum, iron, calcium and other ions. [30]

Within the scope of this study seven metals were quantified for pools at sampling site Vorau. All pools were corrected with the appropriate concentrations of field blanks. Figure 15 shows the relative contributions of quantified metals for the sampling site Vorau ( $\text{PM}_{10}$ ). In view of the fact that a seasonal trend of  $\text{PM}_{10}$  mass could be observed, investigated elements showed differences, respectively no seasonal pattern. The highest portion is contributed to aluminum and concentrations ranged between  $169 \text{ ng} \cdot \text{m}^{-3}$  to  $1435 \text{ ng} \cdot \text{m}^{-3}$ . At some pools also amounts of chromium and barium could be quantified. The concentrations of chromium and barium varied between 5 to  $37 \text{ ng} \cdot \text{m}^{-3}$  respectively 2 to  $15 \text{ ng} \cdot \text{m}^{-3}$ . These variations are independent from seasonal and meteorological impacts. A decreasing trend can be observed for manganese and iron, which reaches its maximum at New Year's Eve. Elevated concentrations of barium were observed at NYE. Because of this fact, the following two days of NYE were handled as special events for sampling sites

in Graz and not summarized with other days. The amount of iron shows high fluctuations which ranged between 27 to 343 ng\*m<sup>-3</sup>. Emission of barium and iron can be caused by anthropogenic processes preferably from traffic related aerosols like brake abrasion or resuspension of road dust. A seasonal trend can be observed for the concentrations of zinc, which reaches its maximum during the winter time. Besides levoglucosan and potassium, also zinc is emitted during the combustion of biomass, but can also be caused by traffic related aerosols like abrasion products from brakes and tires. [31]  
In summary, no clear trend could be seen for any metal; and all quantified metals underlie high variations.

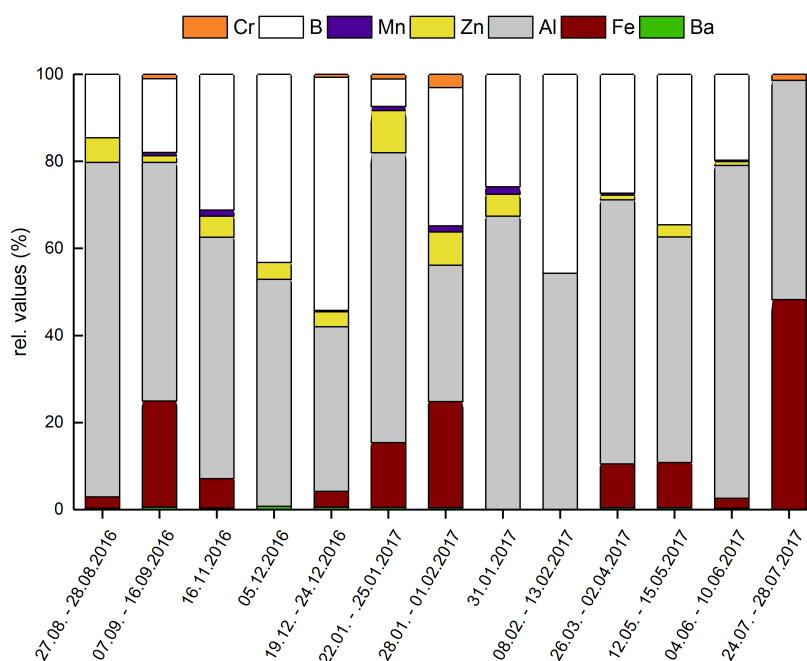


Figure 15: Annual relative contribution (%) of quantified metals for sampling site Vorau (PM<sub>10</sub>)

Previous studies used different methods to classify in crustal or non- crustal emission the method of Crustal enrichment factors was chosen. [17]

To describe the crustal influence of the emissions of crustal and trace elements caused by erosion and resuspension, enrichment factors were calculated. The comparison of element concentrations found in particulate matter with element concentrations in crustal material shows the enrichment relative to the crustal source of the earth. Aluminum is used as reference element for the calculation of CEF and the chemical composition of the upper earth crust was used. [32]

Formula 3: Calculation of crustal enrichment factor [30]

$$CEF = \frac{\left(\frac{C_{i,PM}}{C_{Al,PM}}\right)}{\left(\frac{C_{i,crust}}{C_{Al,crust}}\right)}$$

$C_{i,PM}$  ..... concentration of element i in PM  
 $C_{i,crust}$  ..... concentration of element i in earth crust  
 $C_{Al,PM}$  ..... concentration of Al in PM  
 $C_{Al,crust}$  ..... concentration of Al in earth crust

Figure 16 shows the crustal enrichment factors for quantified elements, they grey drawn line marks a CEF of 10. Summer and winter pools are presented separately, whereas the average CEF of summer pools (VO 1 - 2, VO 10 – 13) is drawn as red line and the average CEF of winter pools (VO 3 – 9) as black line. CEF values greater than 10 mark enriched elemental concentrations relative to the earth's crustal composition. [30]

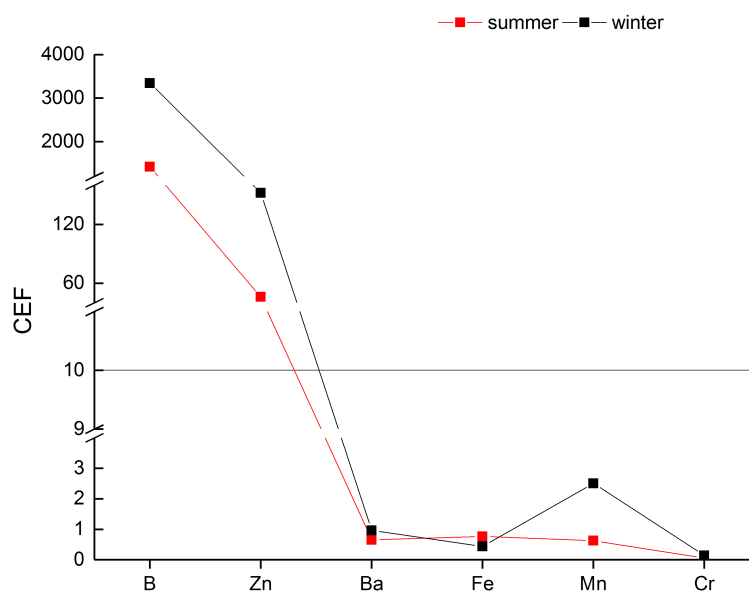


Figure 16: Median crustal enrichment factors (CEF) for  $PM_{10}$  elemental concentrations of sampling site Vorau based on the elemental profile for the primitive mantle of the earth by Taylor et al. The grey drawn line marks a CEF of 10. Red drawn line is the average CEF of summer pools (VO 1-2, VO 10 - 13) while the black drawn line presents the average CEF of winter pools (VO 3-9)

Generally higher CEFs can be observed during winter period than during summer period. Especially high CEFs can be observed for boron and zinc; those high concentrations can be ascribed to non geogenic sources. Sources of these elevated concentrations of boron could be burning of biomass which contains wood preservation agents, the use of flame protection agents or agricultural fertilization.[33] Like already mentioned, an annual trend of zinc can be observed, which can be caused by biomass burning. The CEFs of iron, manganese, barium and chromium ranged below 1 and indicate no enrichment. High barium and iron emission can be attributed to traffic related aerosols like brake abrasion and resuspensions of road dust. [31]

## 5.6 Conclusion - Vorau

Within the project “CleanAir by Biomass” first measurements of quartz fiber filters took place in Vorau from August 2016 to September 2017. This sampling site counted eight exceedances of the  $PM_{10}$  limit value of  $50 \mu g \cdot m^{-3}$ , which occurred during January 2017. To represent the situation of ambient air quality in Vorau, 13 sample pools of  $PM_{10}$  samples were analyzed. To identify the impact of different sources filter were divided into sample pools where the aspect of the occurrence of precipitation was considered. Precipitation cleans the atmosphere and so a lower concentration of PM and other air pollutants can be measured. So, the precipitation of the background site at Masenberg (1260 m) was considered. Because of the different sea levels at these sampling sites (Vorau and Masenberg) and consequently different meteorological conditions, only prominent amounts of precipitation  $> 10 L \cdot m^{-2}$  were respected.

Analysis of several components like elemental carbon (EC), organic carbon (OC), soluble ions, anhydrosugars, humic like substances and polycyclic aromatic hydrocarbons were done. The source apportionment was carried out with the macro-tracer approach which was developed within the AQUELLA and AQUELLIS studies at TU Wien. [1]

The major particle sources, which were effective during pollution periods in Vorau are:

- Secondary inorganic aerosol
- Wood burning aerosol
- Traffic related aerosols and not identified organic material (including HULIS)

The annual trends are summarized in Figure 17; in general, quite similar trends of aerosol which are preferably found during winter, can be observed. An increasing trend of SIA, wood burning aerosol and total PM concentration can be observed during the cold period. On 31.01.2017 the maximum value of SIA was measured with  $58 \mu g \cdot m^{-3}$  (corresponds to 56 % of  $PM_{10}$  mass) and the maximum value of wood burning aerosol was also measured with  $20 \mu g \cdot m^{-3}$  (corresponds to 20 % of total  $PM_{10}$  mass). This was also the day with the maximum  $PM_{10}$  concentration of  $95 \mu g \cdot m^{-3}$  during the whole sampling period. Derived from the concentrations trends of ammonium, nitrate and sulfate a regional transport of air masses may be the source for this high contribution of SIA. The contribution of mineral dust underlies high fluctuations which ranged between 0,6 to  $3,0 \mu g \cdot m^{-3}$  which corresponds to 1 – 16 % of total  $PM_{10}$  mass.

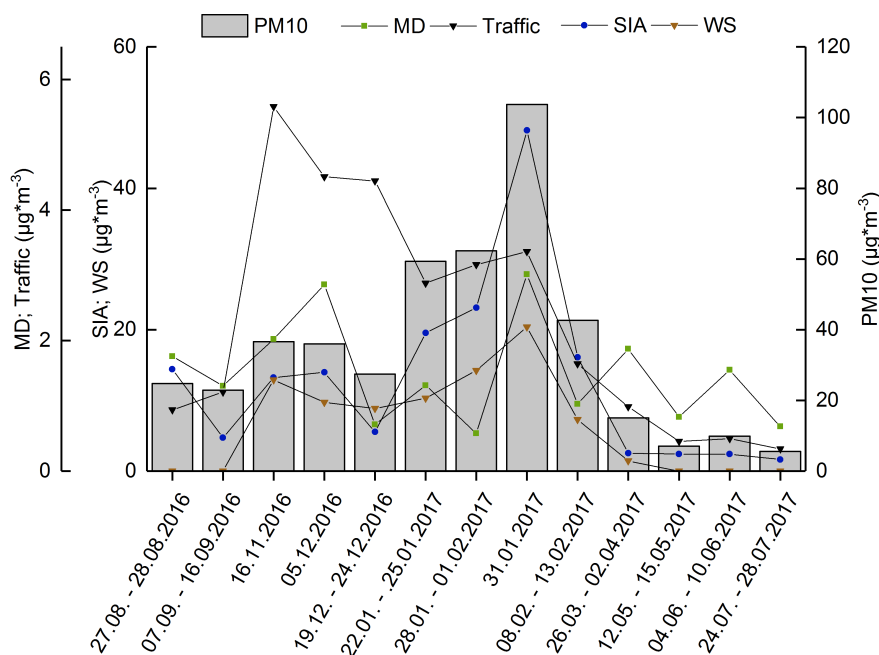


Figure 17: Annual trend of secondary inorganic aerosol, wood burning aerosol, mineral dust and traffic related aerosols (exhaust and abrasion) ( $\mu\text{g}\cdot\text{m}^{-3}$ ) and total  $\text{PM}_{10}$  concentration ( $\mu\text{g}\cdot\text{m}^{-3}$ ) over sampling period - Vorau

To sum up, a clear difference in  $\text{PM}_{10}$  concentrations and the resulting source apportionment, which is shown in Figure 18, can be observed. During winter time, a clear impact of wood burning aerosol and secondary inorganic aerosol can be observed. This can be attributed to lower average temperatures and a higher amount of small scale heating. Furthermore, low temperatures support the formation of semi volatile aerosol components. During summer time an increasing trend of mineral dust and not defined PM can be observed. This can be attributed to a higher impact of agricultural activities and bioaerosols.

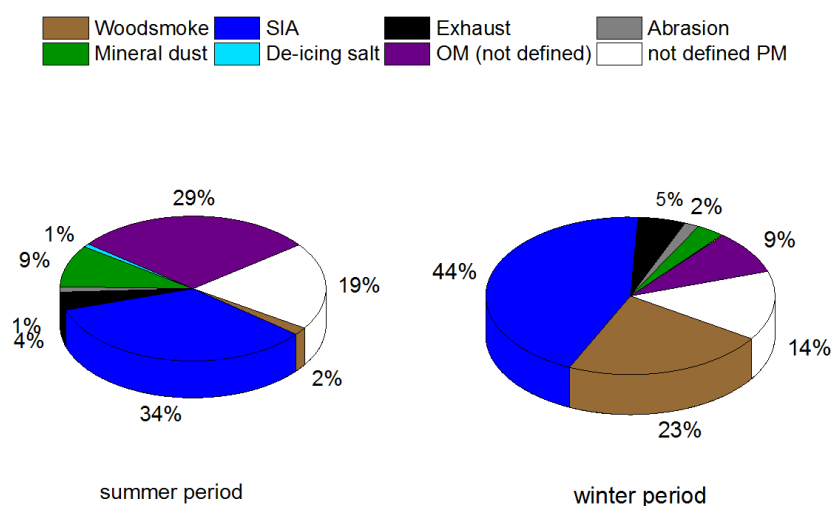


Figure 18: Comparison of the average source apportionment of summer and winter period for sampling site Vorau ( $\text{PM}_{10}$ )

# 6 Sampling site - Graz

## 6.1 PM<sub>10</sub> and PM<sub>2.5</sub> sampling sites in Graz

In the scope of this work, sampling of different particulate matter fractions (PM<sub>10</sub> and PM<sub>2.5</sub>) took place at three sites in Graz, Styria. Sampling was performed by the respective Air Quality Network (Department 17C) of Land Steiermark. Figure 19 shows the three different sampling sites Graz Don Bosco, Graz Süd and Graz Ost. [34]

For quantification PM<sub>2.5</sub> samples of sampling sites Graz Don Bosco and Graz Süd and PM<sub>10</sub> samples of Graz Ost were available.

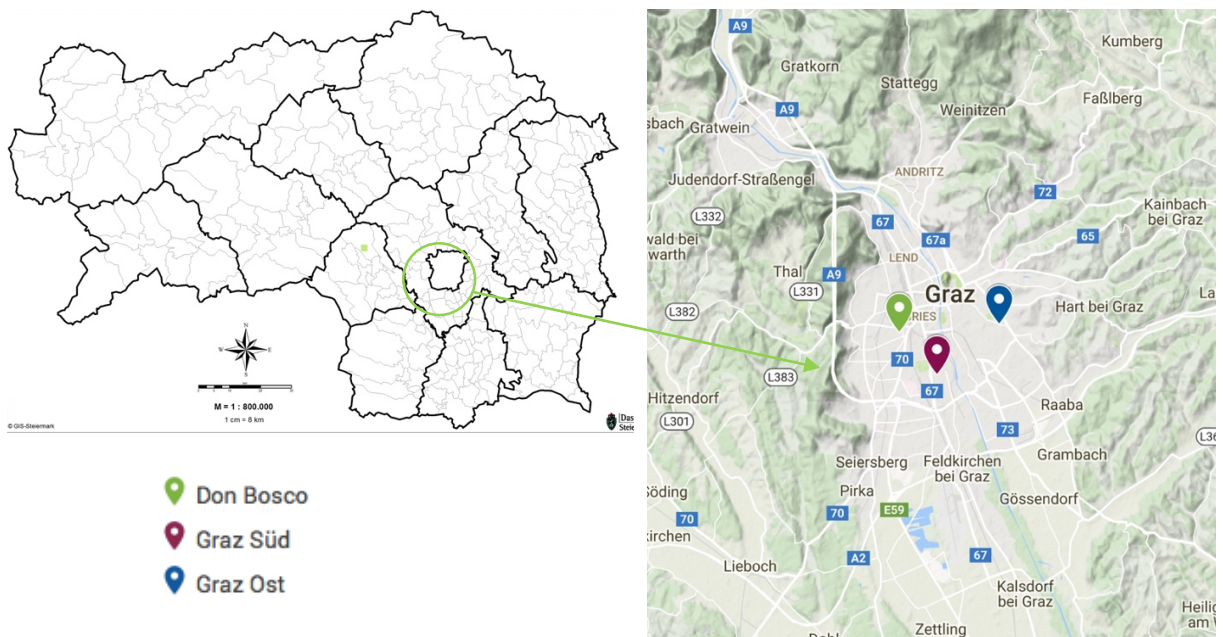


Figure 19: Map of sampling sites in Graz, Austria [34],[27]

## 6.2 Classification of sample pools

---

Gravimetric analysis of the quartz fiber filter was performed by Land Steiermark. After the gravimetric analysis, the filters were folded and stored in PE- bags at -20 °C until they were transferred to TU Wien for further investigations. Due to the fact of several exceedances at the sampling site Graz Don Bosco, the arrangement of the pools was based on the mass concentration  $PM_{10}$  at this site. Chosen pools cover a different number of days, but always the same range of  $PM_{10}$  concentrations. For chemical analysis  $PM_{2.5}$  samples of Graz Don Bosco and Graz Süd and  $PM_{10}$  samples of Graz Ost were available.

For the time period of January and February 2017 following classification was chosen:

- Three pools which characterize days with a maximum concentration of  $PM_{10} > 80 \mu g \cdot m^{-3}$
- Five pools which characterize moderate polluted periods with  $PM_{10}$  concentrations within 50 to  $80 \mu g \cdot m^{-3}$
- Three pools which characterize low polluted periods with  $PM_{10}$  concentrations  $< 30 \mu g \cdot m^{-3}$

Analyses are focused on the sampling site Graz Don Bosco, because there the highest amounts of pollution were observed. To compare the individual time periods which were mentioned before, sample pools of the other two sampling sites were analyzed as well. Therefore, five pools for the sampling site Graz Ost and four pools for the sampling site Graz Süd were quantified. This enables the conclusion if the contribution of all sampling sites in Graz had been similar.

- Furthermore, pools of the time period of March 2017 were analyzed. These pools characterize the situation of ambient air quality after the high polluted period of January and February. In any case the total PM concentrations were lower than  $< 30 \mu g \cdot m^{-3}$ , but still in the cold season. The focus was again set at the sampling site Graz Don Bosco with three pools. For the sampling sites Graz Süd and Graz Ost one pool was analyzed.
- Because of the different situation of ambient air quality caused by fireworks, New Year's Eve was handled as special event. Because of its different contribution of the trace element Barium, the following two days after NYE were named as post NYE pools and represent one pool for each sampling site.

Table 12 lists the chosen sample pools of the sampling sites in Graz. The naming of pS marks the situation of post NYE (02.01. and 03.01.2017).

Table 12: List of sample pools Graz

	PM <sub>10</sub> mass [ $\mu\text{g}\cdot\text{m}^{-3}$ ]	Time period	Graz Don Bosco	Grad Süd	Graz Ost
January and February	50-80	02.01. -03.01.2017	DBpS17	GSps17	GOpS17
	80+	11.01. - 12.01.2017	DB1		
	50-80	18.01. - 21.01.2017	DB2		
	80+	22.01. - 23.01.2017	DB3	GS 3	GO3
	50-80	27.01. - 30.01.2017	DB4		
	80+	31.01. - 02.02.2017	DB5	GS5	GO5
	50-80	09.02. - 17.02.2017	DB6		GO6
	30+	21.02. - 23.02.2017	DB7		
	<30	05.01. - 08.01.2017	DB8	GS8	GO8
	<30	03.02. - 08.02.2017	DB9		
March	<30	24.02. - 28.02.2017	DB10		
	<30	01.03. - 10.03.2017	DBM1	GSM	GOM
	<30	17.03. - 21.03.2017	DBM2		
	<30	27.03. - 31.03.2017	DBM3		
also, blank filters have been analyzed for each period of time					

### 6.3 PM<sub>2.5</sub> and PM<sub>10</sub> concentration trends

Figure 20 shows the daily means of gravimetric measured PM<sub>10</sub> and PM<sub>2.5</sub> concentrations of all sampling sites in Graz. Exceedances of the daily limit value for PM<sub>10</sub> concentration (red line) can mostly be observed at cold temperatures. If temperature increased, the daily means of PM<sub>10</sub> mass were within the limit value for the daily mean of PM<sub>10</sub>.

During the sampling period from 01.01.2017 to 31.03.2017, obvious exceedances of the limit value can be observed. At sampling site Graz Don Bosco, 34 days of exceedance of PM<sub>10</sub> limit value were measured. Already 21 of them occurred during January 2017. For sampling site Graz Süd, 33 days of exceedance during sampling period and 19 of them during January were observed. At sampling site Graz Ost in total 28 days of exceedance were measured, 16 of them occurred in January 2017.

Because of high PM masses caused by fireworks, New Year's Eve was handled as special event. On 01.01.2017 the maximum concentration of  $157 \mu\text{g}\cdot\text{m}^{-3}$  of  $\text{PM}_{10}$  mass was measured at sampling site Graz Don Bosco. On NYE, also higher  $\text{PM}_{10}$  concentrations were observed at the other two sampling sites Graz Süd and Graz Ost. Furthermore, high concentrations of daily means of the  $\text{PM}_{10}$  mass were measured on 23.01.2017. On this day, the  $\text{PM}_{10}$  mass counted  $133 \mu\text{g}\cdot\text{m}^{-3}$  at sampling site Graz Süd, which is lower than on NYE. A higher  $\text{PM}_{10}$  concentration of  $127 \mu\text{g}\cdot\text{m}^{-3}$  was measured on 23.01.2017 than at NYE at sampling site Graz Ost.

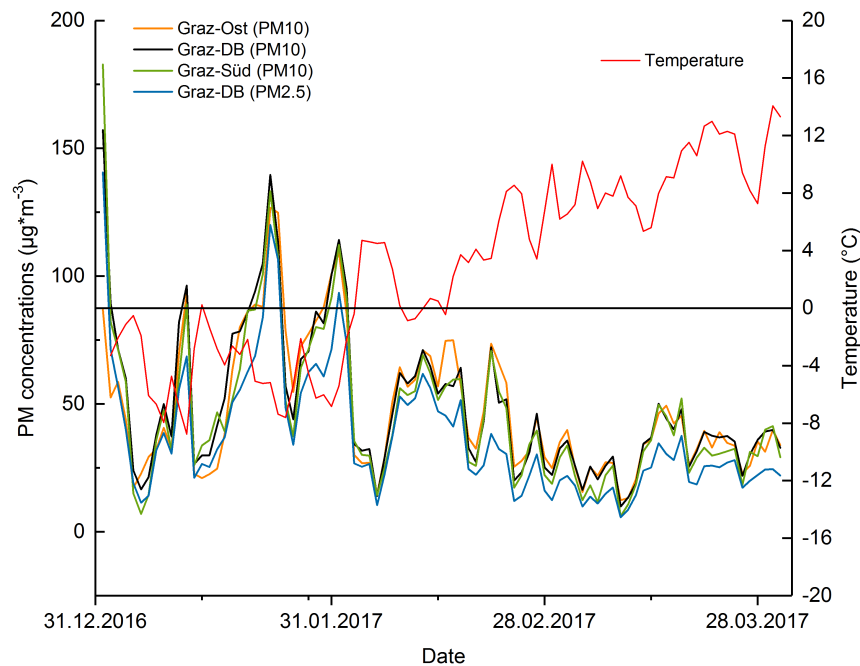


Figure 20: Comparison of  $\text{PM}_{10}$  and  $\text{PM}_{2.5}$  concentrations ( $\mu\text{g}\cdot\text{m}^{-3}$ ) of different sampling sites in Graz and the trend of temperature ( $^{\circ}\text{C}$ )

With minor differences between the sampling sites, the trends of the  $\text{PM}_{10}$  concentrations are quite similar. Especially on days with high concentrations of PM a similarity is visible. Because of this Graz shows a largely constant/similar pollution situation in the spatial scale.

The ratios of the gravimetric measured  $\text{PM}_{10}$  to  $\text{PM}_{2.5}$  concentrations of the sampling site Graz Don Bosco, which reflect the contribution of coarse mode particles, ranged between 1,1 and 1,9. Till 22.02.2017 ratios were by trend lower (1,1 to 1,5) than observed later on (1,3 to 1,9). The highest ratios were measured on the beginning of March, and were represented with the pool DB M1 (01.03. – 10.03.2017).

In January and February 2017 high PM concentrations were measured in most regions of Austria; this was predominately caused by the meteorological situation (low temperature). To show this phenomenon the daily means of  $\text{PM}_{10}$  mass of Graz Don Bosco were compared with the daily means of the background site Bockberg. So, the trend of local and regional pollution by PM can be observed. The sampling site Bockberg (449 m) was

already used as background site within several other studies to describe the regional pollution. [1]

Figure 21 shows the daily means of the PM<sub>10</sub> concentration of the sampling site Graz Don Bosco (black line) and additionally the daily means of PM<sub>10</sub> concentration of the background site Bockberg (grey bars). During the first days of January, the concentration of the background site Bockberg was clearly different than the concentration at Graz Don Bosco (urban impact). Particularly on New Year's Eve a high difference caused by local emissions of fireworks in urban area, can be seen. The increasing concentrations in the time ranges of 11.01. - 12.01.2017, 21.01. – 24.01.2017, 31.01. – 02.02.2017 and 09.02. – 17.02.2017 can be observed at the urban sites as well as at the background site. These similar trends are caused by a pollution episode covering a larger region. In urban area as well as at the background site elevated concentrations can be observed. The background site reached a maximum value of 123 µg\*m<sup>-3</sup> on 23.01.2017.

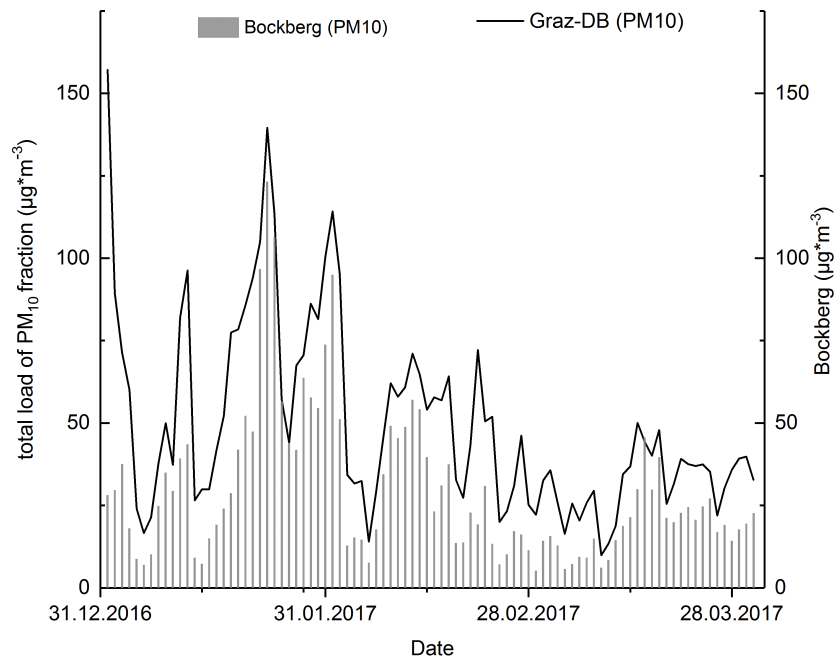


Figure 21: Trend of daily means of PM<sub>10</sub> concentrations (µg\*m<sup>-3</sup>) at Graz Don Bosco as well as the daily means of PM<sub>10</sub> (µg\*m<sup>-3</sup>) of the background site Bockberg

In Figure 22 the PM<sub>10</sub> and PM<sub>2.5</sub> concentrations of the sampling site Graz Don Bosco and the ratio of the continuous measured PM<sub>10</sub> mass of Graz Don Bosco to Bockberg (grey bars) are shown. The red highlighted area marks ratios between 1,0 and 1,5. Ratios within this area mark similar PM concentrations on the urban and the background site. Which means that the PM<sub>10</sub> concentration of Graz Don Bosco was maximum 1,5 times as high as at the background site.

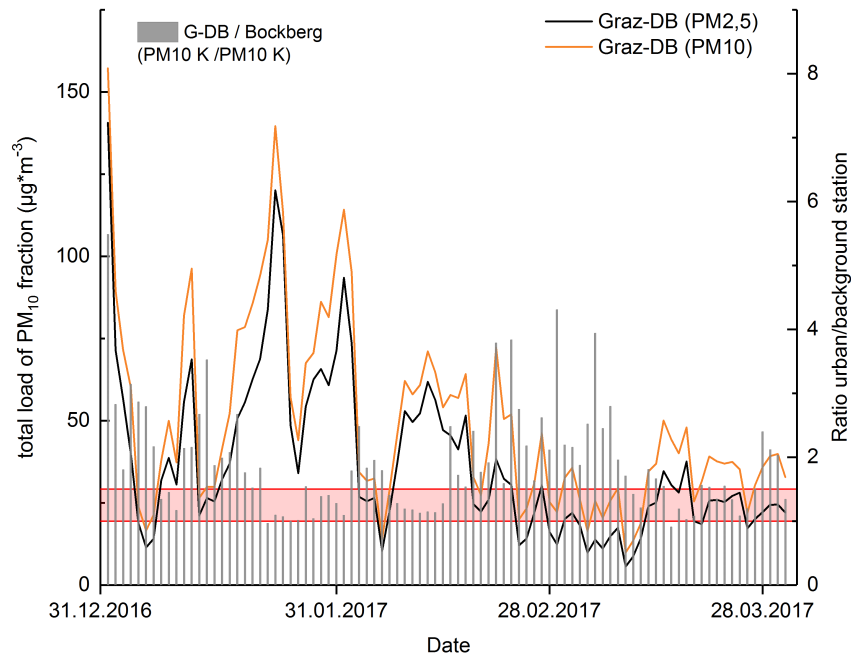


Figure 22: Daily means of  $PM_{10}$  and  $PM_{2.5}$  concentration ( $\mu\text{g}\cdot\text{m}^{-3}$ ) of the sampling site Graz Don Bosco and the ratio of daily means of  $PM_{10}$  concentration of urban and background site. The red highlighted area marks ratios between 1,0 to 1,5.

At the beginning of the time period under investigation clearly different concentrations can be observed at urban and the background site. During the time period of 01.01. – 03.01.2017 the ratios between this two sampling sites ranged between 8 and 3. This marks a much higher PM concentration at the urban site Graz Don Bosco of 140 to 57  $\mu\text{g}\cdot\text{m}^{-3}$ , while lower concentrations of 28 to 37  $\mu\text{g}\cdot\text{m}^{-3}$  were observed at the background site Bockberg. With increasing time the concentrations adapt to each other and the ratios varied between 0,8 and 1,2 during days with highest PM concentrations. Only one day (with a  $PM_{10}$  concentration  $>80 \mu\text{g}\cdot\text{m}^{-3}$ ) overstepped the red highlighted area. This was the case for the time period of 20.01. – 05.02.2017, with  $PM_{10}$  concentrations  $> 50 \mu\text{g}\cdot\text{m}^{-3}$ . Noticeable high ratios were measured 02.03.2017 and 06.03.2017. They are included in the Pool DB M1 which describes a time period of 01.03. – 10.03.2017. Generally, precipitation leads to a cleaning effect of the atmosphere and decreasing concentrations of PM. So, the comparison of periods with different ratios between urban and background site was possible.

Like already mentioned NYE marks a special case with a high pollution situation caused by fireworks. So, the pollution in urban area was higher than at the background site which marks an urban pollution situation.

In summary at the beginning of the sampling period quite different  $PM_{10}$  concentrations of the sampling sites Graz Don Bosco and Bockberg can be observed. Quite different ratios can especially be noticed on days with relatively low  $PM_{10}$  concentrations. At days with especially high  $PM_{10}$  concentrations, a similar pollution occurred at Graz Don Bosco and Bockberg.

The classification of sampling pools was carried out on the basis of different  $PM_{10}$  concentrations which were measured at sampling site Graz Don Bosco. In Figure 23 shows the concentrations of  $PM_{10}$  and  $PM_{2.5}$  mass of Graz Don Bosco. The light grey and dark grey highlighted areas mark the time periods of selected sampling pools.

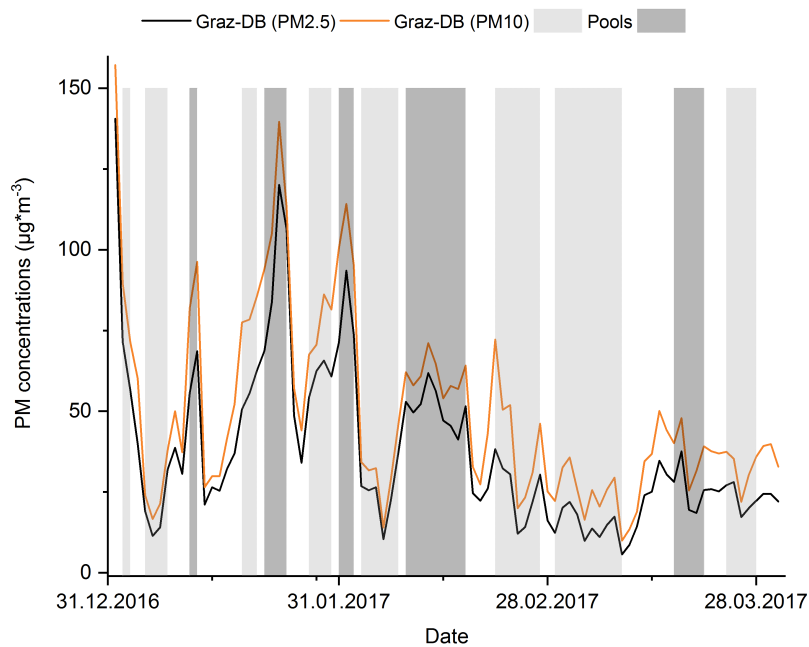


Figure 23: Temporal trend of  $PM_{10}$  and  $PM_{2.5}$  concentrations ( $\mu\text{g}\cdot\text{m}^{-3}$ ) at sampling site Graz Don Bosco and time periods of chosen sample pools

The selected pools of the sampling site Graz Don Bosco covered different  $PM$  concentrations. A lower number of pools, which cover the same time periods as chosen for Graz Don Bosco, were taken of the sampling sites Graz Ost and Graz Süd. So, the comparison of the different sampling sites among the same time periods was possible.

## **6.4 Source apportionment with macro-tracer approach - Graz**

---

This chapter comprises the results of source apportionment with the macro-tracer approach. All concentrations and the calculated source contributions are listed in the Annex.

Because of the before mentioned classification three different situations can be discussed for January and February 2017. These are pools with high loads, mid loads and low loads of  $PM_{10}$  concentration. The classification was carried out on basis of the  $PM_{10}$  concentrations of the sampling site Graz Don Bosco. A fourth group of samples characterizes the situation of March 2017. Additionally, pools of New Year's Eve (2016 & 2017) were analyzed and discussed as a special event.

It has to be kept in mind, that the quantification of  $PM_{2.5}$  concentration was carried out of the sampling sites Graz Don Bosco and Graz Süd and of the  $PM_{10}$  concentration of the sampling site Graz Ost. Because of these different trends in source apportionment can be seen.

### **6.4.1 Days with maximum PM concentrations (January and February)**

#### **(Sample pools which characterize $PM_{10}$ concentrations $> 80 \mu g \cdot m^{-3}$ – Graz Don Bosco)**

---

This group includes three pools of sampling site Graz Don Bosco: DB 1, DB 3 and DB 5. The average daily means of  $PM_{10}$  concentration are for DB1  $88 \mu g \cdot m^{-3}$ , for DB3  $114 \mu g \cdot m^{-3}$  and for DB5  $96 \mu g \cdot m^{-3}$ . Two pools of sampling sites Graz Süd (GS3, GS5) and Graz Ost (GO3, GO5) which cover same time periods as DB3 and DB5, were measured within this group.

The quantification of  $PM_{2.5}$  samples was carried out for the sampling sites Graz Don Bosco and Graz Süd. This fraction is a subset of  $PM_{10}$  and thus shows lower mass concentrations. The ratios of gravimetric measured  $PM_{10}$  to gravimetric measured  $PM_{2.5}$  concentration ranged between 1,2 to 1,4 for selected pools of sampling site Graz Don Bosco. A clear difference can be observed at DB1 where the amount of  $PM_{10}$  mass was very high.

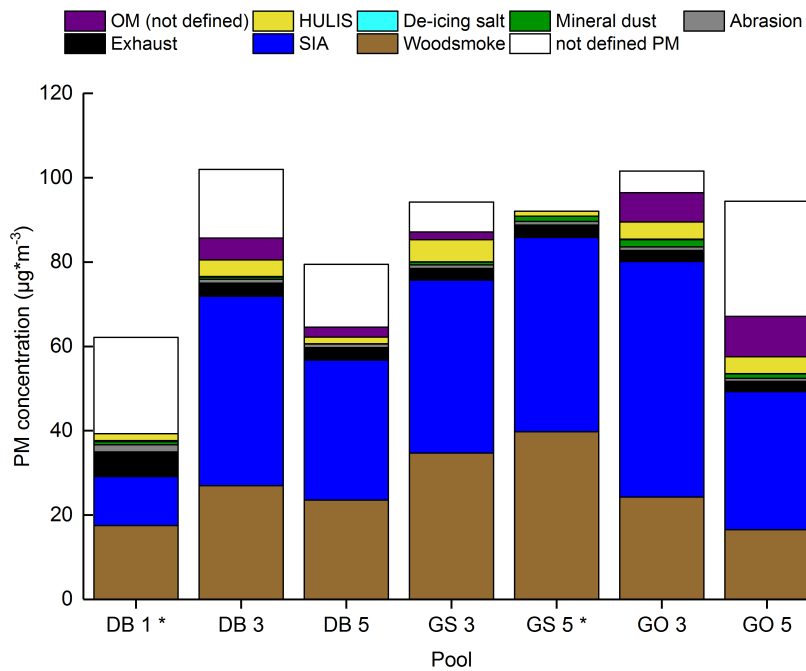


Figure 24: Presentation of pools with  $PM_{10}$  concentrations  $> 80 \mu g * m^{-3}$  for Graz Don Bosco ( $PM_{2.5}$ ), Graz Süd ( $PM_{2.5}$ ) and Graz Ost ( $PM_{10}$ )

Figure 24 shows the concentrations observed for pools with  $PM_{10}$  concentrations  $> 80 \mu g * m^{-3}$  while Figure 25 shows the relative contribution of pollution categories. The absolute PM concentrations ranged from 62 to  $102 \mu g * m^{-3}$ . Only for pools of the sampling site Graz Ost the concentration of mineral dust is noticeable. The reason for this is that at the sampling site Graz Ost analysis was carried out of the  $PM_{10}$  samples, while the quantification for the  $PM_{2.5}$  samples for the other sampling sites Graz Don Bosco and Graz Süd was carried out. With exclusion of DB 1 and GO 5 the macro-tracer approach enabled the characterization of mostly 80 % of the total PM. Pools which are marked with a \*, like GS 5\*, highlight an overestimation of the overall mass by the calculation. The overestimation at pool GS 2\* counted 29 %, which means, that the macro-tracer approach calculated 29 % more mass, than gravimetrically determined. Such overestimations occurred only at pools of the sampling site Graz Süd and was always connected to a relative high amount of wood burning aerosol. It cannot be excluded, that the model calculation of the macro-tracer approach overestimates the amount for this sampling site. In case of pool DB 1\*, the recovery was lower. This pool is marked with \* because the calculation of wood burning aerosol led to an overestimation of organic material. For this pool, the macro-tracer approach enabled the characterization of 64 % of total PM. Also, the contribution of sources of particulate matter distinguishes DB 1 from the other pools of this period. Because of already mentioned differences (the difference of the ratio of  $PM_{10}$  concentrations of the urban and background site as well as elevated fraction of coarse mode particles), DB 1 is discussed separately.

Comparison of sampling sites Graz Don Bosco and Graz Süd

Both figures show (except DB 1) a predominance of secondary inorganic aerosol. The pools GS 3, GS 5, GO 3 and GO 5 cover the same time period as DB 3 and DB 5. So, for this time period measurements of all three sampling sites were available. The absolute concentrations of secondary inorganic aerosol for the pools of sampling site Graz Don Bosco ranged between 45 to 33  $\mu\text{g}\cdot\text{m}^{-3}$ , which represented a contribution of 42 – 44 %. The ratios of Graz Süd were slightly higher but quite similar with absolute concentrations of 41 – 46  $\mu\text{g}\cdot\text{m}^{-3}$  which represented a contribution of 43 – 65 %.

Wood burning aerosol constituted the second important particle source. At all sampling sites, over 20 % of total PM were attributed to wood burning aerosol. The relative contributions ranged between 26 – 30 % for sampling site Graz Don Bosco and 37 – 56 % for sampling site Graz Süd. Absolute concentrations varied between 24 – 27  $\mu\text{g}\cdot\text{m}^{-3}$  and 35 – 40  $\mu\text{g}\cdot\text{m}^{-3}$ , so higher concentrations can be observed at sampling site Graz Süd.

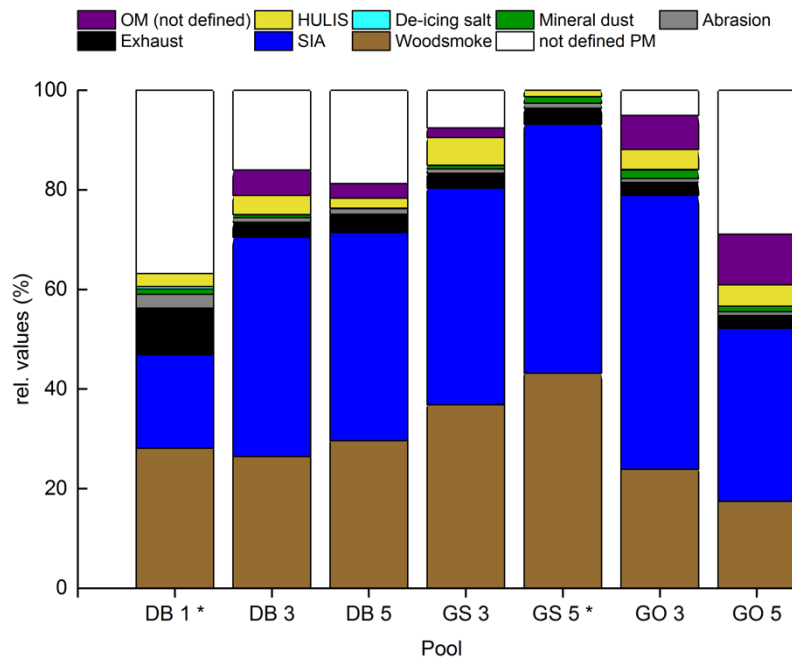


Figure 25: Presentation of source apportionment with  $\text{PM}_{10}$  concentrations  $> 80 \mu\text{g}\cdot\text{m}^{-3}$  for sampling site Graz Don Bosco ( $\text{PM}_{2.5}$ ), Graz Süd ( $\text{PM}_{2.5}$ ) and Graz Ost ( $\text{PM}_{10}$ )

The contributions of traffic related carbonaceous aerosol (exhaust and abrasion) were lower and contributed 4 % for Graz Don Bosco, 4 – 5 % for Graz Süd. For a complete evaluation, it has to be considered that an essential amount of nitrates which is formed of the precursor  $\text{NO}_x$  is contributed to SIA. These  $\text{NO}_x$  emissions are particularly caused by traffic related aerosols. [31], [35]

The contribution of humic like substances and not defined organic material varied between 3 – 6 %. The amounts of mineral dust are contributed to maximum of 1 % at sampling site Graz Don Bosco.

To sum up no clear difference of the importance of particle sources at days with maximum  $PM_{10}$  concentrations  $> 80 \mu g \cdot m^{-3}$  can be observed between the sampling sites Graz Don Bosco and Graz Süd.

#### Comparison of sampling site Graz Don Bosco with Graz Ost

In comparison, higher absolute concentrations and relative contributions of SIA were measured at sampling site Graz Ost ( $PM_{10}$ ). They ranged between  $33 - 56 \mu g \cdot m^{-3}$  (35 – 55 %) for SIA and  $16 - 24 \mu g \cdot m^{-3}$  (17 – 24 %) for wood burning aerosol. The amount of traffic related aerosols (exhaust and abrasion) varied between  $3 - 4 \mu g \cdot m^{-3}$  (3 %) and the amount of mineral dust accounted  $1 \mu g \cdot m^{-3}$  (1 %). The measured concentration for humic like substances was  $4 \mu g \cdot m^{-3}$  (4 %) and the amount of not defined organic material ranged between  $7 - 10 \mu g \cdot m^{-3}$  (5 – 7 %). The predominance of SIA followed by wood burning aerosol can also be found at this sampling site Graz Ost. The contribution of not defined organic material, humic like substances and traffic related aerosols complete the dominant particle sources at this sampling sites. Particle sources which occur preferably in the so called coarse fraction ( $PM_{10-2.5}$ ) can be clearly detected in the analyzed  $PM_{10}$  samples.

#### Specific characteristic of DB 1

DB 1 is the only pool of this period where a predominance of wood burning aerosol was detected. The absolute concentration was slightly lower than in following pools of sampling site Graz Don Bosco and Graz Süd; but the relative contribution (28 %) was similar to the results of DB 3 and DB 5. There was a noticeable low contribution of secondary inorganic aerosol (19 %) and a high contribution of traffic related aerosols (exhaust and abrasion: 12 %). Also, some impact of de-icing salt (0,5 % of total PM mass) can be observed at DB 1. Still this amount is negligible, as earlier studies considered this contribution only if the impact was at least 1 % of total PM mass. [1] These results correlate with the before mentioned trend of increasing  $PM_{10}$  concentration at sampling site Graz Don Bosco. Within this time period (DB 1: 11.01. – 12.01.2017) a higher increase of  $PM_{10}$  mass at the urban site than at the background site Bockberg can be observed. So, DB 1 represents a dominant contribution of urban particle sources, while the impact of SIA, which represents the regional transport of air pollutants, decreases. So, the first pollution peak (11.01. – 12.01.2017) is caused by local sources and clearly different to following episodes. Similar differences of days with high PM concentrations in Graz were observed in earlier projects (report LU-08/07). [1]

### 6.4.2 Days with medium PM concentrations (January and February)

#### (Sample pools, which characterize PM<sub>10</sub> concentration between 50 - 80 µg\*m<sup>-3</sup> – Don Bosco)

This group includes five pools of sampling site Graz Don Bosco: DB pS17, DB2, DB4, DB6 and DB7. The average daily means of PM<sub>10</sub> concentration for DB pS17 were 76 µg\*m<sup>-3</sup>, for DB2 79 µg\*m<sup>-3</sup>, for DB4 72 µg\*m<sup>-3</sup>, for DB6 57 µg\*m<sup>-3</sup> and for DB7 57 µg\*m<sup>-3</sup>. For sampling site Graz Süd only one pool GS pS17, representing the time period of DB pS17, was analyzed. Two pools of sampling sites Graz Ost (GO pS17 and GO 6) which cover the time periods of DB pS17 and DB 6 were analyzed. Pools with the identification “pS” mark the situation of the two days after NYE (02.01. and 03.01.2017). Because of their different contribution of elements caused by fireworks (especially Barium) they were summarized to one pool and not associated with following days.

The quantification of PM<sub>2.5</sub> samples was carried out for the sampling sites Graz Don Bosco and Graz Süd. The ratios of gravimetric measured PM<sub>10</sub> to gravimetric measured PM<sub>2.5</sub> concentration ranged between 1,1 to 1,7 for selected pools of sampling site Graz Don Bosco.

The macro-tracer approach enabled the characterization of at least 79 % of measured particulate matter. Pool GS pS17 was overestimated, caused by the calculation + 6 % were contributed to particle sources.

The absolute concentrations of pools with medium PM<sub>10</sub> concentration within 50 to 80 µg\*m<sup>-3</sup> are shown in Figure 26, while Figure 27 shows the relative contributions of these pools.

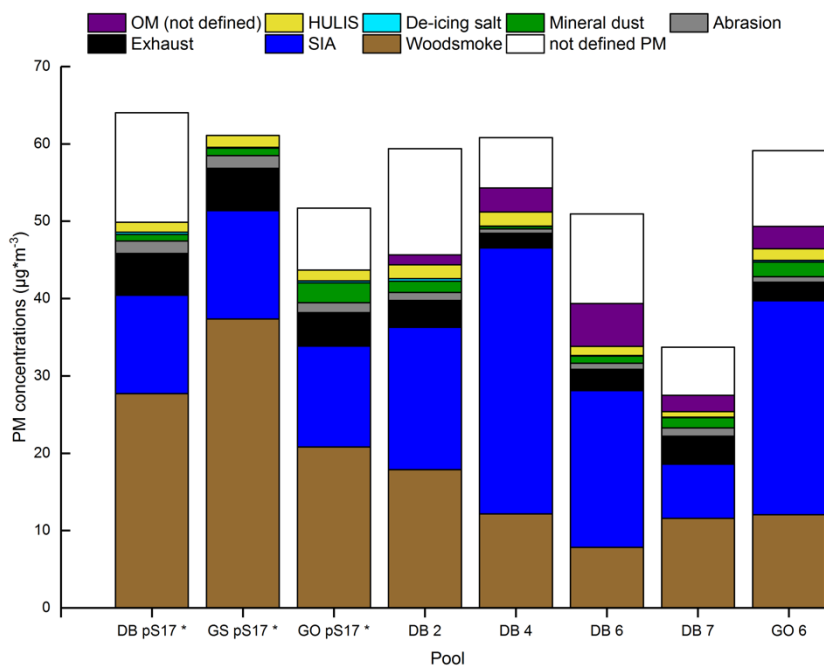


Figure 26: Presentation of source apportionment with PM<sub>10</sub> concentrations within 50 - 80 µg\*m<sup>-3</sup> for sampling site Graz Don Bosco (PM<sub>2.5</sub>), Graz Süd (PM<sub>2.5</sub>) and Graz Ost (PM<sub>10</sub>)

Comparison of sampling sites Graz Don Bosco and Graz Süd

DB pS17, GS pS17 and GO pS 17 characterize the situation post New Year's Eve (02.01 – 03.01.2017). DB 2 to DB 7 characterize the mid load pools of time period of January and February. The comparison of the pools of sampling site Graz Don Bosco showed a decreasing trend of  $PM_{2.5}$  concentration as well as a decreasing trend of wood burning aerosol. DB 7 shows the lowest PM concentration of  $57 \mu g \cdot m^{-3}$  of all pools in this section. Only DB 7, the latest pool of this time period, showed a higher concentration of wood burning aerosol ( $12 \mu g \cdot m^{-3}$ ; 34 %) which is similar to DB 4 ( $12 \mu g \cdot m^{-3}$ ; 20 %). On the contrary to the decreasing trend of wood burning aerosol an increasing trend of secondary inorganic aerosol can be observed. Furthermore, no explicit predominance of SIA or wood burning aerosol can be detected. For all pools of sampling site Graz Don Bosco, the concentrations of wood burning aerosol ranged between  $8 - 18 \mu g \cdot m^{-3}$  which corresponds a relative contribution of 15 – 34 %. The concentrations of secondary inorganic aerosol varied between  $7 - 34 \mu g \cdot m^{-3}$  which corresponds a relative contribution of 21 – 57 %. After consideration of the time line a predominance of wood burning aerosol can be seen during the first days of January. Later on, the contribution of secondary inorganic aerosol increased. The concentrations of traffic related aerosols ranged between  $2 - 5 \mu g \cdot m^{-3}$  which corresponds a contribution of 4 – 14 %. During time an increasing contribution can be observed till the end of February. The contributions of HULIS, not defined organic material and mineral dust varied between 2 -3, 1 – 7 and 2 – 4 %.

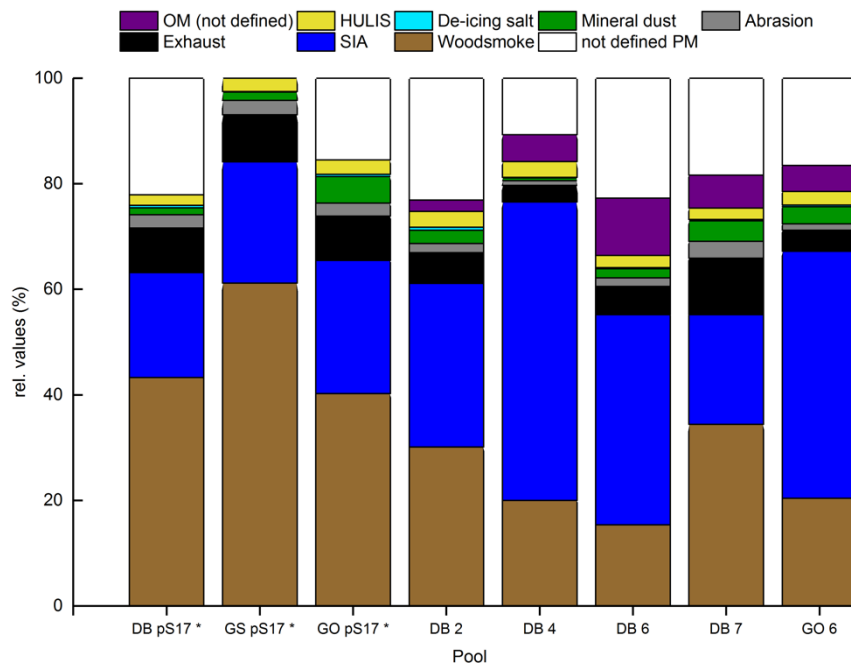


Figure 27: Presentation of source apportionment with  $PM_{10}$  concentrations within  $50 - 80 \mu g \cdot m^{-3}$  for sampling site Graz Don Bosco ( $PM_{2.5}$ ), Graz Süd ( $PM_{2.5}$ ) and Graz Ost ( $PM_{10}$ )

Specific characteristic of post NYE (02.01. and 03.01.2017)

In every case of the post New Year's Eve pools secondary inorganic aerosols captured about 20% of total PM. The contribution of traffic related aerosols counted about 10 %. Noticeable was the high contribution of wood burning aerosol which lead to an overestimation of pools. Because of this, all three post New Year's Eve pools are marked with \*; the overestimation varied between 1 – 7 % of the total concentration of PM. This is caused by the high portion of wood burning aerosol, which is calculated out of the concentration of levoglucosan. This overestimation might be due the conversion factor which is not adopted do special events like fireworks. Yet there is no literature data available which describes the levoglucosan trends during fireworks. Still this situation is very special, the chemical analysis of trace elements differs at New Year's Eve and post NYE pools from the other days. There was also a contribution of humic like substances which ranged between 2 – 3 %. The macro-tracer approach enabled the characterization of 78 to 106% of PM mass measured at the appropriate sampling site. On average about 10% of total PM were contributed to the traffic related aerosols (exhaust and abrasion). Special events like NYE and the following days do not represent regional pollution problems. The macro-tracer approach is not optimized for local events like this, so apportionment is flawed with some uncertainty.

Comparison with the sampling site Graz Ost

A noticeable amount of mineral dust can be observed at all pools of sampling site Graz Ost. Graz Ost is the only sampling site where the PM<sub>10</sub> samples were provided for analysis.

The contribution of pools of sampling site Graz Ost is quite similar to Graz Don Bosco. Only noticeable amounts of sources which preferably occurs in PM<sub>10</sub> samples of PM was found.

**6.4.3 Days with proportionally low PM concentrations (January and February)****(Sample pools, which characterize PM<sub>10</sub> concentrations < 30 µg\*m<sup>-3</sup> – Don Bosco)**

---

Despite the general high PM concentrations during January and February 2017, there were also some days with PM concentrations < 30 µg\*m<sup>-3</sup>. To describe this situation, three pools of sampling site Graz Don Bosco (DB 8, DB 9 and DB 10) were chosen. The average daily means of PM<sub>10</sub> concentration accounted for DB 8 24 µg\*m<sup>-3</sup>, for DB 9 28 µg\*m<sup>-3</sup> and for DB 10 27 µg\*m<sup>-3</sup>. Respectively one pool describes the situation at the other two sampling sites Graz Süd (GS 8\*) and Graz Ost (GO 8) which cover the same time periods as DB 8 (05.01. – 08.01.2017).

The ratios of gravimetric measured  $PM_{10}$  to gravimetric measured  $PM_{2.5}$  concentrations ranged between 1,1 to 1,4 for selected pools of sampling site Graz Don Bosco. The macro-tracer approach enabled the characterization of 59 – 86 % of PM mass. GS 8\*, which is highlighted with \* marks an overestimation of 20 %. Again, the overestimation only occurred at sampling site Graz Süd, because of the high amount of wood burning aerosol determined by the macro-tracer approach.

To represent the pollution situation of PM concentrations  $< 30 \mu\text{g}\cdot\text{m}^{-3}$  three pools of the sampling site Graz Don Bosco are presented in Figure 28 while Figure 29 shows the relative contribution of particle sources.

### Results for the sampling site Graz Don Bosco

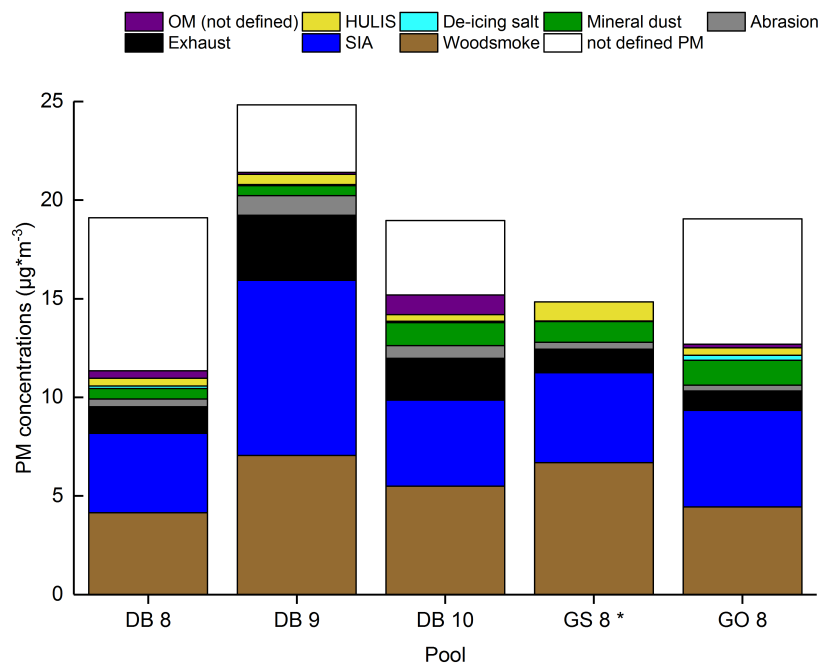


Figure 28: Presentation of source apportionment with  $PM_{10}$  concentrations  $< 30 \mu\text{g}\cdot\text{m}^{-3}$  for sampling site Graz Don Bosco ( $PM_{2.5}$ ), Graz Süd ( $PM_{2.5}$ ) and Graz Ost ( $PM_{10}$ )

Again, a predominance of wood burning aerosol and secondary inorganic aerosol can be observed. The concentrations of wood burning aerosol ranged between  $4 - 7 \mu\text{g}\cdot\text{m}^{-3}$  which corresponds 22 – 29 %. The concentrations of secondary inorganic aerosol varied between  $4 - 9 \mu\text{g}\cdot\text{m}^{-3}$  which corresponds 21 – 36 % of total PM. Therefore, this particle source has a lower impact on days with lower PM concentrations than on days with high PM concentrations. The contribution of traffic related aerosols ranged between 9 – 17 % and is noticeable higher at pools with higher PM concentrations. In every pool, the contribution of mineral dust ranged between 2 – 6 % and the contribution of humic like substances and organic material varied between 2 – 5%.

Comparison with sampling site Graz Süd

The concentrations of secondary inorganic aerosol of sampling site Graz Süd ( $5 \mu\text{g}\cdot\text{m}^{-3}$ ; 37 %) are in line with the concentrations of sampling site Graz Don Bosco. The relative contribution of wood burning aerosol is higher (54 %) but the absolute concentrations are quite similar ( $7 \mu\text{g}\cdot\text{m}^{-3}$ ). These overestimations are caused by an inappropriate conversion factor for this sampling site.

Comparison with sampling site Graz Ost

The results for sampling site Graz Ost corresponds to the expectations. The contribution of mineral dust was 7 %, while it was only 3 % for DB 8.

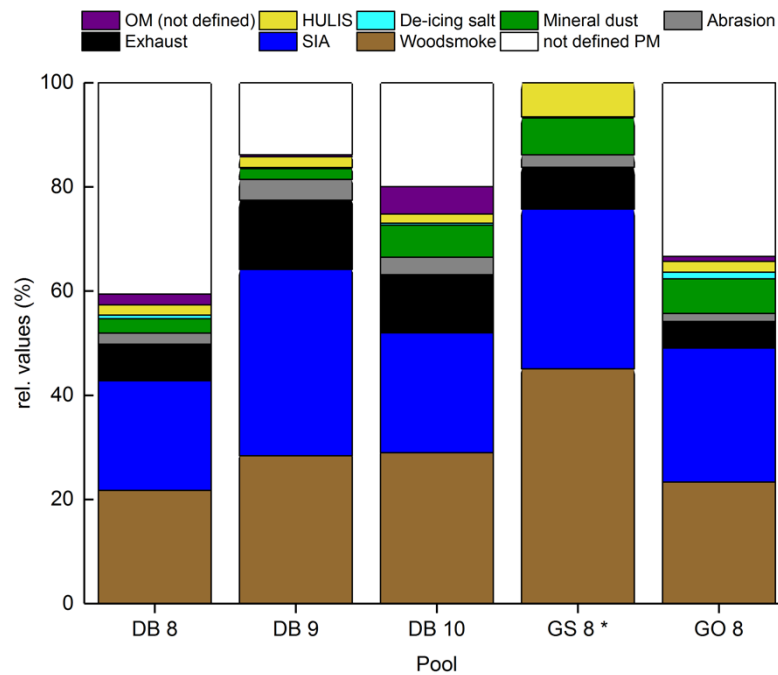


Figure 29: Presentation of source apportionment with  $\text{PM}_{10}$  concentrations  $< 30 \mu\text{g}\cdot\text{m}^{-3}$  for sampling site Graz Don Bosco ( $\text{PM}_{2.5}$ ), Graz Süd ( $\text{PM}_{2.5}$ ) and Graz Ost ( $\text{PM}_{10}$ )

At all three pools of the sampling site Graz Don Bosco less than 40 % of total PM are attributed to wood burning aerosol. In contrast to pools with higher PM concentrations, a higher amount was attributed to traffic related aerosols (exhaust and abrasion). On average, traffic related aerosols contribute to total PM more than 10 %. Furthermore about 25 % of total PM are explained by secondary inorganic aerosols. In case of the pools of other sampling sites a higher amount is contributed to wood burning aerosol than at Graz Don Bosco. 54 % of total PM are contributed to wood burning aerosol at GS 3\* and 23 % at GO 4. GO 4 is the only pool with a visible contribution of de-icing salt. Furthermore GS 3\* and GO 4 are the pools with the lowest PM concentrations of this classification. The total  $\text{PM}_{2.5}$  mass of GS 3\* was  $12 \mu\text{g}\cdot\text{m}^{-3}$  while the total  $\text{PM}_{10}$  mass of GO 4 was  $19 \mu\text{g}\cdot\text{m}^{-3}$ . Different to the three pools of Graz Don Bosco, a higher amount of mineral dust can be observed at GS 3\* (9 %) and GO 4 (7 %). The amount of mineral dust of DB 8, which marks the same time period as GS 3\* and GO 4, was 3 %.

#### 6.4.4 Representation of ambient aerosol concentrations and sources in March

In March, obvious higher temperatures and lower PM concentrations, which were generally below PM concentrations measured in January and February, occurred. Three pools of sampling site Graz Don Bosco (DB M1, DB M2 and DB M3) describe the situation of March.

The average daily means of  $PM_{10}$  concentration accounted for DB M1  $24 \mu\text{g}\cdot\text{m}^{-3}$ , for DB M2  $33 \mu\text{g}\cdot\text{m}^{-3}$  and for DB M3  $34 \mu\text{g}\cdot\text{m}^{-3}$ . For the other two sampling sites Graz Süd (GS M1) and Graz Ost (GO M1) one pool which covers the same time periods as DB M1 (01.03. – 10.03.2017) was chosen.

The ratios of gravimetric measured  $PM_{10}$  to gravimetric measured  $PM_{2.5}$  mass ranged between 1,3 and 1,7 for the selected pools of sampling site Graz Don Bosco. The macro-tracer approach enabled the characterization of 66 – 80 % of PM mass. GS M1\* which is highlighted with \* marks an overestimation of 2 %. Again, the overestimation occurred only at sampling site Graz Süd because of the high amount of wood burning aerosol.

Figure 30 presents the pollution situation at higher temperatures and clearly lower PM concentrations in March. Figure 31 shows the relative contribution of particle sources which have relevant impacts in March.

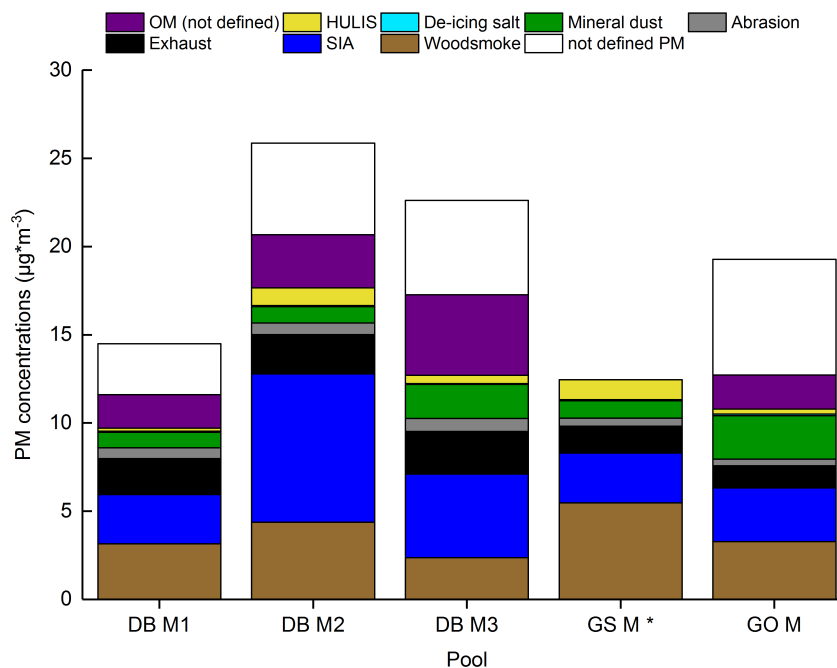


Figure 30: Presentation of source apportionment with  $PM_{10}$  concentrations of March for sampling site Graz Don Bosco ( $PM_{2.5}$ ), Graz Süd ( $PM_{2.5}$ ) and Graz Ost ( $PM_{10}$ )

Results for the sampling site Graz Don Bosco

The pools of the sampling site Graz Don Bosco (DB M1 – 3) almost describe the whole month of March. In comparison of these pools, a decreasing trend of wood burning aerosol can be observed. The absolute concentrations of wood burning aerosol ranged between 2 -4  $\mu\text{g}\cdot\text{m}^{-3}$ , which corresponds to 10 – 22 %. Despite that the contribution of not defined organic material increased. Absolute concentrations varied between 2 – 5  $\mu\text{g}\cdot\text{m}^{-3}$ , which corresponds to 9 – 13 %. Also for secondary inorganic aerosol, a decreasing trend can be observed. The absolute concentrations of SIA ranged between 3 – 8  $\mu\text{g}\cdot\text{m}^{-3}$ , which corresponds a contribution of 19 – 32%. The decrease of wood burning aerosol and secondary inorganic aerosol can be attributed to an increasing trend of temperature. During three pools of March, average temperatures of 8,7 – 11,0 °C occurred. The formation of ammonium nitrate depends on temperature and is preferred at low temperatures. At higher temperatures, there is also a decreasing demand on small scale heating which corresponds to the reduced amount of wood burning aerosol. The contribution of mineral dust also decreases with increasing temperature. The amount, which is contributed to traffic related aerosols (exhaust and abrasion), was higher (3 $\mu\text{g}\cdot\text{m}^{-3}$ , 11 – 18 %) and shows no trend during March.

Finally, the comparison of pools with low PM concentrations during time period of January – February to the pools of March shows a continuously decreasing trend of wood burning aerosol. During January and February, a slowly decreasing trend can be observed, while there was an intense decrease noticeable during March. The contributions of wood burning aerosol decreased from 22 to 10 % during March. Parallel to this an increasing trend of urban sources can be identified from January till March. Urban sources include traffic related aerosols as well as mineral dust. Traffic related aerosols increased from 9 to 14 % while the contribution of mineral dust ranged between 3 to 9 %. The contribution of secondary inorganic aerosol varied between 19 – 36 % from January till March. Whereat on average higher concentrations were measured during January than during March.

The AQUELLA studies show a similarity for the mentioned situation in Graz. The source contributions of the seasonal means of AQUELLA show considerable fluctuations. 2004 there were several exceedances at the sampling site Graz Don Bosco in winter. These were caused by the increase of wood burning aerosol, humic like substances and secondary inorganic aerosols. [1]

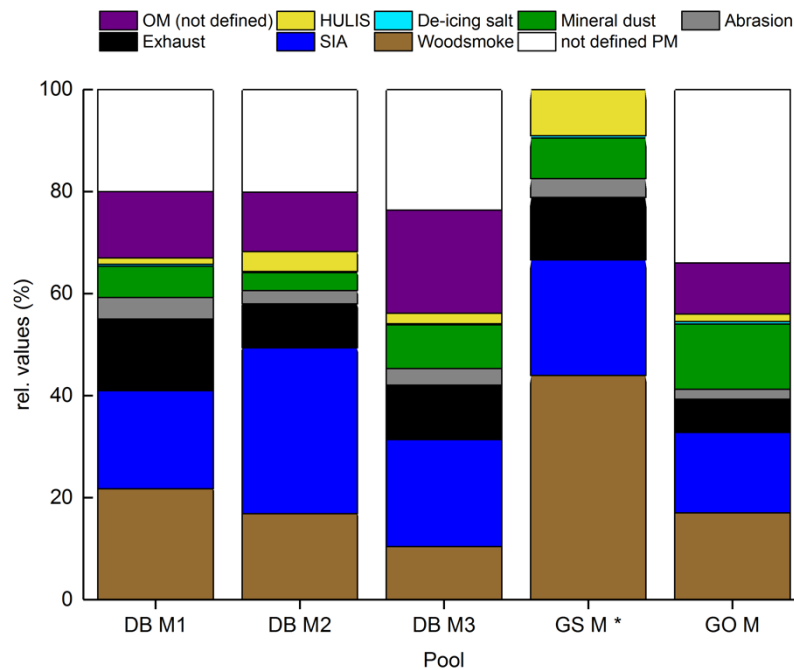


Figure 31: Presentation of source apportionment with  $PM_{10}$  concentrations of March for sampling sites Graz Don Bosco ( $PM_{2.5}$ ), Graz Süd ( $PM_{2.5}$ ) and Graz Ost ( $PM_{10}$ )

#### Comparison of sampling site Graz Don Bosco with Graz Süd

At GS M1\* a noticeable high relative contribution of wood burning aerosol ( $5 \mu\text{g}\cdot\text{m}^{-3}$ ; 44 %) was measured. The comparison with the absolute concentrations shows that this is caused by the especially low  $PM_{2.5}$  concentration ( $12 \mu\text{g}\cdot\text{m}^{-3}$ ) and should not be overrated. Furthermore, in contrast to the sample pools of Graz Don Bosco, several other saccharides than levoglucosan and mannosan were quantified. Besides levoglucosan, also mannosan and galactosan were quantified, which could also indicate additional sources. The contribution of humic like substances was noticeable high with 9 %. GS M1\* is highlighted because an overestimation of organic material occurred; so, the estimation of wood burning aerosol is flawed with an elevated uncertainty.

#### Comparison of sampling site Graz Don Bosco with Graz Ost

Generally, the concentrations of secondary inorganic aerosol, wood burning aerosol and traffic related aerosols were lower than measured in DB M1 ( $PM_{2.5}$ ), but the contribution of mineral dust was higher at sampling site Graz Ost. The concentration of wood burning aerosol counted  $3 \mu\text{g}\cdot\text{m}^{-3}$ , which corresponds to 17 % of total PM. The contribution of secondary inorganic aerosol was 13 % ( $3 \mu\text{g}\cdot\text{m}^{-3}$ ) and the contribution of traffic related aerosols (exhaust and abrasion) accounted 9 % ( $1 \mu\text{g}\cdot\text{m}^{-3}$ ). The concentration of mineral dust was  $13 \mu\text{g}\cdot\text{m}^{-3}$ , which corresponds a contribution of 3 %. The contribution of mineral dust was clearly noticeable at this sampling site, which is caused by the analysis of  $PM_{10}$  samples. The comparison of DB M1, GS M1\* and GO M1 shows a lower contribution of mineral dust (analyzed  $PM_{2.5}$  samples). This phenomenon can also be seen during other pollution periods.

### 6.4.5 Comparison of pools with different ratios PM concentrations between urban and background site

Figure 32 compares two pools of the sampling site Graz Don Bosco with different ratios of PM<sub>10</sub> concentration between urban and background site. DB 3 describes the situation at the end of January (22.01. and 23.01.2017) with a ratio of 1,0; which means quite similar total PM<sub>10</sub> concentrations both sites. The pool DB M1 marks the first ten days of March (01.03. – 10.03.2017) with a ratio of 2,6 between urban and background site. This pool contains days with higher ratios of 4,3 (01.03.2017) and 3,9 (06.03.2017), which mark higher pollutions at the urban sampling site than at the background site. Furthermore, pool DB 3 has an average PM<sub>2,5</sub> mass of 102 µg\*m<sup>-3</sup> and DB M1 14 µg\*m<sup>-3</sup>. The macro-tracer approach enabled the characterization of at least 80 % of the total PM mass.

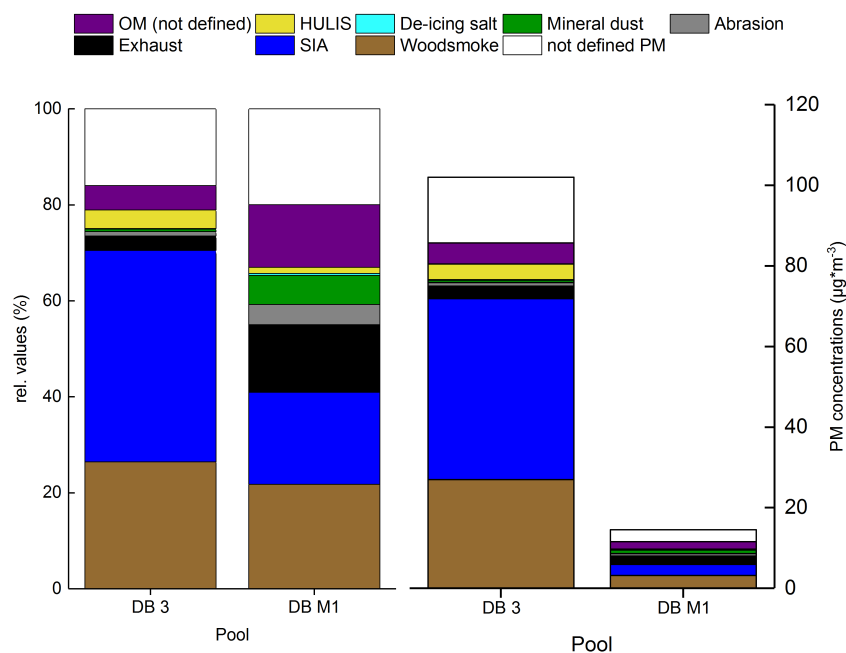


Figure 32: Presentation of source apportionment of pools with different ratios of PM<sub>10</sub> concentrations between urban and background site

Clear differences of source apportionment between these two pools can be seen in Figure 32. The comparison of the absolute concentrations shows a noticeable lower amount of wood burning aerosol during March (3 µg\*m<sup>-3</sup>; 22 %) than during January (27 µg\*m<sup>-3</sup>; 26 %); but the relative contributions were quite similar for both pools. Fluctuations of absolute concentrations as well as for the relative contributions can be observed for secondary inorganic aerosol. The relative contribution of SIA was quite lower during March than during January; the contribution of SIA accounted for DB 3 44 % (45 µg\*m<sup>-3</sup>) while it was 19 % (3 µg\*m<sup>-3</sup>) in DB M1. The relative contribution of traffic related aerosols shows an indirect proportional trend. During March a noticeable higher contribution of 18 % (3 µg\*m<sup>-3</sup>) was detected than in January (4 %; 4 µg\*m<sup>-3</sup>). In January, no contribution of mineral dust could be observed while it increased to 1 % of total PM during March.

The comparison concludes that the pollution of DB 3 is mostly caused by a regional increase of particulate matter and transport of air mass. Low temperatures support the formation of semi volatile aerosol components. Classical urban sources (traffic related aerosols, mineral dust) are less noticeable during January than during March. It has to be kept in mind, that the formation of secondary inorganic aerosol is caused by gaseous precursor substances like  $\text{NO}_x$ ,  $\text{SO}_2$  and  $\text{NH}_3$ , which are emitted in urban area.

#### 6.4.6 Comparison of New Year's Eve 2016 and 2017

Because of the high pollution on New Year's Eve, it was handled as a special event and not combined with other days. To compare the source apportionment two filters of NYE of 2016 and 2017 were analyzed. Generally New Year's Eve 2017 had a much higher total PM concentration ( $141 \mu\text{g}\cdot\text{m}^{-3}$ ) than 2016 ( $89 \mu\text{g}\cdot\text{m}^{-3}$ ). The macro-tracer approach enabled the characterization of 74 % (2016) and 67 % (2017).

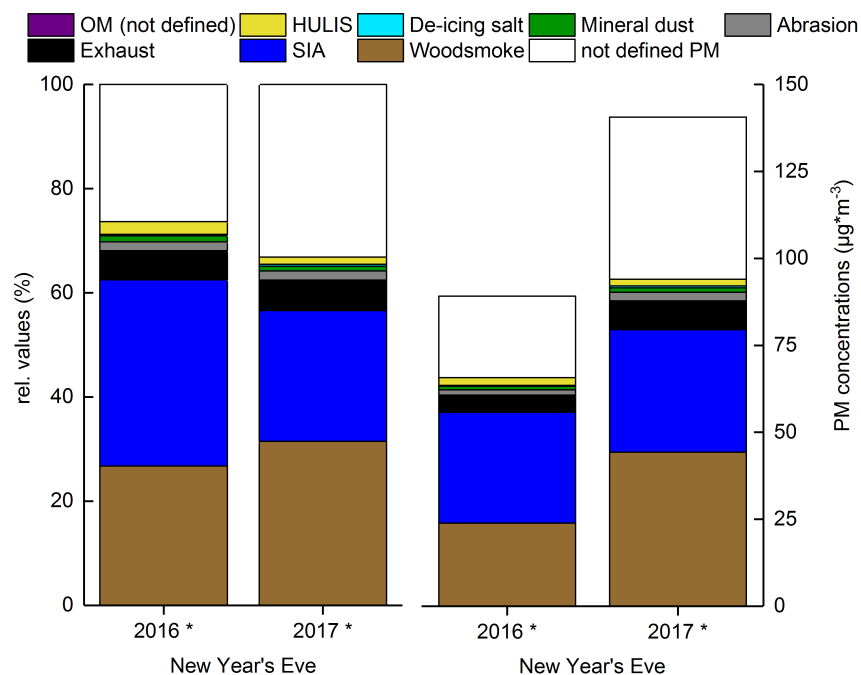


Figure 33: Source apportionment of NYE 2016 and 2017

Besides the source contribution also the total amounts of sources are shown in Figure 33. In both cases 27% (2016) and 32% (2017) of total PM are contributed to wood burning aerosol which corresponds  $24 \mu\text{g}\cdot\text{m}^{-3}$  (2016) and  $44 \mu\text{g}\cdot\text{m}^{-3}$  (2017). Furthermore, a high amount of secondary inorganic aerosols can be observed. At NYE 2016 an amount of 36% ( $32 \mu\text{g}\cdot\text{m}^{-3}$ ) and 2017 an amount of 25% ( $35 \mu\text{g}\cdot\text{m}^{-3}$ ) of total PM is contributed to SIA. The amounts of mineral dust of both years showed a similar trend and captured 1% of total PM. The amount, which is contributed to humic like substances is 4% (2016) and 2% (2017). This corresponds a concentration of  $2 \mu\text{g}\cdot\text{m}^{-3}$  in both cases. Both pools are marked with \*, because no not defined organic material was contributed. This is caused by the high contribution of wood burning aerosol, could also be seen in post NYE pools and was discussed there already.

## 6.5 Polycyclic aromatic hydrocarbons

Because of their persistence and toxicity polycyclic aromatic hydrocarbons play an important role in air quality control. Due to the fact of bioaccumulation, they represent a harm to human or animal health. Generally, PAHs are formed during incomplete combustion processes and are preferably adsorbed at soot particles. [36]

They consist of two or more condensed ring systems and are classified into light and heavy PAHs according to their number of condensed rings. [36], [37]

Because of its high toxicity Benzo(a)pyrene (BaP) is used as a marker substance for air quality control. In human organisms BaP is metabolized to cancerogenic products and influences catalytic biotransformation.[37]

Europe-wide an annual limit value for BaP of  $1 \text{ ng} \cdot \text{m}^{-3}$  in  $\text{PM}_{10}$  samples was set. [5], [38] This value was assumed to Austrian law and is anchored in the IG – L.

Figure 34 shows the absolute values of the marker substance BaP and total  $\text{PM}_{2.5}$  concentrations at sampling site Graz Don Bosco. Higher amounts than  $1 \text{ ng} \cdot \text{m}^{-3}$  can be observed in the time period of January and February. It has to be kept in mind, that the limit value of  $1 \text{ ng} \cdot \text{m}^{-3}$  BaP describes the annual mean value. Although there were some high values measured at the beginning of the year, the annual mean can be maintained. Blue marked bars show pools DB 2 and DB 7 of the sampling site Graz Don Bosco which characterize different ratios between urban and background site.

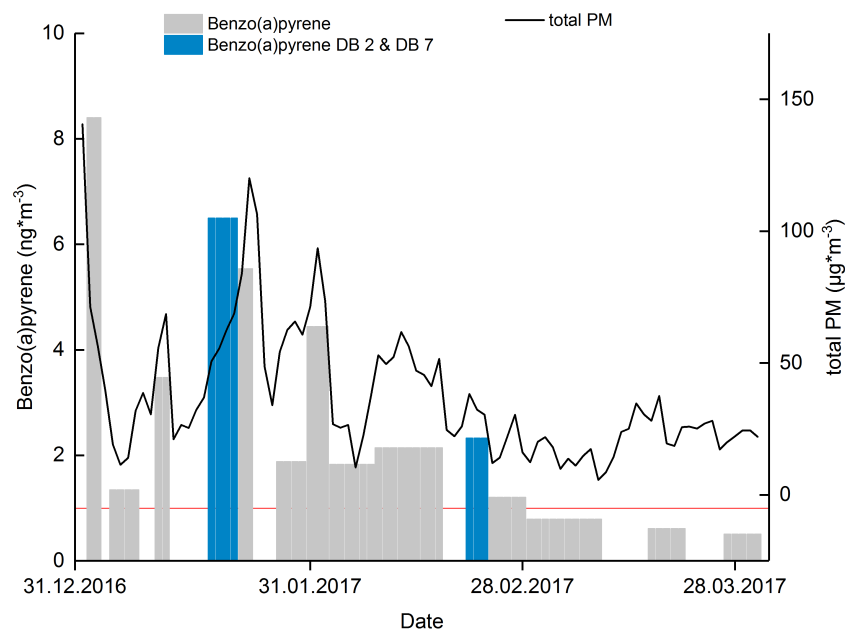


Figure 34: Concentrations of Benzo(a)pyrene ( $\text{ng} \cdot \text{m}^{-3}$ ) and  $\text{PM}_{2.5}$  mass ( $\mu\text{g} \cdot \text{m}^{-3}$ ) at sampling site Graz Don Bosco

Generally, the concentrations of BaP show seasonal trends. These trends depend on the interaction of time trends of emission and dispersion conditions. Main sources for BaP are small scale heating units for biomass and coal as caloric power sites. [6]

In summer, there is a reduced heating demand which correlates with lower BaP concentrations, like they are shown in Figure 34. Noticeable are the already lower concentrations of BaP in March. Generally, a decreasing trend of the concentration of BaP can be observed at all three sampling sites.

The maximum value of  $18 \text{ ng}\cdot\text{m}^{-3}$  was measured at New Year's Eve 2017 and confirms the exceptional pollution caused by fireworks. In contrast to NYE 2017, NYE 2016 showed a remarkably lower concentration of BaP of  $8 \text{ ng}\cdot\text{m}^{-3}$ . The maximum value during the 13 sample pools (except NYE) was measured at DB pS17 with  $9 \text{ ng}\cdot\text{m}^{-3}$ , which describes the two following days after NYE.

Although DB 2 and DB 7 (blue highlighted bars) represent a different ratio of PM concentrations between urban and background site, this trend cannot be seen at the concentrations of BaP. The ratios of  $\text{PM}_{10}$  concentrations accounted 1,9 (DB 2) and 2,5 (DB 7). This means a higher pollution at urban site for both pools. Usually ratios higher than 1 – 1,5 indicate a major influence of local urban sources. The concentration of BaP of DB 2 (18.01. – 21.02.2017) was  $7 \text{ ng}\cdot\text{m}^{-3}$ , while the concentration of BaP of DB 7 (21.02. – 23.02.2017) accounted  $2 \text{ ng}\cdot\text{m}^{-3}$ . Although higher ratios can be observed during later time periods, a decreasing trend of BaP concentration can be observed.

Besides BaP, also levoglucosan is formed during combustion processes. Figure 35 shows the concentrations of levoglucosan and BaP over time for sampling site Graz Don Bosco. The decreasing trend of the concentrations of levoglucosan is in line with the decreasing trend of the concentrations of BaP. At lower temperatures, there is a higher demand of small scale heating, so higher concentrations of levoglucosan and BaP can be measured. At the end of February and March, temperatures clearly over  $0 \text{ }^\circ\text{C}$  were measured and the demand of small scale heating decreased. Increasing temperatures and decreasing combustion leads to decreasing concentrations of combustion tracers levoglucosan and BaP.

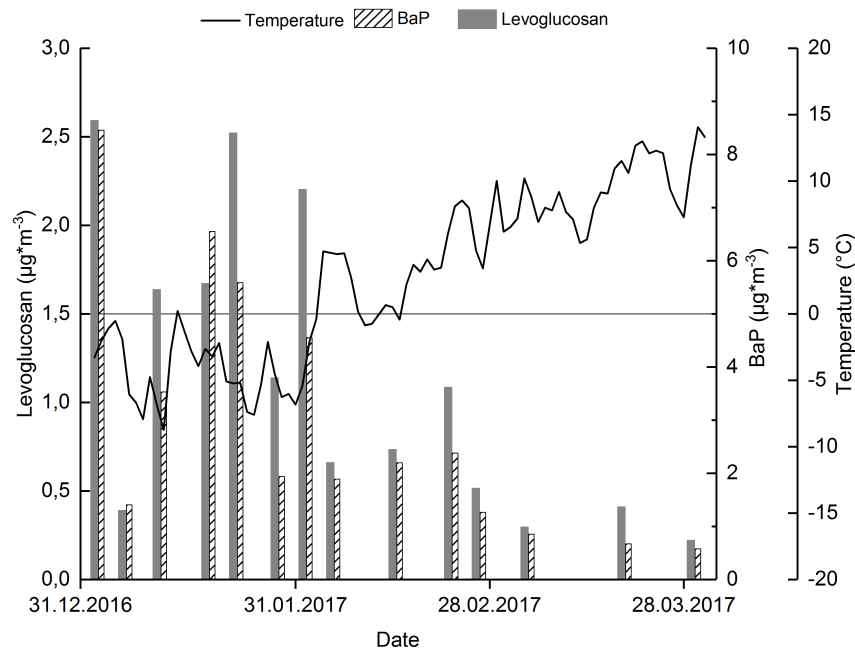


Figure 35: Concentrations of levoglucosan ( $\mu\text{g}\cdot\text{m}^{-3}$ ) and Benzo(a)pyrene ( $\text{ng}\cdot\text{m}^{-3}$ ) over sampling period

Pool DB 1 (11.01. – 12.01.2017) describes the situation at lowest average temperature of  $-8,76\text{ }^{\circ}\text{C}$  and pool DB M3 (27.03. – 31-03.2017) the situation at highest average temperatures of  $+14,05\text{ }^{\circ}\text{C}$  during sampling period. The concentration of BaP while DB 1 was  $4\text{ ng}\cdot\text{m}^{-3}$  and while DB M3  $1\text{ ng}\cdot\text{m}^{-3}$  which marks a clear difference between two pools with different temperature situations.

To determine the situation of ambient air quality based on the concentrations of BaP, every member state of the European Union has to quantify several more PAHs. Within the guideline of EU, five more PAHs have to be measured and they are listed below. [38]

- Benzo (b, k)fluoranthene
- Benzo(j)fluoranthene
- Benz(a)anthracene
- Indeno(1,2,3-c,d)pyrene
- Dibenz(a,h)anthracene

Within the scope of this work Benzo(j)fluoranthene was not quantified, so Benzo(e)pyrene was added additionally.

Figure 36 shows the concentrations of listed PAHs and total PM concentrations for the sampling site Graz Don Bosco over the sampling period.

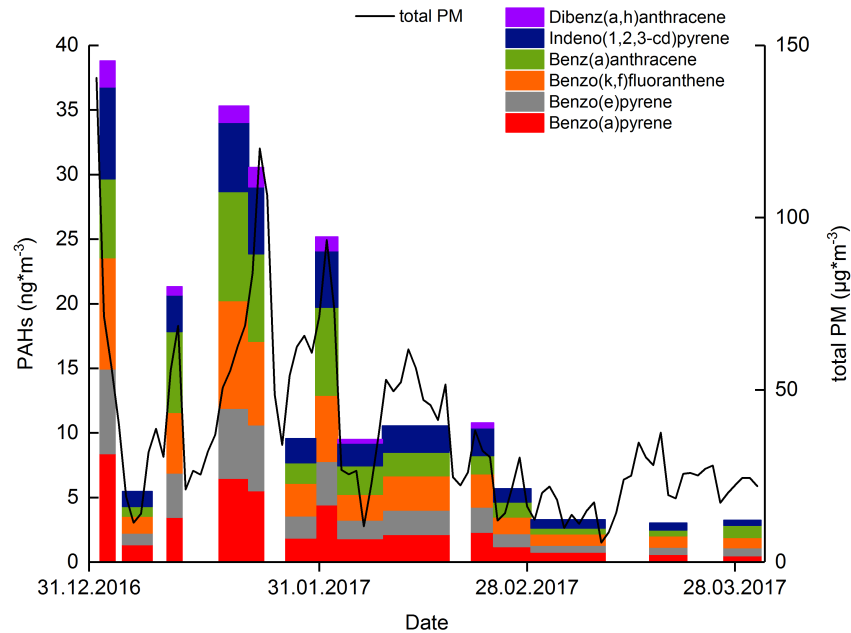


Figure 36: Concentrations of PAHs ( $\text{ng}\cdot\text{m}^{-3}$ ) and PM concentrations ( $\mu\text{g}\cdot\text{m}^{-3}$ ) at sampling site Graz Don Bosco

Higher PM concentrations are in line with higher concentrations of PAHs. The highest concentrations of BaP, excluding NYE and DB pS17, can be observed at DB 2 with  $6 \text{ ng}\cdot\text{m}^{-3}$ , which temporarily exceeded the annual limit value. The absolute concentrations for Benzo(e)pyrene, Benzo(k, f)fluoranthene, Benz(a)anthracene and Indeno(1,2,3-c,d)pyrene ranged between  $5 \text{ ng}\cdot\text{m}^{-3}$  and  $8 \text{ ng}\cdot\text{m}^{-3}$ . Short term exceedances of the annual limit value of  $1 \text{ ng}\cdot\text{m}^{-3}$  can be observed but this does not necessarily lead to an exceedance of the annual limit.

At pools with lower PM concentrations clearly lower concentrations of PAHs could be observed. Dibenz(a, h)anthracene could not be quantified at pools with lower PM concentrations. This polycyclic aromatic hydrocarbon could only be measured in pools with high PM concentrations and they ranged between  $0,2 \text{ ng}\cdot\text{m}^{-3}$  and  $2,0 \text{ ng}\cdot\text{m}^{-3}$  (excluding NYE).

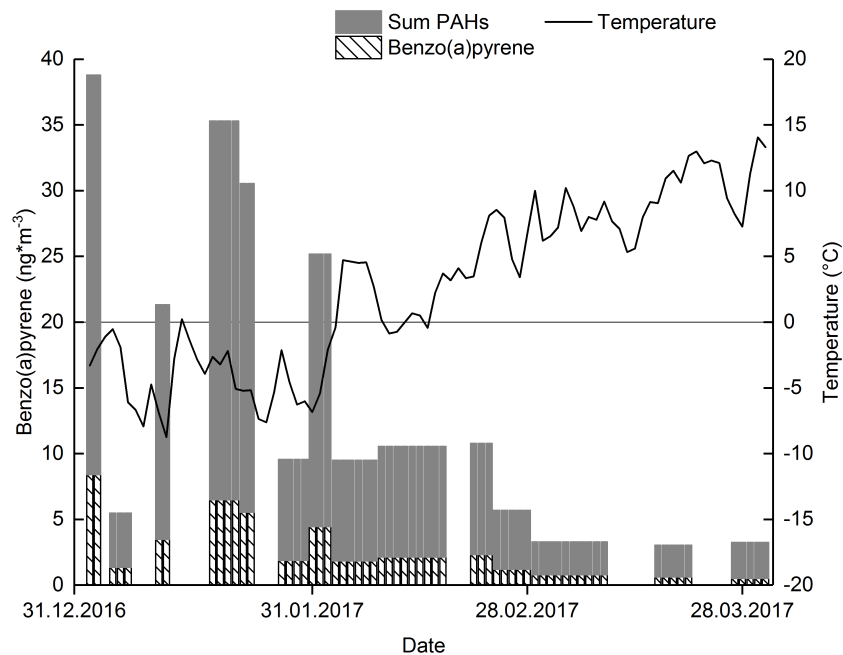


Figure 37: Trend of concentrations of PAHs ( $\text{ng}\cdot\text{m}^{-3}$ ) and temperature ( $^{\circ}\text{C}$ )

Figure 37 shows the absolute concentrations of BaP and the sum of quantified PAHs according to the guideline of EU. [38] The decreasing trend of PAHs with increasing temperature can clearly be observed. In March, generally lower sums of PAHs were measured. Furthermore, high total PM concentrations are in line with higher concentrations of BaP and thus higher sums of PAHs. Because of this correlation BaP is chosen as marker substance for air quality control. According to an international interlaboratory comparison test a clearly lower variety of PAHs could be quantified at low polluted filters. [39]

## 6.6 Conclusion – Graz

Within the project “Aerosolquellenanalyse- Winter Graz” quartz fiber filters were sampled in Graz from the beginning of January to the end of March 2017. The sampling site Graz Don Bosco counted 20 exceedances of the limit value of  $\text{PM}_{10}$  samples of  $50 \mu\text{g}\cdot\text{m}^{-3}$ . To represent the situation of ambient air quality sample pools of the three sampling sites Graz Don Bosco, Graz Süd and Graz Ost were analyzed. For quantification, the  $\text{PM}_{2,5}$  samples of sampling sites Graz Don Bosco and Graz Süd and the  $\text{PM}_{10}$  samples of Graz Ost were available.

To identify the impact of different sources filters were divided into sample pools. These pools represent high, medium and low pollution situations of January and February as well as the situation of March 2017. Because of its different elemental composition (especially for the trace element Barium) New Year's Eve was handled as special event.

Analysis of several components like elemental carbon (EC), organic carbon (OC), soluble ions, anhydrosugars, humic like substances and polycyclic aromatic hydrocarbons were done. The source apportionment was carried out with the macro-tracer approach, which was developed within the AQUELLA and AQUELLIS studies at TU Wien. [1]

In general, quite similar trends of PM mass, with minor differences between the sampling sites, can be observed. This was especially noticeable within pools with high concentrations of PM. The exceedances of the limit value for PM<sub>10</sub> samples of 50 µg\*m<sup>-3</sup> occur preferably at low temperatures. If temperature increased the daily means of PM mass decreased in most cases below 50 µg\*m<sup>-3</sup>. Caused by the meteorological situation a decreasing trend of PM concentrations can be observed.

The comparison of the PM concentrations between sampling site Graz Don Bosco and the background site Bockberg showed a similar trend. The background site Bockberg is used to identify regional transport. Only on the days after New Year's Eve higher concentrations were measured at the urban site Graz Don Bosco than at Bockberg. Because of local emissions caused by fireworks NYE was handled as special event and not summarized with other days to a pool. Also during the first pollution period (11.01. – 12.01.2017) the concentration of the sampling site Graz Don Bosco were noticeable higher than at the background site Bockberg. Later on, the PM<sub>10</sub> concentrations at urban and background site adapted to each other. This indicates that the situation of ambient air quality in Graz is affected also by regional pollution periods. This can especially be observed at days with high PM concentrations, when the ratio between urban and background site is between 1,0 and 1,5, which represents a similar pollution of both sites.

The major particle sources, which were effective during pollution periods in Graz are:

- Secondary inorganic aerosol
- Wood burning aerosol
- Traffic related aerosols

Table 13: List of major particle sources during the different pollution periods in Graz

Pollution Period	Major sources
> 80 $\mu\text{g}\cdot\text{m}^{-3}$	<p>This group includes three pools of sampling site Graz Don Bosco and also two pools of sampling site Graz Süd as well of sampling site Graz Ost. With exception of pool DB 1 the major concentration of PM was contributed to secondary inorganic aerosol followed by wood burning aerosol. Pools of this pollution period represent the time period of January. During this time period low temperatures were measured, which can be seen in the predominance of "winter" sources. The previous impact at background site Bockberg reached similar PM concentrations like the urban sampling site Graz Don Bosco. This marks a regional pollution period and so relative contributions of "urban" sources in Graz are low. During the first pollution period (DB 1) major differences between concentrations of the urban sampling site and the background site can be observed. The relative contribution of "urban" sources can be clearly seen.</p>
50 – 80 $\mu\text{g}\cdot\text{m}^{-3}$	<p>This group includes five pools of sampling site Graz Don Bosco, one pool for Graz Süd and two pools for Graz Ost. The predominance of "winter" sources can be attributed to the low temperatures. The pools of sampling site Graz Don Bosco describe the time period of January and February. Secondary inorganic aerosol represents the major particle source during this pollution period. A decreasing trend of wood burning aerosol (30 – 15 %) can be observed. During time the impact of traffic related aerosols became noticeable.</p> <p>Only pool DB 7 describes a different situation where the contribution of wood burning aerosol is higher (35 %) than the contribution of secondary inorganic aerosol (21 %).</p>
< 30 $\mu\text{g}\cdot\text{m}^{-3}$	<p>Three pools of sampling site Graz Don Bosco describe the situation of lower concentrations of PM. For sampling site Graz Süd and Graz Ost respectively one pool was chosen. At all three pools of sampling site Graz Don Bosco &lt; 30 % of total PM were contributed to wood burning aerosol. In contrary to pools of higher pollution period, the contributions of traffic related aerosols (exhaust and abrasion) were noticeable (9 – 17 %). Furthermore, the contribution of secondary inorganic aerosol ranged between 21 – 36 %. The contribution of wood burning aerosol of pools of the other two sampling sites (Graz Süd and Graz Ost) was higher. The contribution was 54 % for Graz Süd and 23 % for Graz Ost.</p>
< 30 $\mu\text{g}\cdot\text{m}^{-3}$ during March	<p>In March, higher temperatures were observed and generally lower PM concentrations were determined. Three pools of sampling site Graz Don Bosco and one pool of sampling sites Graz Süd and Graz Ost describe the situation in March. The three chosen pools of sampling site Graz Don Bosco describe nearly the whole month. A decreasing trend of wood burning aerosol which drops to 10 % can be observed during March at sampling site Graz Don Bosco. In contrary, an increasing trend of the contribution of mineral dust which ranged between 19 – 32 % can be seen. Especially high contributions of mineral dust occur at sampling site Graz Ost, which is caused by the analyzed <math>\text{PM}_{10}</math> samples. The contributions of mineral dust of sampling site Graz Ost are similar to four times higher than at sampling site Graz Don Bosco.</p> <p>The contribution of secondary inorganic aerosol ranged between 19 – 21 %. During March, it was not possible to identify a major aerosol source.</p>
Special case: NYE	<p>Because of the high pollution on New Year's Eve it was handled as a special event and not combined with other days. To compare the source apportionment two filters of NYE of 2016 and 2017 were analyzed. Generally New Year's Eve of 2017 had a much higher PM mass of 141 <math>\mu\text{g}\cdot\text{m}^{-3}</math> than 2016 with 89 <math>\mu\text{g}\cdot\text{m}^{-3}</math>.</p> <p>Also on NYE wood burning aerosol and secondary inorganic aerosol showed a predominant impact on source contribution. The high amount of wood burning aerosol is flawed with higher uncertainty because the macro-tracer approach is not optimized for situations like these.</p> <p>The different contribution of trace elements (especially Barium) was crucial for the separate quantification of NYE. Barium causes a green flame color and is used in fireworks. In further pools low to not detectable concentrations of Barium were quantified.</p>

# 7 Comparison Graz Don Bosco – Vorau

## 7.1 PM<sub>10</sub> concentrations

---

As expected, higher concentrations of particulate matter were measured at the three sampling sites in Graz than in Vorau. The maximum measured PM<sub>10</sub> concentrations (except NYE) occurred on 23.01.2017 with 139 µg\*m<sup>-3</sup> at sampling site Graz Don Bosco. At sampling site Vorau noticeable lower PM<sub>10</sub> concentrations were measured. The maximum value of measured PM<sub>10</sub> concentration occurred on 31.01.2017 with 104 µg\*m<sup>-3</sup> at sampling site Vorau.

The maximum PM<sub>10</sub> concentrations of sampling site Graz Don Bosco is about 1,8 times higher than the maximum measured PM<sub>10</sub> concentrations of Vorau. With an exception (31.01.2017) the average PM<sub>10</sub> concentration during sampling pools accounted 30 µg\*m<sup>-3</sup>, which is similar to the low measured PM<sub>10</sub> concentrations of sampling site Graz Don Bosco. The above mentioned average PM<sub>10</sub> concentration of sampling site Vorau does not represent an annual average, but rather the average PM<sub>10</sub> mass during selected sampling pools.

## 7.2 Source apportionment with macro-tracer approach

---

Graz represents the situation of a city with special meteorological issues while Vorau is located in the east of Styria, surrounded by mountains and high agricultural activity. Because of the different geographical and meteorological issues, differences in source contributions were expected. Besides this, other great differences between these two sampling sites can be observed. Graz represents the situation of ambient air quality of a city with a about 56 times higher density of population than Vorau. Because of the geographical differences and the different sea levels air masses are transported differently which leads to a different situation of ambient air quality.

In both cases the macro-tracer approach enabled the characterization of the biggest part of particulate matter.

Despite the above-mentioned differences between the sites the general outline of aerosol sources is quite comparable. This reflects the fact, that atmospheric aerosols have a life time of several days and thus can influence larger regions. However, an alternating predominance of the main sources (wood burning aerosol and secondary inorganic aerosol) can be observed in Vorau and Graz.

### 7.2.1 Secondary inorganic aerosol

Although the  $PM_{10}$  concentrations showed strong differences, the contribution of secondary inorganic aerosol was quite similar. The sampling in Graz (01.01. – 01.03.2017) covers the same period as VO 6 – VO 10 of sampling period in Vorau. The contribution of SIA at Graz Don Bosco ranged between 19 – 57 %; while it varied between 39 – 56 % at sampling site Vorau. Figure 38 shows the average concentrations of ammonium, nitrate and sulphate for sampling sites Graz Don Bosco and Vorau during the winter period. Noteworthy are the slightly higher concentrations of all ions at sampling site Vorau.

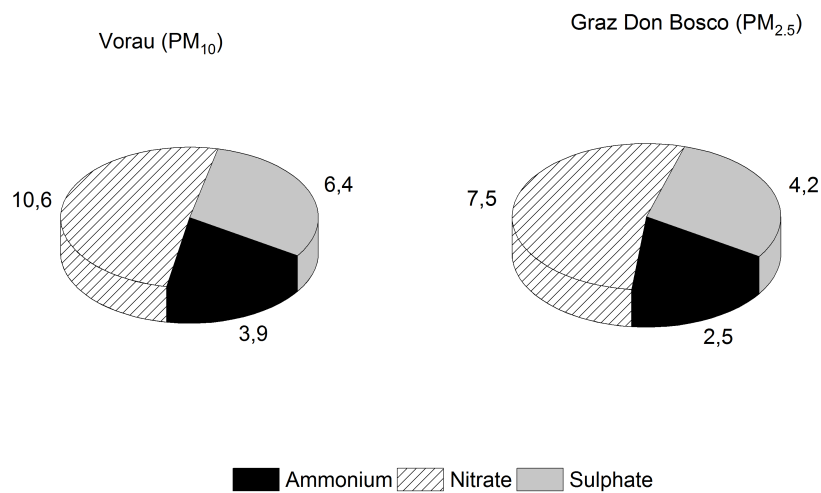


Figure 38: Average concentrations of ammonium, nitrate and sulphate ( $\mu g \cdot m^{-3}$ ) for sampling sites Vorau (PM<sub>10</sub>) and Graz Don Bosco (PM<sub>2.5</sub>) during the winter period

In summary, a higher contribution of secondary inorganic aerosol was observed at sampling site Vorau. Still, a clear difference of the sources of SIA was seen. To discuss the differences between this two sampling sites the calculation of the equivalent concentrations of measured analytes was carried out; an ion balance for both sampling sites is shown in Figure 39.

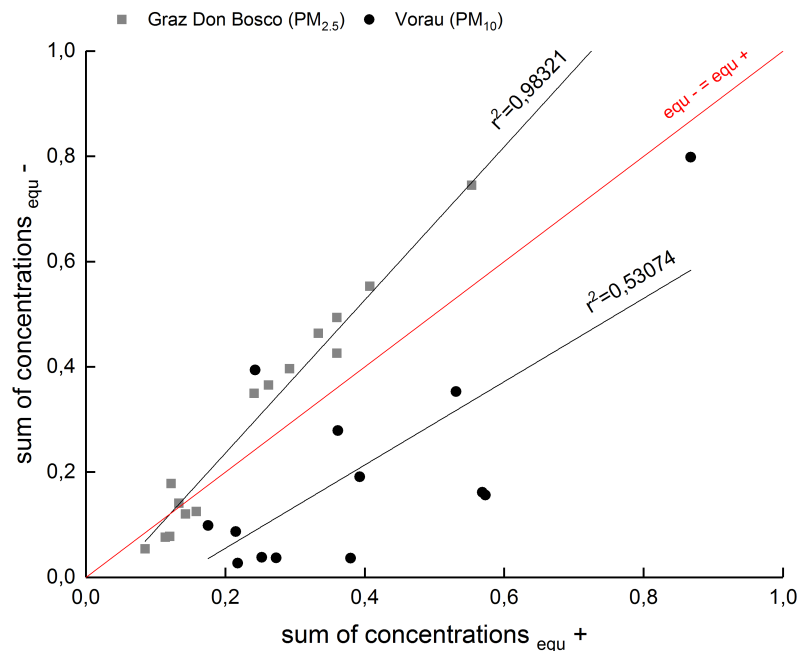


Figure 39: Ion balances of sampling sites Graz Don Bosco ( $PM_{2.5}$ ) and Vorau ( $PM_{10}$ ). The red highlighted line marks the balance between anions and cations ( $C_{equ-} = C_{equ+}$ ).

Figure 39 shows a well-correlated sum of equivalent concentrations ( $r^2=0,98321$ ) for sampling site Graz Don Bosco; the ion balance of Vorau shows some fluctuations ( $r^2=0,53074$ ). Within the scope of this work chloride, nitrite, nitrate and sulphate were quantified. The ion equivalent concentrations at sampling site Graz Don Bosco are above the  $x=y$  line (red). This means, that a higher concentration of anions was measured. The equivalent concentrations of sampling site Vorau show high variations but they are mostly below the  $x=y$  line (red). Which is dedicated to higher measured equivalent concentrations of cations. The chromatograms of sampling site Vorau showed further peaks, which can be ascribed to phosphates in the samples; because of method issues they were not quantified. So, this leads to an imbalance of ion balance at sampling site Vorau.

## 7.2.2 Wood burning aerosol

Anhydrosugars like levoglucosan and its isomers mannosan and galactosan are exclusively produced during the combustion of biomass like cellulose and hemicellulose. Within the macro-tracer approach the impact of wood burning aerosol is calculated on basis of the levoglucosan concentrations. [1], [40]

In Figure 40 the concentrations of levoglucosan and organic carbon during the winter period for the sampling sites Graz Don Bosco ( $PM_{2.5}$ ) and Vorau ( $PM_{10}$ ) are reported. The lines drawn in black mark the maximum ratio of levoglucosan/OC of 0,13 and a rather low, but not the lowest ratio of levoglucosan/OC of 0,08. Two pools of Graz Don Bosco and one pool of Vorau are below the lower ratio line. These three pools have a lower ratio than 0,08 and describe the time period of March, where already higher temperatures were reported and so the demand on small scale heating decreased. The ratio of levoglucosan/OC of all other pools ranged between 0,08 and 0,13. The largest spread of ratios was observed at sampling site Vorau, where the ratios of levoglucosan/OC varied between 0,04 and 0,13.

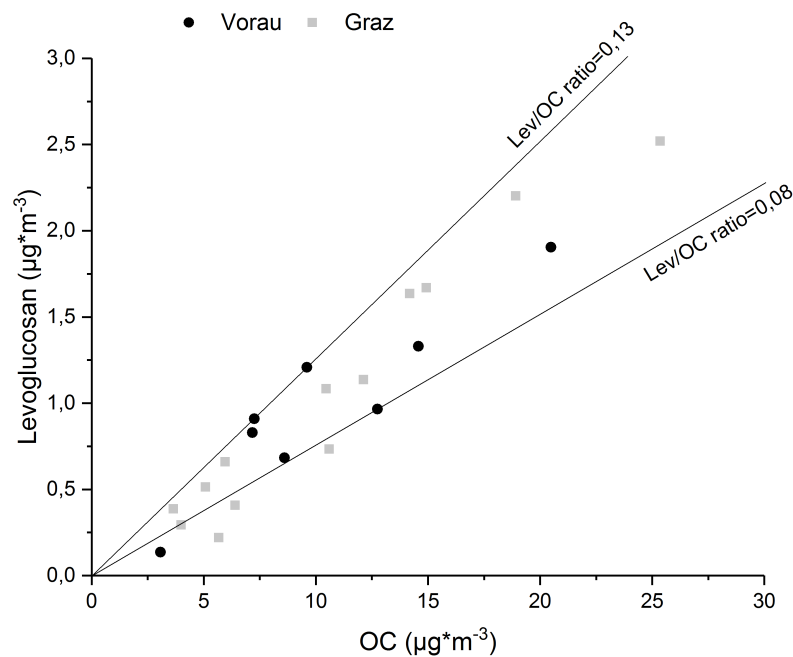


Figure 40: Ratios of levoglucosan to organic carbon ( $\mu\text{g}\cdot\text{m}^{-3}$ ) at sampling sites Graz Don Bosco ( $PM_{2.5}$ ) and Vorau ( $PM_{10}$ ) during winter period

Despite this, the contribution of wood burning aerosol was quite similar at both sampling sites (Graz Don Bosco and Vorau). At sampling site Graz Don Bosco, it ranged between 10 – 34 % of  $PM_{2.5}$  concentration. A similar contribution of pools which cover the same time period of Graz Don Bosco was observed; the contribution of wood burning aerosol of sampling site Vorau varied between 17 – 27 % of  $PM_{10}$  concentration during winter period.

### 7.2.3 Traffic related aerosols

Organic Carbon can be emitted by different sources. So, a classification in primary and secondary organic carbon can be carried out. Primary organic carbon is emitted directly into the atmosphere while secondary organic carbon is formed during gas- to- particle processes in the atmosphere. [41] In the scope of this work the impact of biological and fungal caused organic carbon is neglected, because these sources are not relevant during winter time. Because of this, all following figures focus on winter period of the two sampling sites, Graz and Vorau.

As expected results of the macro-tracer approach show a higher impact of traffic related aerosols at sampling site Graz Don Bosco than at sampling site Vorau. For quantification,  $PM_{10}$  samples of sampling site Vorau and the  $PM_{2.5}$  samples of Graz Don Bosco were available. During VO 6 – VO 10, which cover the same time period as pools of sampling site Graz Don Bosco, average concentrations of 4 % of  $PM_{10}$  concentration are contributed to traffic related aerosols (exhaust and abrasion). While on average 11 % of  $PM_{2.5}$  concentration was contributed to traffic related aerosols at sampling site Graz Don Bosco. This is a slightly three times higher impact of traffic related aerosols in Graz, which is caused by highly traveled streets.

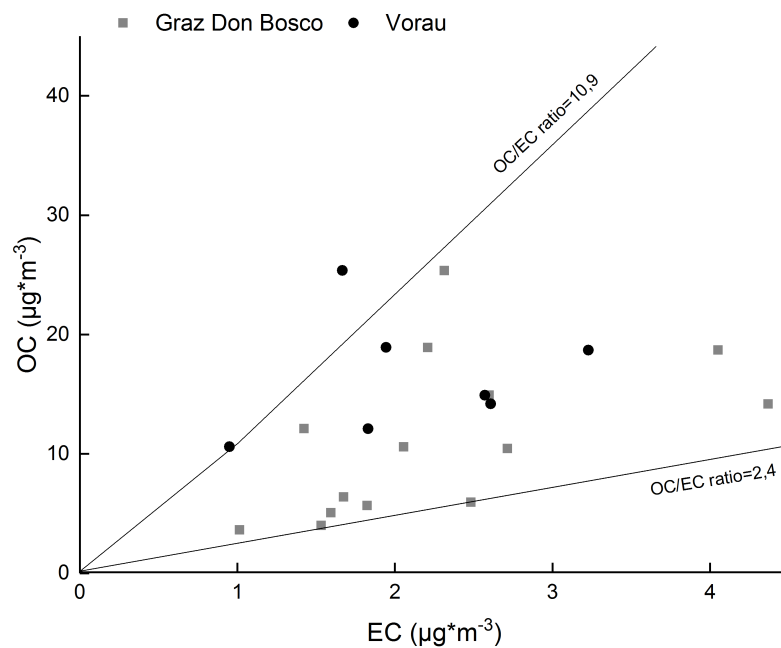


Figure 41: OC vs EC concentrations ( $\mu\text{g}\cdot\text{m}^{-3}$ ) for sampling sites Graz Don Bosco and Vorau during winter period

Figure 41 shows the ratios of OC and EC of the sampling sites Graz Don Bosco ( $PM_{2.5}$ ) and Vorau ( $PM_{10}$ ) as well as the maximum and minimum ratio of OC/EC drawn as lines. In general, lower ratios can be observed at Graz Don Bosco in Vorau. A high OC/EC ratio marks a low impact of traffic and corresponds to low concentrations of EC. This corresponds with the different locations of the sampling sites. The ratios of sampling site Graz Don Bosco varied between 2,5 and 10,9 while they ranged between 2,8 and 10,5 at sampling site Vorau. Previous studies showed, that generally lower OC/EC ratios are associated with a higher impact of traffic related aerosols. [42] To summarize, a higher impact of traffic related aerosols was observed at sampling site Graz Don Bosco.

#### **7.2.4 Mineral dust**

---

Mineral dust can be preferably measured in the coarse fraction ( $PM_{10-2.5}$ ) or  $PM_{10}$  samples and has both natural and anthropogenic sources. Sources of mineral dust in particulate matter of the region of interest are resuspension and erosion. Also dust storm events emit large amounts of mineral dust, but they are neglected within this study.[43]

The average contribution of mineral dust at sampling site Graz Don Bosco was 3 % ( $PM_{2.5}$  samples) while a higher contribution of 5 % was observed at sampling site Graz Ost ( $PM_{10}$  samples). An average contribution of 2 % was quantified during the time period which cover the pools of sampling site Graz Don Bosco at sampling site Vorau. A seasonality of mineral dust can be observed. In following pools which describe later time periods the contribution of mineral dust was higher. During summer pools (April to July) on average 13 % of  $PM_{10}$  mass was attributed by mineral dust at sampling site Vorau. The maximum contribution of mineral dust at sampling site of Graz Ost was also 13 % of  $PM_{10}$  concentration and occurred during the first ten days in March.

## 8 Limitations of the macro-tracer approach and other methods used for source apportionment

Independent from the preferred method several assumptions have to be set to carry out a source apportionment. They include the non- reactivity of measured analytes and no chemical interaction between emissions from different aerosol sources. Usually this does not display real world conditions. For example, primary source emissions may undergo chemical transformations or reactions in the atmosphere (like SIA) before they reach the receptor site, i.e. the sampling site. Furthermore, the appropriate sources have to be considered, so a significant and valid source apportionment is calculated. [21]

In the scope of this work the source apportionment was carried out on basis of the macro-tracer approach. This approach evaluates the contribution of selected particle sources based on the measured atmospheric concentrations of so called macro-tracers, like already mentioned in chapter 2.

Although the macro-tracer approach presents a robust method for source apportionment, some limitations occurred during calculation. For example, the calculation of contributing sources is based on a minor number of tracer substances, so a noticeable uncertainty is given. There are also several factors which influence the transport and formation of these macro-tracers. Furthermore, the used conversion factors have to be evaluated continuously to yield a precise source apportionment.

Within the macro-tracer approach the calculation of the contribution of secondary inorganic aerosol was carried out on the basis of the concentrations of ammonium, nitrate and sulphate. Previous studies showed the impact of several other formation and transformation reactions of inorganic ions in the atmosphere. The formation of  $\text{Ca}(\text{NO}_3)_2$ ,  $\text{K}_2\text{SO}_4$ ,  $\text{NaNO}_3$  or  $\text{NH}_4\text{Cl}$  through heterogeneous reactions or neutralization reactions in the atmosphere is neglected within the macro-tracer approach. The amount of measured calcium is contributed to mineral dust and the amount of chloride to de-icing salt. Whereas the impact of de-icing salt above 1 % of total PM concentration is noticeable and influences the source apportionment. [21]

There are also several factors which influence the emission and formation of wood burning aerosol. The most obvious uncertainties can be attributed to the calculation of organic material, which has several sources and is attributed to emissions caused by biomass burning, water-soluble secondary organic aerosols and not defined organic material. Most likely the overestimation of the PM mass concentrations, which occurred at sampling site Graz Süd, are due to conversion factors not perfectly applicable to this site. The source apportionment of the other three sampling sites showed no inappropriate calculation conditions. Differences of the conversion factor were already observed in further studies. Variabilities can be caused by the sort of used wood type (hard- or softwood), the type of appliance and burning conditions. [12], [15]

Tailored emission factors based on the type of wood sort and the consumption of burning material were used to optimize the calculation of wood burning aerosol within the macro-tracer approach in Piazzalunga et al.. The calculation of real world emission ratios was carried out via Positive matrix factorization and so weighted conversion factors for levoglucosan were used to achieve an optimal source apportionment. Another advantage is, that weighted emission factors can be used for source apportionment at sampling sites which are not well known. [40]

Humic like substances (HULIS) count to the secondary organic aerosols and capture an essential part of water-soluble organic compounds in PM. Previous studies (PMInter) attributed two times the total carbon concentration to HULIS, thus accounting for hetero atoms which definitely will be present. [7] Within this work the contribution of HULIS was calculated as HULIS-C only. Humic like substances can also be partly caused by biomass burning, which was neglected within the calculation used before and is considered with the present approach. Because of the variation of conversion factors the contribution of HULIS and not defined organic material can be biased with some uncertainty.

A further problem was observed in respect to elemental carbon (EC) sources. EC can have different origins; it can be partly caused by the combustion of biomass or traffic related emissions. In the present study, the total concentration of EC was attributed to traffic related emissions. So, the formation of EC during biomass burning was neglected within the scope of this work; which does not display real world conditions. The optimization of used conversion factors for wood burning aerosol would also lead to a different classification of EC caused by biomass burning. This was already conducted in previous studies, but is not adapted to current used burning appliances, so it is flawed with higher uncertainty. [7], [9]

The calculation of mineral dust, which has both anthropogenic and natural sources, is based on the concentrations of aluminum and calcium. Previous studies showed that there is a variety of observational and empirical methods for the calculation of the mineral dust contribution. [43] Within this work the calculation of mineral dust with the macro-tracer approach is based on the fact that the greatest amount of mineral dust consists of carbonates and silicates. So, the calculation is based on the atmospheric concentrations of calcium and silicium. Because quartz fiber filters were used for sampling, the concentration of silicium was indirectly calculated on the basis of the concentration of aluminum. Through this, the contribution of mineral dust is flawed with greater uncertainty. This could be reduced if the calculation is based on several more analytes. Previous studies (Miller-Schulze et al., 2015) used the calculation based on the “oxide model” where the contribution of mineral dust is based on the calculation of an oxide weighted profile. Therefore, the atmospheric concentrations of aluminum, calcium, iron, potassium, magnesium, manganese, sodium, ruthenium, scandium, silicium and titanium are considered. [43]

Within this work the macro-tracer approach enabled the contribution of the greatest amount of particulate matter at all sampling sites. But there are several methods for source apportionment which may consider the impact of several more analytes.

Previous used methods are the “Chemical mass balance” and the “Positive matrix factorization” model. Both methods are based on detailed chemical information about single sources or source groups. [21]

To carry out a source apportionment the knowledge of appropriate sources affecting the area of interest is required. If the major sources are known and chemically identified the fitting can be carried out with a multilinear engine like the Chemical mass balance model. If the chemical knowledge of sources is not well known, several more effects have to be considered, so a Factor Analysis model (like the Positive Matrix Factorization model) has to be applied. [21]

The *Chemical mass balance* (CMB) contributes sources on the basis of representative source categories rather than individual emitters. For this, source profiles have to be generated and they are used for qualification, quantification and calculating the contribution of different sources to PM. Because of great variations depending on location, legislative regulations and emitters individual source profiles have to be generated. [21]

If the knowledge of chemical characteristics is not as well known, there is a great number of impacts, so the source apportionment gets a multilinear problem. To solve this, several approaches like the *PMF model (Positive Matrix Factorization)* is used. It is also a receptor model which allows the quantification of source contribution based on the composition of the fingerprints of sources. This means the contribution is not calculated on basis of tracer substances, so the impact of several more analytes is considered. The calculation is based on a data matrix of measured analytes and number of samples. [44]

Both CMB and PMF are based on extensively statistical analysis and are not trivial. Because of the reduced time resolution, i.e. the number of samples available for the given time period, it was not possible to carry out the source apportionment with the PMF model within the scope of this work. This was caused by several limitations which are listed below:

- To identify sources of different pollution periods, filters were grouped into sample pools. Because of this, the time resolution was minimized and PMF is preferably used for source apportionments with high time resolutions such as those from aerosol mass spectrometers or 24hr PM samples. [44]
- Furthermore, analysis requires a great analytical input which consists of an enhanced knowledge of source profiles as well as profiles from the sampling site.
- The quantification several substances was carried out. The reduction of time resolution leads to a small scope of samples. So, a high number of analytes compared to the small number of sample pools leads to high uncertainties of the source apportionment.
- Furthermore, MLE (Multilinear Engines) do not work without difficulties if the input file contains missing values, if they are for example below the detection limit. So, a simplification for such values has to be considered. If the concentrations are below the detection limit, the source contribution via the macro-tracer approach is neglected. For multilinear engines, a substitution by LOD/2 attended to higher uncertainties can be done.

To sum up, the source apportionment with the macro-tracer approach displays a simple and robust method, which requires a manageable amount of analytical input. So, source apportionment can be conducted based on a small number of tracer substances which are preferably formed of nine sources. The source apportionment with CMB and PMF is based on a great number of quantified analytes and requires on the one hand a great analytical input and on the other hand emission profiles for appropriate sources. To avoid this high analytical and time effort, the macro-tracer method was established and displays a method for everyday source apportionment.

As any model calculation, the macro-tracer method is biased with some uncertainty, if it is applied at regions, which were not investigated in detail earlier. So, for further investigations an over-all uncertainty which includes the uncertainties of all realized analyses and sample preparation methods has to be calculated to yield a precise source apportionment for the region of interest.

## 9 Summary and Conclusions

The identification of dominant sources of PM<sub>10</sub> and PM<sub>2.5</sub> prevailing at different sampling sites in Styria was performed in terms of chemical analysis and the macro-tracer approach. It permits the identification and quantification of nine PM sources. The calculation of the contributions of macro-tracers to different sources, is carried out on the basis of the concentrations of tracer substances with appropriate conversion factors, which are listed in chapter 2.

Sampling was carried out with quartz fiber filters with a High-Volume Sampler at four different sampling sites in Styria. For chemical analysis PM<sub>2.5</sub> samples of the sampling sites Graz Don Bosco and Graz Süd and PM<sub>10</sub> samples of Graz Ost and Vorau were available. Graz represents the situation of a city with special meteorological issues due to its situation in a basin, while Vorau is located in the east of Styria, surrounded by mountains and high agricultural activity.

Since a detailed chemical analysis of all filters was not possible, selected filters were pooled to represent characteristic time periods. Because of several exceedances of the PM<sub>10</sub> limit value at all sampling sites in Graz the classification was based on the different PM<sub>10</sub> mass concentrations. The classification of sample pools for sampling site Vorau was also based on the different PM<sub>10</sub> mass concentrations, but also the occurrence of precipitation was considered. As expected, higher concentrations of particulate matter were measured at the three sampling sites in Graz than in Vorau.

At all sampling sites the macro-tracer approach enabled the characterization of the biggest part of particulate matter. Despite differences between the sites the general outline of the dominant aerosol sources was quite comparable. This reflects the fact, that atmospheric aerosols have a life time of several days and thus can influence larger regions. However, an alternating predominance of the main sources (wood burning aerosol and secondary inorganic aerosol) can be observed in Vorau and Graz. As expected, results of the macro-tracer approach showed a higher impact of traffic related aerosols at sampling site Graz Don Bosco than at sampling site Vorau. On the other hand, a higher amount of not defined organic material was attributed at the pools of sampling site Vorau. This points to sources not considered in the present approach, e.g. bioaerosols.

In general, the macro-tracer approach resulted in a good agreement with gravimetric measured PM mass concentrations at all sampling sites, except Graz Süd. At several pools of this site an overestimation occurred. This was always connected to a relatively high amount of wood burning aerosol. It cannot be excluded, that the model calculation of the macro-tracer approach overestimates the amount for this sampling site. Although the macro-tracer approach represents a robust and simple method for source apportionment, some uncertainty remains. This is caused by the several assumptions which are set during the calculation. To conclude, the used conversion factors have to be evaluated continuously to yield a precise source apportionment.

# 10 List of figures

Figure 1: Sampling site in Vorau, Austria [24][25].....	- 12 -
Figure 2: Comparison of PM <sub>10</sub> concentrations (µg*m <sup>-3</sup> ) of sampling sites in Vorau, Masenberg and Hartberg and trend of temperature (°C) during sampling period. ....	- 14 -
Figure 3: Ratio PM <sub>10</sub> concentrations of Vorau/Hartberg and the total PM <sub>10</sub> concentration (µg*m <sup>-3</sup> ) of Vorau. The red highlighted area marks the ratio between 1,0 and 1,5 which means similar pollutions at the different sampling sites. ....	- 15 -
Figure 4: Trend of PM <sub>10</sub> concentration (µg*m <sup>-3</sup> ) in Vorau and precipitation (L*m <sup>-2</sup> ) on Masenberg. The red highlighted area marks an abrupt decrease of PM <sub>10</sub> concentration caused by a precipitation event. ....	- 16 -
Figure 5: Sampling pools – Vorau. The red drawn line marks the daily limit value of PM <sub>10</sub> concentration. Pools during or after the occurrence of precipitation > 10 L*m <sup>-2</sup> are highlighted blue. ....	- 17 -
Figure 6: Presentation of source apportionment of winter pools (VO 3 – 9) of sampling site Vorau (PM <sub>10</sub> ) .....	- 18 -
Figure 7: Presentation of source apportionment of summer pools (VO 1 – 2 and VO 10 - 13) of sampling site Vorau (PM <sub>10</sub> ) .....	- 19 -
Figure 8: Comparison of the source apportionment of different sampling periods of sampling site Vorau (PM <sub>2,5</sub> ).....	- 20 -
Figure 9: Atmospheric concentrations of ammonium, nitrate or sulphate (µg*m <sup>-3</sup> ) (right inner axis) and secondary inorganic aerosol (µg*m <sup>-3</sup> ) (left axis) over time period. The daily mean of temperature (°C) is shown as a red line. ....	- 23 -
Figure 10: Annual trend of SIA concentrations and left PM (µg*m <sup>-3</sup> ) and temperature (°C).....	- 24 -
Figure 11: Trend of the atmospheric concentrations of wood burning tracers levoglucosan and potassium (µg*m <sup>-3</sup> ) and temperature (°C) over sampling period, Vorau. The concentration of levoglucosan dropped below the LOD (< 0,03 µg*m <sup>-3</sup> ), so quantification was not possible during summer time. ....	- 25 -
Figure 12: Relative contribution of wood burning aerosols and left PM and trend of temperature. The width of showed bars displays the number of days which are summarized to a pool.....	- 27 -
Figure 13: Annual trend of levoglucosan and mannosan. The grey highlighted area marks pools during autumn/winter period .....	- 27 -
Figure 15: Annual trend of relative values of mineral dust (%) and trend of temperature (°C) – Vorau .....	- 29 -
Figure 16: Annual relative contribution of quantified metals for sampling site Vorau (PM <sub>10</sub> ) .....	- 30 -
Figure 17: Median crustal enrichment factors (CEF) for PM <sub>10</sub> elemental concentrations of sampling site Vorau based on the elemental profile for the primitive mantle of the earth by Taylor et al. The grey drawn line marks a CEF of 10. Red drawn line is the average CEF of summer pools (VO 1-2, VO 10 – 13) while the black drawn line presents the average CEF of winter pools (VO 3-9).....	- 31 -
Figure 18: Annual trend of secondary inorganic aerosol, wood burning aerosol, mineral dust and traffic related aerosols (exhaust and abrasion) (µg*m <sup>-3</sup> ) and total PM <sub>10</sub> concentration (µg*m <sup>-3</sup> ) over sampling period – Vorau .....	- 33 -
Figure 19: Comparison of the average source apportionment of summer and winter period for sampling site Vorau (PM <sub>10</sub> ) .....	- 33 -
Figure 19:Map of sampling sites in Graz, Austria [32],[25].....	- 34 -
Figure 21: Comparison of PM <sub>10</sub> and PM <sub>2,5</sub> concentrations (µg*m <sup>-3</sup> ) of different sampling sites in Graz and the trend of temperature (°C) .....	- 37 -

Figure 22: Trend of daily means of PM <sub>10</sub> concentrations at Graz Don Bosco as well as the daily means of PM <sub>10</sub> of the background site Bockberg .....	- 38 -
Figure 23: Daily means of PM <sub>10</sub> and PM <sub>2.5</sub> concentration of the sampling site Graz Don Bosco and the ratio of daily means of PM <sub>10</sub> concentration of urban and background site. The red highlighted area marks ratios between 1,0 to 1,5.....	- 39 -
Figure 24: Temporal trend of PM <sub>10</sub> and PM <sub>2.5</sub> concentrations at sampling site Graz Don Bosco and time periods of chosen sample pools.....	- 40 -
Figure 25: Presentation of pools with PM <sub>10</sub> concentrations > 80 µg*m <sup>-3</sup> for Graz Don Bosco (PM <sub>2.5</sub> ), Graz Süd (PM <sub>2.5</sub> ) and Graz Ost (PM <sub>10</sub> ) .....	- 42 -
Figure 26: Presentation of source apportionment with PM <sub>10</sub> concentrations > 80 µg*m <sup>-3</sup> for sampling site Graz Don Bosco (PM <sub>2.5</sub> ), Graz Süd (PM <sub>2.5</sub> ) and Graz Ost (PM <sub>10</sub> ) .....	- 43 -
Figure 27: Presentation of source apportionment with PM <sub>10</sub> concentrations within 50 - 80 µg*m <sup>-3</sup> for sampling site Graz Don Bosco (PM <sub>2.5</sub> ), Graz Süd (PM <sub>2.5</sub> ) and Graz Ost (PM <sub>10</sub> ) .....	- 45 -
Figure 28: Presentation of source apportionment with PM <sub>10</sub> concentrations within 50 - 80 µg*m <sup>-3</sup> for sampling site Graz Don Bosco (PM <sub>2.5</sub> ), Graz Süd (PM <sub>2.5</sub> ) and Graz Ost (PM <sub>10</sub> ) .....	- 46 -
Figure 29: Presentation of source apportionment with PM <sub>10</sub> concentrations < 30 µg*m <sup>-3</sup> for sampling site Graz Don Bosco (PM <sub>2.5</sub> ), Graz Süd (PM <sub>2.5</sub> ) and Graz Ost (PM <sub>10</sub> ) .....	- 48 -
Figure 30: Presentation of source apportionment with PM <sub>10</sub> concentrations < 30 µg*m <sup>-3</sup> for sampling site Graz Don Bosco (PM <sub>2.5</sub> ), Graz Süd (PM <sub>2.5</sub> ) and Graz Ost (PM <sub>10</sub> ) .....	- 49 -
Figure 31: Presentation of source apportionment with PM <sub>10</sub> concentrations of March for sampling site Graz Don Bosco (PM <sub>2.5</sub> ), Graz Süd (PM <sub>2.5</sub> ) and Graz Ost (PM <sub>10</sub> ) .....	- 50 -
Figure 32: Presentation of source apportionment with PM <sub>10</sub> concentrations of March for sampling sites Graz Don Bosco (PM <sub>2.5</sub> ), Graz Süd (PM <sub>2.5</sub> ) and Graz Ost (PM <sub>10</sub> ) .....	- 52 -
Figure 33: Presentation of source apportionment of pools with different ratios of PM <sub>10</sub> concentrations between urban and background site .....	- 53 -
Figure 34: Source apportionment of NYE 2016 and 2017 .....	- 54 -
Figure 35: Concentrations of Benzo(a)pyrene and PM <sub>2.5</sub> mass at sampling site Graz Don Bosco .....	- 55 -
Figure 36: Concentrations of levoglucosan (µg*m <sup>-3</sup> ) and Benzo(a)pyrene (ng*m <sup>-3</sup> ) over sampling period.....	- 57 -
Figure 37: Concentrations of PAHs (µg*m <sup>-3</sup> ) and PM concentrations (µg*m <sup>-3</sup> ) at sampling site Graz Don Bosco .....	- 58 -
Figure 38: Trend of concentrations of PAHs (ng*m <sup>-3</sup> ) and temperature (°C) .....	- 59 -
Figure 39: Average concentrations of ammonium, nitrate and sulphate (µg*m <sup>-3</sup> ) for sampling sites Vorau (PM <sub>10</sub> ) and Graz Don Bosco (PM <sub>2.5</sub> ) during the winter period .....	- 63 -
Figure 40: Ion balances of sampling sites Graz Don Bosco (PM <sub>2.5</sub> ) and Vorau (PM <sub>10</sub> ). The red highlighted line marks the balance between anions and cations (C <sub>equ</sub> - = C <sub>equ</sub> +) .....	- 64 -
Figure 41: Ratios of levoglucosan to organic carbon (µg*m <sup>-3</sup> ) at sampling sites Graz Don Bosco (PM <sub>2.5</sub> ) and Vorau (PM <sub>10</sub> ) during winter period .....	- 65 -
Figure 42: OC vs EC concentrations (µg*m <sup>-3</sup> ) for sampling sites Graz Don Bosco and Vorau during winter period.....	- 66 -

# 11 List of tables

Table 1: List of conversion factors to calculate the source contribution I.....	- 3 -
Table 3: Parameters of the anion chromatography system .....	- 6 -
Table 4: Parameters of the cation chromatography system .....	- 6 -
Table 5: Parameters of the Saccharides chromatography system .....	- 7 -
Table 6: Parameters of HULIS quantification [19].....	- 8 -
Table 7: Parameters of PAH quantification .....	- 8 -
Table 8: Parameters of crustal and trace element quantification.....	- 9 -
Table 9: List of limits of detection.....	- 11 -
Table 10: List of sample pools Vorau .....	- 13 -
Table 10: Concentration of ammonium, nitrate and sulphate ( $\mu\text{g}\cdot\text{m}^{-3}$ ), contribution of secondary inorganic aerosol (%) to PM mass and average temperature ( $^{\circ}\text{C}$ ) of all pools of sampling site Vorau.....	- 22 -
Table 11: Concentration of levoglucosan ( $\mu\text{g}\cdot\text{m}^{-3}$ ), contribution of wood burning aerosol (%) and average temperature ( $^{\circ}\text{C}$ ) of winter pools - Vorau .....	- 26 -
Table 12: List of sample pools Graz.....	- 36 -
Table 13: List of major particle sources during the different pollution periods in Graz .....	- 61 -
Table 14: Atmospheric concentrations of quantified analytes of sampling site Vorau. Results of soluble ions, anhydrosugars and carbonaceous fractions in $\mu\text{g}\cdot\text{m}^{-3}$ , results of crustal and elemental elements in $\text{ng}\cdot\text{m}^{-3}$ .....	i
Table 15: List of concentrations of contributed sources of $\text{PM}_{10}$ ( $\mu\text{g}\cdot\text{m}^{-3}$ ) of sampling site Vorau ( $\text{PM}_{10}$ ) .....	ii
Table 16: List of relative source apportionment of $\text{PM}_{10}$ (%) of sampling site Vorau .....	iii
Table 17: Atmospheric concentrations ( $\mu\text{g}\cdot\text{m}^{-3}$ ) of quantified analytes of sampling site Graz Don Bosco ( $\text{PM}_{2.5}$ ).....	iv
Table 18: Atmospheric concentrations ( $\mu\text{g}\cdot\text{m}^{-3}$ ) of quantified analytes of sampling site Graz Süd ( $\text{PM}_{2.5}$ ) and Graz Ost ( $\text{PM}_{10}$ ) .....	v
Table 19: List of concentrations of contributed sources of PM ( $\mu\text{g}\cdot\text{m}^{-3}$ ) of sampling site Graz Don Bosco ( $\text{PM}_{2.5}$ ).....	vi
Table 20: List of concentrations of contributed sources of PM ( $\mu\text{g}\cdot\text{m}^{-3}$ ) of sampling site Graz Süd ( $\text{PM}_{2.5}$ ) and Graz Ost ( $\text{PM}_{10}$ ) .....	vii
Table 21: List of relative source apportionment of PM (%) of sampling site Graz Don Bosco ( $\text{PM}_{2.5}$ ).....	viii
Table 22: List of relative source apportionment of PM (%) of sampling site Graz Süd ( $\text{PM}_{2.5}$ ) and Graz Ost ( $\text{PM}_{10}$ ) .....	ix

## 12 Bibliography

- [1] Bauer et al., “‘Aquella Steiermark Endbericht’ (LU-08/07),” 2007.
- [2] M. Stafoggia, E. Samoli, E. Alessandrini, E. Cadum, B. Ostro, and G. Berti, “EHP – Short-term Associations between Fine and Coarse Particulate Matter and Hospitalizations in Southern Europe: Results from the MED-PARTICLES Project,” vol. 1026, no. 9, pp. 1026–1034, 2013.
- [3] P. V. Hobbs, Introduction to atmospheric chemistry: a companion text to Basic physical chemistry. Cambridge University Press, 2000.
- [4] D. D. I. für N. e. V. ; Kr. K. R. der L. im V. und DIN, Feinstaub und Stickstoffdioxid : Wirkung - Quellen - Luftreinhaltepläne - Minderungsmaßnahmen, 1. Auflage. Berlin, 2006.
- [5] Bundesgesetz Österreich, Bundesgesetz zum Schutz vor Immissionen durch Luftschadstoffe (Immissionsschutzgesetz - Luft, IG - L). .
- [6] U. Spangl Nagl, “Jahresbericht der Luftgütemessungen in Österreich 2016,” 2017.
- [7] Kistler et al., “Projekt PMInter, Filteranalysen und 14C Messungen in Feinstaubproben,” 2013.
- [8] C. Schmidl et al., “Chemical characterisation of fine particle emissions from wood stove combustion of common woods growing in mid- European Alpine regions,” Atmos. Environ., vol. Vol. 42, pp. 126–141.
- [9] C. Schmidl et al., “Endbericht für das Projekt ‘AQUELLIS-FB’ Aerosolquellen - Verbrennung fester Brennstoffe,” 2008.
- [10] M. Kistler, “Particulate matter and odor emission factors from small scale biomass combustion units (Dissertation),” Vienna, 2012.
- [11] M. Handler et al., “Size and composition of particulate emissions from motor vehicles in the Kaisermühlen-Tunnel,” Atmos. Environ., vol. 249, no. 1–3, pp. 85–101, 2008.
- [12] A. Caseiro, H. Bauer, C. Schmidl, C. A. Pio, and H. Puxbaum, “Wood burning impact on PM10 in three Austrian regions,” Atmos. Environ., vol. 43, no. 13, pp. 2186–2195, 2009.
- [13] Limbeck et al., “Carbon-specific analysis of humic-like substances in atmospheric aerosol and precipitation samples,” Anal. Chem., vol. 77, no. 22, pp. 7288–7293, 2005.

- [14] B. R. T. Simoneit et al., "Levoglucosan, a tracer for cellulose in biomass burning and atmospheric particles," *Atmos. Environ.*, vol. 33, no. 2, pp. 173–182, 1999.
- [15] C. Schmidl et al., "Particulate and gaseous emissions from manually and automatically fired small scale combustion systems," *Atmos. Environ.*, vol. 45, no. 39, pp. 7443–7454, 2011.
- [16] S. Zappoli et al., "Inorganic, organic and macromolecular components of fine aerosol in different areas of Europe in relation to their water solubility," *Atmos. Environ.*, vol. 33, pp. 2733–2743, 1999.
- [17] A. Limbeck, M. Handler, C. Puls, J. Zbiral, H. Bauer, and H. Puxbaum, "Impact of mineral components and selected trace metals on ambient PM10 concentrations," *Atmos. Environ.*, vol. 43, no. 3, pp. 530–538, 2009.
- [18] Y. Iinuma, G. Engling, H. Puxbaum, and H. Herrmann, "A highly resolved anion-exchange chromatographic method for determination of saccharidic tracers for biomass combustion and primary bio-particles in atmospheric aerosol," *Atmos. Environ.*, vol. 43, no. 6, pp. 1367–1371, 2009.
- [19] T. Steinkogler, "Praktikumsbericht - HULIS," no. 1125590, pp. 1–34, 2017.
- [20] DIN Deutsches Institut für Normung e. V. ; KRdL Kommission Reinhaltung der Luft im VDI, "Luftbeschaffenheit- Messverfahren zur Bestimmung der Konzentration von Benzo(a)pyren in Luft; Deutsche Fassung EN 15549:2008," 2008.
- [21] G. Argyropoulos, C. Samara, E. Diapouli, and K. Eleftheriadis, "An iterative method for evaluating the inter-comparability between chemical mass balance and multivariate receptor models," *Chemom. Intell. Lab. Syst.*, vol. 155, pp. 97–108, 2016.
- [22] J. Bauer et al., "Characterization of the sunset semi-continuous carbon aerosol analyzer.," *J. Air Waste Manag. Assoc.*, vol. 59, no. 7, pp. 826–833, 2009.
- [23] F. Cavalli, M. Viana, K. E. Yttri, J. Genberg, and J. P. Putaud, "Toward a standardised thermal-optical protocol for measuring atmospheric organic and elemental carbon: The EUSAAR protocol," *Atmos. Meas. Tech.*, vol. 3, no. 1, pp. 79–89, 2010.
- [24] M. Bonta, B. Hegedus, and A. Limbeck, "Application of dried-droplets deposited on pre-cut filter paper disks for quantitative LA-ICP-MS imaging of biologically relevant minor and trace elements in tissue samples," *Anal. Chim. Acta*, vol. 908, pp. 54–62, 2016.
- [25] K. E. Yttri et al., "An intercomparison study of analytical methods used for quantification of levoglucosan in ambient aerosol filter samples," *Atmos. Meas. Tech.*, vol. 8, pp. 125–147, 2015.
- [26] Google Maps, "Map of sampling site in Vorau."
- [27] GIS- Steiermark, "Steiermark Landkarte mit Gemeinden," 2018. [Online]. Available: [http://gis2.stmk.gv.at/gis2.stmk.gv.at/gis/content/karten/download/BezStmkmitGemeinden\\_2015.jpg](http://gis2.stmk.gv.at/gis2.stmk.gv.at/gis/content/karten/download/BezStmkmitGemeinden_2015.jpg). [Accessed: 20-Mar-2018]
- [28] Umweltbundesamt, "Luftschadstoffe- NOx." [Online]. Available: <http://www.umweltbundesamt.at/umweltsituation/luft/luftschadstoffe/nox/>. [Accessed: 26-Jan-2018].

- [29] Umweltbundesamt, "Luftschadstoffe, SO<sub>2</sub>." [Online]. Available: <http://www.umweltbundesamt.at/umweltsituation/luft/luftschadstoffe/so2/>. [Accessed: 26-Jan-2018].
- [30] N. Clements et al., "Concentrations and source insights for trace elements in fine and coarse particulate matter," *Atmos. Environ.*, vol. 89, pp. 373–381, 2014.
- [31] N. Jankowski, "Particulate matter characterization of mobile emissions and source apportionment in an industrialized region in Austria," Technische Universität Wien, Dissertation, 2010.
- [32] H. K. Wedepohl, "The composition of the continental crust," *Geochim. Cosmochim. Acta* 59, pp. 1217–1232, 1995.
- [33] M. Srebnik et al., *Contemporary aspects of boron: chemistry and biological applications*. Boston Elsevier, 2005.
- [34] Google Maps, "Map of sampling sites in Graz, Austria." [Online]. Available: <https://www.google.com/maps/d/print?hl=en&mid=1cJldj6bpbvZeYgKgOJV8B6gTK5s&pagew=842&pageh=595&llsw=47.008157%2C15.328098&llne=47.106275%2C15.53392&cid=mp&cv=TANlucihyk.en>.
- [35] N. Jankowski et al., "AQUELLA Linz - Oberösterreich, Aerosolquellenanalyse für Linz - Oberösterreich," 2009.
- [36] K. Kögeler, "Untersuchung des Extraktionsverhaltens Polycyclischer Aromatischer Kohlenwasserstoffe aus Böden mittels SPE, Soxhlet- und Ultraschallextraktion," Wien, 1995.
- [37] K. Fent, *Ökotoxikologie*, 3. Auflage. Thieme, 2007.
- [38] Amtsblatt der Europäischen Union, "Richtlinie 2004/107/EG des Europäischen Parlaments und Rates," vol. 2006, no. 593, pp. 6–16.
- [39] A. Riccio et al., "Real-world automotive particulate matter and PAH emission factors and profile concentrations: Results from an urban tunnel experiment in Naples, Italy," *Atmos. Environ.*, vol. 141, pp. 379–387, 2016.
- [40] A. Piazzalunga et al., "Estimates of wood burning contribution to PM by the macro-tracer method using tailored emission factors," *Atmos. Environ.*, vol. 45, no. 37, pp. 6642–6649, 2011.
- [41] C. Pio et al., "OC/EC ratio observations in Europe: Re-thinking the approach for apportionment between primary and secondary organic carbon," *Atmos. Environ.*, vol. 45, no. 34, pp. 6121–6132, 2011.
- [42] B. Kirchsteiger et al., "Aerosolquellenanalyse für Graz , Winter 2017," 2017.
- [43] J. P. Miller-Schulze et al., "Seasonal contribution of mineral dust and other major components to particulate matter at two remote sites in Central Asia," *Atmos. Environ.*, vol. 119, pp. 11–20, 2015.
- [44] G. Norris, R. Duvall, S. Brown, and S. Bai, "EPA Positive Matrix Factorization (PMF) 5.0 Fundamentals and User Guide," p. 136, 2014.

## 13 Annex

Table 14: Atmospheric concentrations of quantified analytes of sampling site Vorau. Results of soluble ions, anhydrosugars and carbonaceous fractions in  $\mu\text{g}\cdot\text{m}^{-3}$ , results of crustal and elemental elements in  $\text{ng}\cdot\text{m}^{-3}$

Pool	Na <sup>+</sup>	NH <sub>4</sub> <sup>+</sup>	Ca <sup>2+</sup>	Cl <sup>-</sup>	NO <sub>3</sub> <sup>-</sup>	SO <sub>4</sub> <sup>2-</sup>	Levo-glucosan	OC	EC	Aluminum	Barium	Iron	Boron	Zinc	Manganese	Chromium
VO 1	0,7	3,4	0,2		2,1	7,5	<LOD	5,0	0,5	1435	5	49	272	106	<LOD	<LOD
VO 2	0,6	1,1	0,2	0,0	0,6	3,7	<LOD	4,7	0,7	771	8	343	238	22	11	14
VO 3	1,0	3,6	0,4	0,5	5,7	2,8	1,2	9,6	3,2	1254	9	152	705	111	32	<LOD
VO4	1,1	4,4	0,7	0,4	6,3	2,0	0,9	7,3	2,6	1104	15	<LOD	915	82	<LOD	<LOD
VO 5	0,6	1,3	0,1	0,3	3,2	1,9	0,8	7,2	2,6	564	9	54	798	51	5	10
VO 6	1,3	4,9	0,2	1,0	9,7	8,0	1,0	12,8	1,7	944	7	211	90	137	14	15
VO 7	0,7	1,2	0,1	0,8	13,9	7,1	1,3	14,6	1,8	381	6	296	386	93	17	37
VO 8	1,0	8,9	0,8	0,7	28,6	15,3	1,9	20,5	1,9	1121	<LOD	<LOD	430	84	28	<LOD
VO 9	1,7	3,6	0,1	0,2	7,0	7,7	0,7	8,6	1,0	875	<LOD	<LOD	736	<LOD	<LOD	<LOD
VO 10	3,9	0,8	0,5	0,1	0,1	1,4	0,1	3,1	0,6	794	5	132	357	14	6	<LOD
VO 11	2,9	0,3	0,2	0,1	1,2	0,8	<LOD	2,1	0,3	277	2	55	185	15	<LOD	<LOD
VO 12	3,6	0,4	0,3	0,1	0,8	1,0	<LOD	3,0	0,3	888	4	27	229	10	4	<LOD
VO 13	2,9	0,1	0,2	0,1	0,9	0,5	<LOD	2,0	0,2	169	<LOD	162	<LOD	<LOD	<LOD	5

Table 15: List of concentrations of contributed sources of  $PM_{10}$  ( $\mu g * m^{-3}$ ) of sampling site Vorau ( $PM_{10}$ )

Pool	Wood smoke	Exhaust	Abrasion	Mineral dust	SIA	OM not defined	NaCl	remaining PM	average PM concentration
VO 1	0,0	0,7	0,2	1,8	14,4	6,8	0,0	0,9	24,8
VO 2	0,0	0,9	0,3	1,3	5,9	6,3	0,0	8,2	22,9
VO 3	12,9	4,3	1,3	2,0	13,3	0,3	0,1	2,5	36,6
VO4	9,7	3,5	1,0	2,9	14,0	0,2	0,1	4,6	36,0
VO 5	8,9	3,4	1,0	0,7	6,9	0,9	0,0	5,6	27,5
VO 6	10,3	2,2	0,7	1,3	25,0	8,4	0,1	11,4	59,3
VO 7	14,2	2,4	0,7	0,6	24,4	7,3	0,1	12,5	62,3
VO 8	20,4	2,6	0,8	3,0	58,0	10,2	0,1	8,6	103,7
VO 9	7,3	1,3	0,4	1,0	20,1	5,4	0,1	7,1	42,6
VO 10	1,5	0,8	0,2	1,9	2,6	2,9	0,2	5,1	15,1
VO 11	0,0	0,4	0,1	0,8	2,4	2,2	0,1	1,0	7,0
VO 12	0,0	0,4	0,1	1,5	2,4	4,1	0,2	1,2	9,9
VO 13	0,0	0,3	0,1	0,7	1,6	2,6	0,1	0,3	5,6

*Table 16: List of relative source apportionment of PM<sub>10</sub> (%) of sampling site Vorau*

Pool	Wood smoke	Exhaust	Abrasion	Mineral dust	SIA	OM not defined	NaCl	% PM attributed
VO 1	0	3	1	7	58	27	0	97
VO 2	0	4	1	6	26	27	0	64
VO 3	35	12	4	6	36	1	0	93
VO4	27	10	3	8	39	1	0	87
VO 5	32	12	4	3	25	3	0	80
VO 6	17	4	1	2	42	14	0	81
VO 7	23	4	1	1	39	12	0	80
VO 8	20	2	1	3	56	10	0	92
VO 9	17	3	1	2	47	13	0	83
VO 10	10	5	2	12	17	19	1	66
VO 11	0	5	1	12	34	32	2	86
VO 12	0	4	1	16	24	42	2	88
VO 13	0	5	1	12	29	45	2	95

Table 17: Atmospheric concentrations ( $\mu\text{g}\cdot\text{m}^{-3}$ ) of quantified analytes of sampling site Graz Don Bosco ( $\text{PM}_{2,5}$ )

Pool	Na <sup>+</sup>	NH <sub>4</sub> <sup>+</sup>	Ca <sup>2+</sup>	Cl <sup>-</sup>	NO <sub>3</sub> <sup>-</sup>	SO <sub>4</sub> <sup>2-</sup>	Levo-glucosan	OC	EC	BaP	BeP	B(k,f)F	B(a)A	I(1,2,3-cd)P	DiB(a,h)A	HULIS-C	Aluminum
Sil 16	0,3	1,8	0,1	8,3	11,6	15,6	2,2	17,8	3,8	8,1	6,7	9,0	7,6	8,1	1,9	2,2	1,7
Sil 17	1,8	0,9	0,1	16,2	7,1	24,0	4,1	26,2	6,2	18,1	14,9	51,3	20,1	14,3	3,8	1,9	1,8
DB pS 17	2,3	1,5	0,3	6,6	7,1	3,0	2,6	18,7	4,1	8,4	6,6	8,6	6,1	7,1	2,0	1,3	0,0
DB 1	2,3	1,8	0,3	6,8	5,6	3,2	1,6	14,2	4,4	3,5	3,4	4,7	6,3	2,8	0,7	1,6	0,0
DB 2	2,5	2,9	0,4	7,7	9,3	4,6	1,7	14,9	2,6	6,5	5,4	8,3	8,4	5,4	1,3	1,8	0,2
DB 3	0,8	8,0	0,1	1,7	20,0	12,9	2,5	25,4	2,3	5,5	5,1	6,5	6,8	5,2	1,5	3,9	0,1
DB 4	0,7	5,3	0,1	1,1	16,8	9,1	1,1	12,1	1,4	1,9	1,7	2,5	1,6	1,9	<LOD	1,8	0,2
DB 5	0,3	6,3	0,0	0,5	15,6	8,3	2,2	18,9	2,2	4,4	3,4	5,1	6,8	4,4	1,1	1,6	0,0
DB 6	1,5	3,3	0,3	0,9	8,9	6,2	0,7	10,6	2,1	2,1	1,9	2,7	1,8	2,0	<LOD	1,2	0,3
DB 7	1,4	0,7	0,5	0,9	4,1	1,6	1,1	10,5	2,7	2,3	1,9	2,6	1,4	2,2	0,4	0,7	0,1
DB 8	1,5	0,6	0,2	2,1	2,3	0,7	0,4	3,6	1,0	1,3	0,9	1,3	0,7	1,2	<LOD	0,4	0,0
DB 9	0,7	1,4	0,1	0,7	4,2	2,5	0,7	6,0	2,5	1,8	1,4	2,0	2,2	1,8	<LOD	0,5	0,2
DB 10	1,3	0,4	0,4	0,4	2,4	1,2	0,5	5,1	1,6	1,2	1,0	1,3	1,1	1,0	<LOD	0,3	0,2
DB M1	1,1	0,1	0,3	0,3	1,6	0,8	0,3	4,0	1,5	0,8	0,5	0,9	0,5	0,7	<LOD	0,2	0,2
DB M2	1,2	1,1	0,3	0,2	4,9	1,6	0,4	6,4	1,7	0,6	0,6	0,9	0,5	0,5	<LOD	1,0	0,3
DB M3	1,1	0,4	0,6	0,2	2,3	1,6	0,2	5,7	1,8	0,5	0,6	0,8	0,9	0,4	<LOD	0,5	0,5

Table 18: Atmospheric concentrations ( $\mu\text{g}\cdot\text{m}^{-3}$ ) of quantified analytes of sampling site Graz Süd ( $\text{PM}_{2,5}$ ) and Graz Ost ( $\text{PM}_{10}$ )

Pool	Na <sup>+</sup>	NH <sub>4</sub> <sup>+</sup>	Ca <sup>2+</sup>	Cl <sup>-</sup>	NO <sub>3</sub> <sup>-</sup>	SO <sub>4</sub> <sup>2-</sup>	Levo-glucosan	OC	EC	BaP	BeP	B(k,f)F	B(a)A	I(1,2,3-cd)P	DiB(a,h)A	HULIS-C	Aluminium
GS pS 17	0,7	1,7	0,2	1,6	7,7	3,4	3,0	20,8	4,1	4,2	3,4	4,3	2,6	<LOD	0,6	1,5	0,2
GS1	0,5	7,8	0,2	0,8	18,2	11,2	2,8	26,4	2,1	5,9	5,2	6,9	8,8	<LOD	1,0	5,2	0,1
GS 2	0,4	9,3	0,2	0,6	20,4	12,1	3,2	18,3	2,2	6,4	6,2	7,7	10,0	5,4	0,8	1,2	0,2
GS 3	0,4	0,6	0,1	0,5	2,6	1,0	0,5	3,7	0,9	1,5	1,2	1,5	1,0	1,1	0,1	1,0	0,4
GSM	1,1	0,1	0,3	0,2	1,6	0,8	0,4	4,0	1,1	0,8	0,6	0,9	0,7	0,7	0,1	1,1	0,1
GO pS 17	1,8	1,5	0,6	5,4	7,7	2,6	1,7	13,6	3,2	10,4	8,2	12,4	6,2	10,4	0,9	1,4	0,8
GO 1	1,3	8,3	0,5	3,4	23,2	19,3	2,0	22,8	2,0	3,9	4,0	6,2	2,6	4,2	0,6	4,1	0,2
GO 2	0,6	5,3	0,2	0,7	13,5	11,0	1,3	20,2	1,8	3,6	3,6	3,6	2,9	3,8	0,6	4,0	0,3
GO 3	2,1	3,4	0,7	3,8	12,3	9,5	1,0	10,8	1,8	3,0	3,4	4,8	2,7	2,7	0,6	1,5	0,3
GO 4	2,1	0,6	0,4	5,6	2,9	1,0	0,4	3,2	0,7	1,6	1,3	1,9	0,6	1,4	<LOD	0,4	0,2
GO M	1,5	0,1	0,9	1,0	1,8	0,9	0,3	3,7	0,9					*		0,3	0,2

Table 19: List of concentrations of contributed sources of PM ( $\mu\text{g}\cdot\text{m}^{-3}$ ) of sampling site Graz Don Bosco ( $\text{PM}_{2,5}$ )

Pool	Wood smoke	Exhaust	Abrasion	Mineral dust	SIA	HULIS	OM not defined	NaCl	remaining PM	average PM concentration
Sil 16	23,9	5,0	1,5	1,6	31,9	2,2	0,0	0,2	23,5	89
Sil 17	44,3	8,2	2,5	1,9	35,2	1,9	0,0	0,5	46,6	141
DB pS 17	27,7	5,4	1,6	0,8	12,7	1,3	0,0	0,3	14,1	64
DB 1	17,5	5,8	1,7	0,7	11,6	1,6	0,0	0,3	22,9	62
DB 2	17,9	3,5	1,0	1,3	18,4	1,8	1,3	0,3	13,7	59
DB 3	27,0	3,1	0,9	0,5	44,9	3,9	5,2	0,1	16,3	102
DB 4	12,2	1,9	0,6	0,3	34,4	1,8	3,1	0,1	6,5	61
DB 5	23,6	2,9	0,9	0,0	33,2	1,6	2,4	0,0	14,9	79
DB 6	7,8	2,7	0,8	1,0	20,3	1,2	5,5	0,1	11,6	51
DB 7	11,6	3,6	1,1	1,4	7,0	0,7	2,1	0,1	6,2	34
DB 8	4,2	1,3	0,4	0,6	4,0	0,4	0,4	0,1	7,7	19
DB 9	7,1	3,3	1,0	0,5	8,9	0,5	0,1	0,0	3,4	25
DB 10	5,5	2,1	0,6	1,1	4,4	0,3	1,0	0,1	3,8	19
DB M1	3,2	2,0	0,6	0,9	2,8	0,2	1,9	0,1	2,9	14
DB M2	4,4	2,2	0,7	1,0	8,4	1,0	3,0	0,1	5,2	26
DB M3	2,4	2,4	0,7	2,0	4,7	0,5	4,6	0,1	5,4	23

Table 20: List of concentrations of contributed sources of PM ( $\mu\text{g}\cdot\text{m}^{-3}$ ) of sampling site Graz Süd ( $\text{PM}_{2,5}$ ) and Graz Ost ( $\text{PM}_{10}$ )

Pool	Wood smoke	Exhaust	Abrasion	Mineral dust	SIA	HULIS	OM not defined	NaCl	remaining PM	average PM concentration
GS pS 17	37,4	5,5	1,6	0,7	14,0	1,5	0,0	0,1	*	58
GS1	34,7	2,8	0,8	0,6	41,0	5,2	1,8	0,0	7,1	94
GS 2	39,8	3,0	0,9	0,6	46,0	1,2	0,0	0,0	*	71
GS 3	6,7	1,2	0,4	0,6	4,6	1,0	0,0	0,0	*	12
GS M	5,5	1,5	0,5	1,0	2,8	1,1	0,0	0,1	*	12
GO pS 17	20,8	4,3	1,3	2,3	13,1	1,4	0,0	0,2	8,0	52
GO 1	24,2	2,7	0,8	1,4	55,9	4,1	6,9	0,2	5,1	102
GO 2	16,5	2,4	0,7	0,9	32,8	4,0	9,6	0,0	27,3	94
GO 3	12,1	2,4	0,7	2,0	27,7	1,5	2,9	0,2	9,8	59
GO 4	4,4	1,0	0,3	1,2	4,9	0,4	0,2	0,3	6,4	19
GO M	3,3	1,3	0,4	2,5	3,0	0,3	1,9	0,1	6,6	19

Table 21: List of relative source apportionment of PM (%) of sampling site Graz Don Bosco (PM<sub>2.5</sub>)

Pool	Wood smoke	Exhaust	Abrasion	Mineral dust	SIA	HULIS	OM not defined	NaCl	% PM attributed
Sil 16	27	6	2	2	36	2	*	0	74
Sil 17	32	6	2	1	25	1	*	0	67
DB pS 17	43	8	3	1	20	2	*	0	78
DB 1	28	9	3	1	19	3	*	0	63
DB 2	30	6	2	2	31	3	2	1	77
DB 3	26	3	1	0	44	4	5	0	84
DB 4	20	3	1	1	57	3	5	0	89
DB 5	30	4	1	0	42	2	3	0	81
DB 6	15	5	2	2	40	2	11	0	77
DB 7	34	11	3	4	21	2	6	0	82
DB 8	22	7	2	3	21	2	2	1	59
DB 9	28	13	4	2	36	2	0	0	86
DB 10	29	11	3	6	23	2	5	0	80
DB M1	22	14	4	6	19	1	13	0	80
DB M2	17	9	3	4	32	4	12	0	80
DB M3	10	11	3	9	21	2	20	0	76

Table 22: List of relative source apportionment of PM (%) of sampling site Graz Süd (PM<sub>2.5</sub>) and Graz Ost (PM<sub>10</sub>)

Pool	Wood smoke	Exhaust	Abrasion	Mineral dust	SIA	HULIS	OM not defined	NaCl	% PM attributed
GS pS 17	65	9	3	1	24	3	*	0	*
GS 3	37	3	1	1	43	6	2	0	92
GS 5	56	4	1	1	65	2	*	0	*
GS 8	54	10	3	5	37	8	*	0	*
GS M	44	12	4	8	23	9	*	0	*
GO pS 17	40	8	3	4	25	3	*	0	85
GO3	24	3	1	1	55	4	7	0	95
GO5	17	3	1	1	35	4	10	0	71
GO 6	20	4	1	3	47	3	5	0	83
GO 8	23	5	2	6	26	2	1	1	67
GO M	17	7	2	13	16	1	10	0	66

